AN ABSTRACT OF THE THESIS OF

Hardeepak (Happy) Singh Gill for the degree of Master of Science in Chemical Engineering presented on October 4, 1996. Title : Stimulated Jet Break-up for Production of Uniform Size Microgel Beads from Crosslinked Sodium Alginate Solutions.

Abstract approved: _____

Willie E. Rochefort

The goal of this thesis was to develop a process of producing small monodisperse alginate gel beads. The phenomenon of controlled jet break-up of alginate solution jet with assisted vibration was used to form uniform sodium alginate droplets which were subsequently crosslinked with divalent calcium ion to form gel beads. Producing uniform alginate beads below 500 microns has been a problem which previous researchers have faced. Also, there is no commercially viable system available which can produce microbeads of uniform size. This study was an attempt to solve some of these problems.

Vibration was applied to the alginate solution jet in both axial and transverse direction to cause jet break-up. Also, different modes of transmitting the vibration to the jet, like vibrating the full assembly or vibrating a diaphragm, were investigated. This resulted in construction of different types of bead generator apparatus. The droplet formation involves the formation of a jet through an orifice and superposition of vibration in order to control the break-up the jet. Both of these fluid flow phenomena depend on the properties of the liquid used to form the droplets. Specifically, the viscoelastic properties of the liquid play a major role in determining the break-up dynamics of the jet. The rheology of the Keltone LV (alginate) solutions (1-2% w/v) was studied using a rotational Bohlin CS-50 Rheometer and a Clark High Shear Capillary Viscometer.

The best results were obtained by using the axial vibrating diaphragm droplet generator. Good monodispersed beads (160-1000 microns) were produced by using two different size orifices 100 micron and 200 microns. The vibration frequency range used was 200 - 6000 Hz and the flowrate range was 2-7 ml/min. The alginate droplets were

crosslinked in 0.1 M calcium chloride and the shrinkage of the alginate droplets due to gelation was studied over a period of 7 days. Based on our study a design for producing sub-100 micron size beads has been proposed which uses a piezoceramic crystal for producing high frequency vibrations.

Stimulated Jet Break-up for Production of Uniform Size Microgel Beads from Crosslinked Sodium Alginate Solutions

by

Hardeepak (Happy) Singh Gill

A THESIS

submitted to

Oregon State University

in partial fulfillment of

the requirements for the

degree of

Master of Science

Completed October 4, 1996

Commencement June 1997

Master of Science thesis of Hardeepak (Happy) Singh Gill presented on October 4, 1996

APPROVED:

Major Professor, representing Chemical Engineering

Head of Chemical Engineering Department

Dean of Graduate School

I understand that my thesis will become part of the permanent collection of Oregon State University libraries. My signature below authorizes release of my thesis to any reader upon request

Redacted for privacy

Hardeepak (Happy) Singh Gill, Author

ACKNOWLEDGMENTS

First and foremost, I would like to thank The God "*WAHEGURU*" for making this dream come true and answering all my prayers.

As a lion hearted boy of Punjab who found his new den in Oregon, this has been a very fulfilling, exciting, and educational time of my life. The success of my stay and study is, in most part, due to the many fine people that I had the pleasure to interact with. Personally, when reading *a* thesis, I usually find the acknowledgments the most interesting with their effusions. In any endeavor which takes as long and becomes as stressful as this research project, there are certain people whose contributions have been very important. So, now it is my turn to be effusive with praise and gratitude. Please read on so that I can thank those persons who have helped me over the years.

Special thanks go to my advisor, Dr. W. E. *"Skip"* Rochefort, whose scholarly advice and concern were inspirational and invaluable. Skip's philosophy of Polymer Science and methodical approach to research were some of my most professionally valuable experiences. I extend my gratitude to Skip and Jackie (Mrs. Rochefort), for providing me shelter in their cozy house when I went "homeless". I admire Skip for his "Koolness", inspite of all the crazy things I did especially when the cops came knocking at his door at four in the morning, making our house their daily rendezvous and me their favorite subject. He counseled me when I was down and through his trust in me, contributed in my own. I would like to thank him specially for all his support, advice and friendship. Hats off to Skip!!

I would like to acknowledge the efforts of my committee members, Dr. Skip Rochefort, Dr. Goran Jovanavic, Dr. Jim Ayers and Dr. Ron Miner. They have been very helpful and have given me their precious time whenever I needed it.

As everyone knows that good research cannot be completed without bread and butter, I would like to thank Dr. Skip Rochefort, OSU and Mr. Ross Clark, Kelco Co. for providing the necessary funds and support.

I wish to thank my father, Dr. J.S. Gill and my mother, Dr. R. J. Hans Gill, for encouraging and supporting me at every step of my life and to my elder sister, Ramneek Gill, for allowing me to play with her beautiful friends when I was a kid and older. Special thanks to her husband, Kanwalpreet for making my California visits a blast. Believe me, that really helped my confidence. I would like to show my gratitude to my ***grandparents*** for all their prayers and to whom this thesis is dedicated.

Many thanks to Dr. Paul Reboa, HP (Corvallis) for letting me use his rheometers and to Charles Lind for his time and effort in doing some rheological tests.

I would like to acknowledge Rada Vukmirovic for her work on the *contraction of alginate gel beads as they undergo gelation*. She was a great help in the last minutes of putting this manuscript together.

I would like to convey my appreciation to my friend, Manu. We went through high school, BS and now MS together. I always found that I need not worry about my grades if he's around. His open attitude about the class assignments allowed me to concentrate on other worldly matters. Of course I had to ensure that we both enrolled for the same classes. I also wish to thank his wife Jyoti for the meals that she ordered Manu to make for me off and on.

Mr. Eric Hekkala deserves my gratitude for keeping my lab in order and for his constructive criticisms.

My thanks to Sanjeev Tyagi, Brijeesh Singla and Adil Nassir for helping me in my initial settlement in Corvallis. Sanjeev has always been and will always remain a great friend. He was a great room mate even though I had to get used to his snoring. If it was not for him, I probably would have never gone to all the *Kool* places in Eugene. Thanks to Adil "chef" who cooked me food whenever I was hungry in the days I was tremendously busy writing my thesis.

Josh "my best buddy", gets my thanks for the escapades from Corvallis that refreshed me and revitalized my efforts at work. Thanks to him for letting me stay at his houseboat whenever I wanted to hide from civilization.

Nick deserves my sincere gratitude for showing my way around the department network and lending me his tools which often I lost track off. I also wish to thank Debbie, Valerie "sweetheart", Paula "sweety", Ron "the womanizer", Kaj "the decent guy", Neeta Singh "sis" and Shibashis for enlivening my stay. Special thanks to Maureen and Susana Alvarez "Susy", who spent countless hours assisting and guiding me with the writing of this thesis.

Tom Smith "IBM fan" kept me busy with his jokes about Macs and helped me whenever the printer broke down while printing my thesis. And thanks to Jim Philips who kept his mouth sealed about all the parties I had in Nick's office. I would also like to thank my labmates Zafar Malik, Bin Xu, Abed Al-Amri and Lance C. Kim.

I will not be able to forget Claudia Gil for her warmth, friendship, and making the last days of my stay a wonderful memory.

Lastly I would like to show my appreciation to my special friend Teena Singh for her enchanting smiles and dreamy eyes, giving me confidence that life is worth living.

TABLE OF CONTENTS

TABLE OF CONTENTS (continued)

TABLE OF CONTENTS (continued)

TABLE OF CONTENTS (continued)

LIST OF FIGURES

LIST OF FIGURES (continued)

LIST OF TABLES

LIST OF APPENDIX FIGURES

LIST OF APPENDIX FIGURES (continued)

"This thesis is dedicated to my loving grandparents

Smt. Bhagwan Kaur

Late Sardar Malkiat Singh Gill

Late Smt. Gurdeep Kaur

Late Sardar Gursher S. Hans"

"Where the mind is without fear and the head is held high,

Where knowledge is free,

Where the world has not been broken up into fragments by narrow domestic walls,

Where words come out from the depth of truth,

striving stretches its arms towards perfection,

has not lost its way into the dreary sand of dead habit,

ever-widening thought and action.....

Father let my country awake."

Rabindranath Tagore

Stimulated Jet Break-up for Production of Uniform Size Microgel Beads from Crosslinked Sodium Alginate Solutions

CHAPTER 1

1. INTRODUCTION

Several methods have been developed for formation of crosslinked calcium alginate beads due to their growing use in the fields of immobilization and microencapsulation of biologically active molecules, tissues, cells and enzymes. Immobilization and microencapsulation helps the biological material to remain viable and in a protected state within a semipermeable membrane which allows the passage of low weight molecular substances like nutrients, oxygen etc., but not to high molecular weight proteins of immune system. Some of the applications include immobilization of living or dead cells in bioreactors, immobilization of plant protoplasts for micropropagation, immobilization of hybridoma cells for production of monoclonal antibodies, entrapment of animal cells for implantation of artificial organs, etc. Various other possible applications of the calcium alginate microgel beads are presented in Chapter 3.

There have been numerous investigators who have made crosslinked alginate gel beads. In this work, controlled jet break-up of alginate solution jet with assisted vibration has been used to form uniform sodium alginate droplets which are subsequently crosslinked with divalent calcium ion to form gel beads. Producing uniform alginate beads below 500 microns has been a problem which previous researchers have faced. Also, there is no commercially viable system available which can produce microbeads of uniform size.

The current study involved the construction and testing of an apparatus which solved the above mentioned problems. The effect of flowrate, frequency of vibration and concentration of alginate solution on the size of microgel beads was investigated. Although this apparatus was constructed on a laboratory scale, it can easily be scaled up to a commercially viable process. Also fluid rheology of alginate solutions was studied to

determine their non-Newtonian properties. Gelation of sodium alginate with calcium chloride solution was investigated through qualitative and rheological properties of calcium alginate gels.

The procedure developed for making crosslinked alginate beads can be used for immobilization and entrapment, as it can be carried out in a single step process under very mild conditions and is therefore compatible with most living cells. The material to be entrapped or immobilized is mixed with sodium alginate solution, and the mixture extruded through the Axial Vibrating Diaphragm Droplet Generator, where the jet is broken up into uniform size droplets with controlled vibration. For a particular size orifice, the size of the uniform droplets can be changed within a limited range by changing the frequency of vibration and velocity of the alginate solution jet. This makes this particular technique very versatile in producing uniform alginate droplets of various sizes from the same orifice. The droplets are then immersed in the crosslinking solution containing divalent ions like calcium or trivalent ions like aluminum. Here the alginate solution droplets undergo crosslinking and form gel beads.

The final size of the gel beads is smaller than the alginate solution droplet as calcium alginate gels shrink during gel formation, leading to loss of water and an increase in polymer concentration relative to the alginate solution. This shrinkage depends on alginate source, alginate concentration in the solution, concentration of sodium ion in sodium alginate solution, type of crosslinking ion (divalent, trivalent etc.), concentration of crosslinking ion, time of gelation, size of alginate solution droplet and temperature.

The key questions which were addressed in this study are as follows:

1) Is it possible to obtain monodispersed alginate beads by stimulated alginate jet break-up and subsequent crosslinking?
2) Can a commercially viable apparatus based on the above principle, be constructed with relative ease?
3) Can the bead size be changed easily and can the operating conditions be predetermined so as to produce alginate beads of a certain size?
4) What are the effects on alginate bead size for different alginate concentrations and other operating conditions?

CHAPTER 2

2. BACKGROUND

2.1 Unstimulated Liquid Jet Break-up

A liquid column is inherently unstable due to pressure increase at points of reduced diameter. Ideally, it will form a series of uniformly spaced droplets with the spacing dependent on the fastest growing wave. Unstimulated liquid jet break-up has been studied in great detail by previous investigators. A brief summary of their work is given in this section. A schematic of a typical jet break-up is shown in Figure 2-1. Newtonian and Non-Newtonian fluids show different behavior in liquid jet break-up and therefore will be discussed separately.

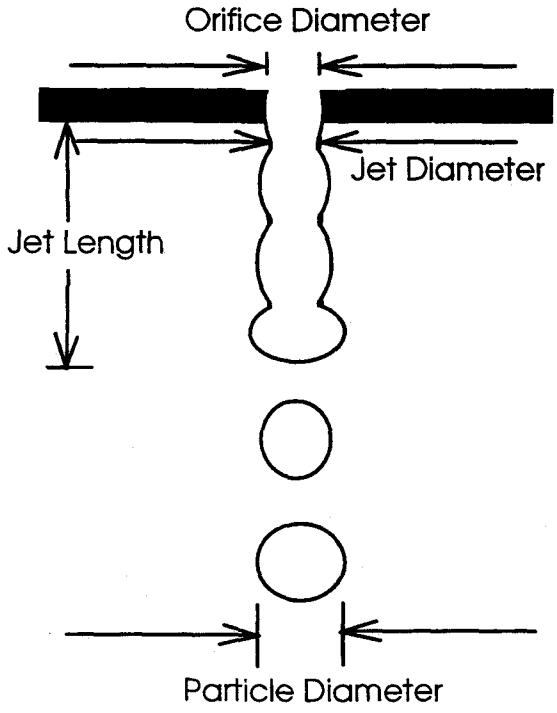

Figure 2.1 LIQUID JET BREAK-UP

2.1.1 Newtonian Liquid Jet Break-up

The liquids which were used to form the jet by the investigators in this section were Newtonian in character. The phenomenon of liquid jet break-up was first studied experimentally by Savart (1833) and Plateau (1873). When a liquid issues from an orifice into another immiscible fluid (liquid or gas), droplets form at the end of the jet due to capillary instability. Capillary instability arises as a result of interfacial tension whenever the wavelength of the surface disturbance exceeds the circumference of the cylindrical liquid jet. In other words, capillary instability is caused by long disturbance waves. Rayleigh (1878) used rigorous theoretical analysis to show that, from an initially small disturbance, a number of unstable waves may form on the jet surface and the wave that causes the jet to break-up , the "most unstable wave", is that which has the maximum growth rate in amplitude. Though, Rayleigh's maximum instability theory was applicable to inviscid fluids, it had only a limiting solution for viscous fluids. Weber (1931), derived a dispersion equation for a viscous liquid jet issuing into gas and found that for viscous jets, the most unstable wavelength is longer than that predicted by Rayleigh for inviscid jet break-up. The above discussion is elaborated in the following paragraphs.

2.1.1.1 Minimum Disturbance Wavelength

It was Plateau (1873) who determined that if a liquid jet with an equilibrium diameter D_J, is disturbed slightly such that the diameter, D is defined by:

$$D = (D_J/2) + \theta \cos(\omega t) \qquad (2\text{-}1)$$

where, θ = disturbance amplitude.

and if the wavelength (λ) of the disturbance is greater or equal to the circumference of the liquid jet (πD_J), the disturbance will grow in time as the liquid moves away from the nozzle. Therefore, the minimum wavelength for which a jet is unstable and a small disturbance will grow is given by the equation (2-2).

$$\lambda_{min} = \pi D_J \tag{2-2}$$

The above was discussed by Goren (1963) as follows, "For a liquid with finite surface tension, the array/droplets has a lower free energy than the cylinder and is consequently thermodynamically more stable".

This means that in order for two disturbances to grow, they must be at least apart by a value equal to the circumference of the jet. Plateau's theory limits the minimum wavelength, that is the maximum frequency between disturbances, but it does not provide any theoretical maximum wavelength i.e. minimum frequency.

2.1.1.2 Optimum Disturbance Wavelength

In 1879, Rayleigh showed that a cylindrical column or jet of inviscid liquid is unstable with respect to an axially symmetric sinusoidal perturbation in radius, if the wavelength of the perturbation (λ) is greater than the circumference of the liquid cylinder (D_J). This phenomenon is also known as Rayleigh's instability. He derived the optimum wavelength, λ_{opt} for a disturbance to be most unstable as follows:

$$\lambda_{opt} = 4.508\ D_J \tag{2-3}$$

Rayleigh determined that a circumferential disturbance on an inviscid, incompressible, cylindrical liquid jet sprayed into a vacuum, will grow exponentially as:

$$\frac{\theta}{\theta_o} = e^{qt} \tag{2-4}$$

$$q = \left[\frac{8\sigma_L}{\rho_L (D_J)^3}\right]^{\frac{1}{2}} \phi\left[\frac{\pi D_J}{\lambda}\right] \tag{2-5}$$

where,

θ = disturbance amplitude

θ_o = initial disturbance amplitude

ϕ = function involving Bessel's function

σ_L= surface tension of the liquid

ρ_L= density of the liquid

The maximum rate of growth of a disturbance occurs when q is maximum, which occurs at the condition given by equation (2-3). This means that the jet will break-up the fastest when the disturbances are 4.508 D_J apart. Thus from equation (2-3) and applying the principle of conservation of mass, the theoretical optimum droplet diameter is given by the following relation:

$$D_{P,opt} = 1.89\, D_J \tag{2-6}$$

Break-up of low viscosity liquid jet is close to Rayleigh's prediction, although smaller drops also known as satellites are also formed along with bigger drops.

Rayleigh (1892) found that for an incompressible, viscous, cylindrical jet without inertia the optimum wavelength, λ_{opt} tends to infinity for the fastest growing disturbances. In other words, it means that viscous liquid jets tend to break-up at distant intervals. Viscous fluids tend to form shorter ligaments between the main droplets, thus reducing the chance of satellite droplets. Thus the effect of viscosity is to reduce the growth rate, reduce the satellite droplet formation and to produce larger main drops.

Weber (1931) modified the relation for viscous liquids as the drops produced by jet break-up are larger in size. For viscous liquids with viscosity μ_L ,the optimum diameter of the droplets is given by

$$D_{P,opt} = 1.89 D_j \left[1 + \frac{3\mu_L}{(\sigma_L \rho_L D_J g_c)^{1/2}} \right]^{1/6} \tag{2-7}$$

Basset (1894) found that viscosity of the liquid tends to produce stability in the cylindrical jet while the surrounding medium, the air, produces instability. He also found that surface tension tends to produce stability or instability depending on whether the wavelength is less than or greater than the circumference of the jet. In addition he investigated the effect of charge on the jet.

Weber (1931) extended the work done by Rayleigh by finding that the optimum wavelength of disturbances to grow most rapidly is given by the equation (2-8).

$$\frac{\lambda_{opt}}{D_J} = \frac{\pi}{0.707}\sqrt{1+\left(\frac{9\mu^2}{\rho\sigma D_J}\right)^{\frac{1}{2}}} \qquad (2\text{-}8)$$

Tyler (1933) found that the value of the optimum wavelength was 4.75 D_J.

2.1.1.3 Weber Number

Weber number (We) is a dimensionless quantity and is defined as the ratio of inertial forces to the surface tension forces.

$$We = \frac{\rho D_J V_J^{\,2}}{2\sigma} \qquad (2\text{-}9)$$

Also the wave number (k) is a dimensionless representation of the reciprocal of the wavelength of the jet disturbance. It is given by the following equation:

$$k = \frac{\pi D_J}{\lambda} \qquad (2\text{-}10)$$

where λ, is the wavelength of the applied disturbance. All the results of Rayleigh's work can also be expressed in terms of Weber number.

2.1.1.4 Jet Length

Jet instability leads to the formation of droplets. Therefore, the concept of jet break-up length is very important. Jet length is defined as the continuous part of the liquid stream before it breaks up into droplets. In the absence of assisted vibration, jet break-up is dominated by the wavelength with the highest growth rate. Jet break-up as a function of jet velocity is illustrated qualitatively in Figure 2-2.

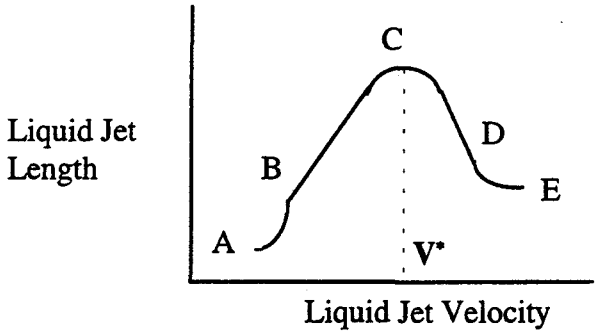

Figure 2.2 EFFECT OF JET VELOCITY ON JET LENGTH

The break-up of a jet can be divided into several regimes. There are two critical velocities which are represented by points B and C in the above figure. At these points the slope changes suddenly. Point A represents the drip limit, below which the kinetic energy of the jet is insufficient to generate the new surface required to form a continuous jet.

Tyler and Watkin (1932) suggested that that critical velocity at point B might be due to the droplet formation at smaller jet lengths. This droplet formation influences the disturbances and causes the jet to break-up at unusually small lengths.

Tyler and Richardson (1925) described the shape of the length versus velocity curve to be a composite of three different phases which may be superimposed. In the first one, there is a straight line relationship between the length and velocity, the disruptions involving surface tension effects. The second phase, is at small jet lengths when the ratio of length to velocity is increasing due to drop formation near the jet. The third phase consists of the hyperbolic relation between the length and the velocity, in which the break-up of the jet is due to viscosity.

The linear-laminar portion of the break-up curve is represented by B-C. The works of Rayleigh and Weber describe this type of jet instability. Weber (1933) determined that this regime is defined by the equation:

$$\frac{L}{D_J} = \left[\ln\left(\frac{D_j/2}{\theta_o} \right) \right] \left(We^{\frac{1}{2}} + \frac{3We}{Re} \right) \tag{2-11}$$

where θ_o is assumed to be an initial amplitude of oscillation and We is the Weber number. Re is the dimensionless Reynolds number and is defined as the ratio of inertial forces to the viscous forces ($Re = DV_L \rho_L / \mu_L$ where V_L is the velocity of the fluid). The value of the log term in equation (2-11) was found to be on the order of 12.

But, Tyler and Watkin (1932) found that the logarithmic term did not have a constant value when the liquids differed greatly in viscosity. As the velocity of the jet increases , the effects of aerodynamic instability and viscosity of the environment became significant. Both can be expected to shorten the break-up length from that obtained by Rayleigh instability alone. Grant and Middleman (1966) obtained an empirical relationship to describe the region above the drip limit. It is given in the following equation:

$$\frac{L}{D_J} = 19.5 \left(We^{1/2} + 3\frac{We}{Re} \right)^{0.85} \tag{2-12}$$

At higher velocities, the break-up length has been observed to reach a maximum and then decrease. The velocity at the maximum jet length is designated as the critical velocity, V^*. Viscosity of the environment is largely responsible for this phenomenon. Grant and Middleman (1966) found that the critical velocity could be represented by the following equation:

$$Re^* = 3.25Z^{-0.28} \tag{2-13}$$

in which the Re^* is the Reynolds number at the critical velocity and Z is the Ohnesorge number defined by $Z = \left[\frac{We^{\frac{1}{2}}}{Re} \right]$.

A minimum break-up length has been observed beyond the critical velocity above which the liquid jet length starts to slightly increase again.

2.1.1.5 Jet Diameter

The diameter of the jet, D_J is important as the relationships for minimum and optimum wavelengths are give in terms of this quantity. Harmon (1955) predicted that for a given laminar jet with no gravitational force, the diameter of the jet is given as follows:

$$D_J = 0.866\, D_O \qquad (2\text{-}14)$$

where D_O is the diameter of the orifice used to form the liquid jet.

Middleman and Gavis (1960) found in their studies that the ratio of the final jet diameter to the initial jet diameter was a function of Reynolds number and Weber number. Goren and Wronski (1965) found that the jet diameter increases monotonically with axial distance for Reynolds number less than 12. When Reynolds number is greater than 17, the jet diameter decreases monotonically with axial distance. But when Reynolds number is between 12 and 17, the diameter of the jet decreases at first and then increases.

Lindblad and Schneider (1965) found experimentally that the ratio of final jet diameter to initial jet diameter is about 0.8 which compare closely with values predicted by previous investigators.

2.1.1.6 Minimum Jet Velocity

It is known that a minimum liquid velocity is needed to form a jet and that this velocity depends on the properties of the liquid.

Lindblad and Schneider (1965) derived that a minimum liquid velocity is needed to form a liquid jet from a capillary,

$$V_{J,min} = \left[\frac{8\sigma_L}{\rho_L D_J}\right]^{\frac{1}{2}} \tag{2-15}$$

where σ_L is the surface tension, ρ_L is the density of the liquid and D_J is the jet diameter.

As the velocity of the jet is increased, the break-up process changes. Any surface wave which exists is reinforced by velocity by lowering the pressure on wave crests due to the higher local velocity at the crest than at the trough. As the velocity increases three general regimes have been identified. The first regime consists of a jet which looks like Rayleigh's symmetric bulges and contractions. It is called the varicose or symmetric oscillation regime. Here the unbroken jet length becomes larger as the velocity is increased and the drops become smaller and less uniform. The second regime is sinusoidal or transverse oscillation regime. In this regime the jet oscillates irregularly in a S-fashion. The jet becomes shorter and the drops become larger. The third regime is the atomization in which there is highly chaotic break-up into small droplets.

2.1.2 Non-Newtonian Liquid Jet Break-up

Non-Newtonian liquids are liquids which do not obey the Newton's law of viscosity. Their viscosity changes with shear rate. Liquid jet break-up for non-Newtonian fluids has not been studied as extensively as the Newtonian liquid jet break-up.

The stability of non-Newtonian jets in an inviscid medium was first analyzed be Middleman (1965), who predicted theoretically that laminar jets of linear viscoelastic fluid would be less stable than Newtonian jets.

Bousefield et. al. (1984) studied dynamics of non-Newtonian liquid filament break-up and observed that jets of polymer solutions generally take longer to break-up into droplets than purely viscous jets of comparable viscosity, and sometimes do not break-up at all. They found that the growth rate of the disturbance is initially more rapid for a non-Newtonian liquid (Maxwell fluid) than for a viscous Newtonian fluid, but for

longer times the growth is retarded and the filament approaches a configuration approximated by a long cylinder of uniform radius connecting two large droplets. The stabilization of jets of polymer solutions is attributed to resistance to extensional deformations. It is this nonlinear behavior resulting from the buildup of extensional stresses that inhibits the break-up of the viscoelastic jets.

The above discussion clearly points out the fact that the jet break-up process directly depends on the rheological characteristics of the non-Newtonian fluid. In polymer solutions, affects such as the role of extensional viscosity and die swell may play an important role depending on whether the storage modulus (elastic component) is significant.

2.2 Stimulated Liquid Jet Break-up

A cylindrical liquid jet is unstable to mechanical disturbances due to which it breaks up into droplets. If these mechanical disturbances are generated by an outside source at a constant frequency within some limited range having sufficient amplitude and then applied to a constant velocity liquid jet, the jet will break-up into droplets having the same size. The droplet generators described in this work is based on the above principle.

2.2.1 Assisted Vibration Mode For Newtonian Liquid Jets

The frequency of the disturbance of a jet undergoing natural break-up tends to be limited to the wave number corresponding to maximum growth rate and thus the range of droplet diameters are severely limited. Also as, the natural break-up is a dynamic process, the wave number keeps changing which gives polydisperse droplets instead of equal size droplets. To increase the range of droplet diameters achievable for a given jet diameter and to obtain monodisperse droplets, many investigators have used vibrations to assist the break-up of the jet. Assisted vibration gives the wavelength corresponding to the

wavelength of the vibration a head start over wavelengths of other disturbances present in the environment. Therefore, a desired droplet size can be obtained by dialing in the right wavelength. The amplitude of the wave with the desired wavelength but less than the maximum inherent growth rate, will dominate the droplet forming process. The amplitudes required to select a wavelength of choice are relatively small.

The wavelength of the disturbance can be calculated as follows. The velocity of the liquid jet is equal to the product of the wavelength. (λ) and the frequency (F) of excitation of the transducer :

$$V_J = F \times \lambda \tag{2-19}$$

Also, it is known that the size of the droplet can be found from the volume of the drop (Schneider and Hendricks) which is:

$$v = \pi(D_J/2)^2\lambda \tag{2-20}$$

where v is the volume of the droplet and D_J is the diameter of jet. The diameter of the droplets that will form was given by Berglund (1972) in the equation:

$$Dp = \left[\frac{6Q}{\pi F}\right]^{\frac{1}{3}} \tag{2-21}$$

Droplets cannot be made arbitrarily small by making disturbance wavelengths, λ, smaller and smaller by increasing the frequency modulation or by decreasing the velocity of the jet. The reason for this is that the liquid cylinder remains stable with respect to displacements from equilibrium for wavelengths less than πD_J.

Thus, one established limitation not to be exceeded is the maximum frequency or minimum λ,

$$\lambda_{min} = \pi D_J \tag{2-22}$$

The upper limit on λ is determined by experimental limitations; increasing λ or jet velocity leads to operating difficulties because the range of the disturbing wavelength may be exceeded which causes the aerosol to become non-uniform with apparently little effect resulting from the mechanical disturbance. With these limitations, Schneider and

Hendricks(1964) gave an empirical relation which indicated that the droplet size could be changed in a trouble free manner by varying the wavelength(λ) between

$$3.5< (\lambda/D_J)>7 \qquad (2\text{-}23)$$

where D_J is the diameter of the jet.

However, Welding (1974) showed that the above relation is not applicable to all the orifice diameter and the range can be determined by the relation

$$Q/(F_{max}\, A_J\, D_J) \leq (\Lambda/D_J) \leq Q/(F_{min}\, A_J\, D_J) \qquad (2\text{-}24)$$

where Q is the flow rate of the liquid

F_{max} is the maximum frequency

F_{min} is the minimum frequency

A_J is the area of the jet

D_J is the diameter of the jet

The values of the optimum wavelength as found by different investigators are given in the table below:

Table 2.1 VALUES OF OPTIMUM WAVELENGTH

Investigator	Year	Optimum Wavelength, λ_{opt}	Liquid used to form jet	Remarks
Ryley and Wood	1963	4.5 D_J	Water	Vibrating capillary
Crane	1964	5.44 D_J	Water	Vibrating orifice
Schnieder and Hendricks	1964	3.5 D_J to 7 D_J	Water	Vibrating capillary

Table 2.1 (CONTINUED)

Strom	1969	4.51 D_J	Water	Vibrating orifice

Goedde and Yuen (1970), examined capillary instability of vertical liquid jets of different viscosity by imposing audio-frequency disturbances. They found that non-linear effects dominate the growth processes of the disturbance. This causes the liquid jet to disintegrate into drops with ligaments in between. The sizes of these ligaments decrease with increasing wave-number, as the non-linear effects are more pronounced at smaller wave numbers. These ligaments subsequently roll up to form satellite droplets as a sphere is the most stable configuration, which under some conditions may coalesce with the main drop. They found that inviscid fluids (like water) and viscous fluids (like glycerin-water) behave similarly except for the fact that in viscous liquids, the viscous damping causes the growth rate of the disturbance to be lower and the maximum growth rate to shift to a lower wave-number.

Numerous investigators have conducted research on making micro droplets, and a list with their respective methods is given in Table 2-2. Aerosol particles (less than 50 μ) have been made with low viscosity fluids using a vibrating orifice with a coaxial shearing fluid, using an air stream. The Vibrating Orifice Aerosol Generator (VOAG) is a commercial instrument manufactured by T.S.I., Inc.(Minneapolis, MN) based on this two-fluid oscillating orifice technique for producing aerosols. It was originally proposed by Berglund and Liu (1973). A list of different types of liquids used to form droplets by assisted vibration is given in Figure C-1 (Appendix C).

Summary of previous experimental work on vibrating droplet generators using Newtonian fluids is given below in Table 2-2.

Table 2.2 LIST OF INVESTIGATORS WHO USED VIBRATING DROPLET GENERATORS

Investigator	Year	Droplet Diameter (microns)	Nozzle Type	Type of Oscillation	Equipment used for oscillation
Savart	1833	---	Capillary	---	Tuning fork
Dimock	1950	100-300	Capillary	Longitudinal	Electromagnet
Magarvey and	1956	300-2500	Capillary	Longitudinal	Earphone
Taylor		2500-10,000	Copper tube	Longitudinal	Earphone
		10,000-20,000	Copper tube	Longitudinal	Plunger driven motor
Schotland	1960	300-1000	Capillary	Longitudinal	Electromagnet
Ryley and Wood	1963	300-1350	Capillary	Transverse	Vibrator
Mason et al	1963	30-1000	Capillary	Transverse	Earphone
Crane,Birch and McCormack	1964	---	Orifice	Transverse	Electric Vibrator
Schneider and Hendricks	1964	50-2000	Capillary	Longitudinal	Piezoelectric transducer
Donnely and Glaberson	1965	---	Capillary	Transverse	Audio speaker
Sweet	1965	73	Capillary	Longitudinal	Magnetostricti-ve Transducer
Fulwyler	1965 1969	50	Orifice	Longitudinal	Piezoelectric transducer and coupling rod

Table 2.2 (CONTINUED)

Atkinson and Miller	1965	400-1540	Capillary	Longitudinal	Inline electric pump operated out of range
Park and Crosby	1965	250-1650	Capillary	Longitudinal	Vibrating diaphragm
Lindblad and Schneider	1965	50-700	Capillary	Longitudinal	Piezoelectric bimorph crystal
Dabora	1967	290-950	Capillary	Longitudinal	Speaker coil
Hendricks and Tsui	1968	600	Orifice	Longitudinal	Ion drag pump
Strom	1969	15-40	Orifice	Longitudinal	Electrostrictive discs
Goedde and Yuen	1969	1820-4550	Capillary	Longitudinal	Electrostatic force and loudspeaker
Wissema and Davies	1969	900-2000	Capillary	Transverse	Philips vibration exciter
Raabe	1970	---	Orifice	Longitudinal	Piezoelectric transducer and coupling rod
Rutland and Jameson	1971	---	Capillary	Transverse	Loudspeaker
Berglund and Lui	1973	12-46	Orifice	Longitudinal	Piezoelectric transducer

Table 2.2 (CONTINUED)

Rajagopalan and Tien	1973	---	Capillary	Transverse	Vibrator
Wedding and Stukel	1974	3-25	Orifice	Longitudinal	Piezoceramic crystal
Wedding	1975	0.8-30	Orifice	Longitudinal	Piezoceramic crystal
Haas	1975	500-1500	Co-axial capillary	Longitudinal	Piezoelectric transducer
Lafrance	1975	6500-11,000	Capillary	Longitudinal	Electrostatic force
Taub	1976	---	Nozzle assembly	Longitudinal	Vibrator
Pimbley and Lee	1977	---	Capillary	Longitudinal	Magnetostricti-vely
Araki and Masuda	1978	700-1300	Nozzle assembly	Longitudinal Transverse	Mechanical vibrator
Chaudhary and Maxworthy	1980	200-1200	Nozzle assembly	Longitudinal	Piezoelectric transducer
Sakai and Hoshino	1980	600-1100	Capillary	Longitudinal	Audio speaker
Kurabayaski and Karasawa	1982	1250-2120	Rectangular Orifice	Transverse	Loudspeaker
Nakayama and Takahashi	1982	---	Nozzle assembly	Longitudinal	Magnetostricti-ve vibrator
Schummer and Tebel	1982	---	Nozzle assembly	Longitudinal	Vibrator

Table 2.2 (CONTINUED)

Lui and Pui	1982	25	Orifice	Longitudinal	Piezoceramic crystal
Barr, Carpenter and Newton	1984	15	Orifice	Longitudinal	Piezoceramic crystal
Tramper	1985	1300-2500	Capillary	Longitudinal	Vibrator
Lin, Eversol and Campillo	1990	5-80	Orifice	Longitudinal	Piezoceramic crystal
Warnica, Reenen,Renksizbulut and Strong	1993	---	Orifice	Longitudinal	Piezoceramic crystal
Blaisot, Ledoux, Ducret and Vendel	1994	100-500	Capillary	Transverse	Piezoceramic crystal
Charuau, Tierce and Birocheau	1994	0.1-1	Open beaker	Longitudinal	Ultrasound Transducer
Moon, Kim, Lim, Go, Lee and Chang	1995	5-200	Orifice	Longitudinal	Piezoceramic crystal

2.2.2 Assisted Vibration Mode For Non-Newtonian Liquid Jets

There has been no significant work reported in literature on the formation of droplets by break-up of non-Newtonian liquid jets with assisted vibration. But there has been some significant work by Schummer et. al. (1984), on study of extensional viscosity of dilute polymer jets issuing from a harmonically vibrating nozzle. The jets of polymer solutions under vibration form droplets connected by filaments. Though this phenomenon is present in the Newtonian liquid jet break-up, it is not as pronounced as in the case of non-Newtonian liquid jet break-up. This is merely due to the fact that polymer solutions are more elastic than Newtonian solutions of comparable viscosities. Therefore, as in Newtonian case there is a regular jet surface with drop regions and filaments in between, but due to elastic properties the filaments disappear only asymptotically. It can be approximated like a purely elongational flow where a cylindrical rod is stretched continuously in the axial direction. The frequency of vibration, amplitude of vibration and the velocity of the jet are the operating parameters which influence elongational flow. In this study, Keltone LV (sodium alginate) solution, a shear thinning liquid was used to form a jet which was subsequently broken-up into uniform droplets with the help of vibrations.

2.3 Methods of Production of Alginate Beads

Alginate is one of the widely used immobilizing system due to its properties which make it is compatible with most of the biocatalysts.. Two main methods of dispersion are mainly applied to the production of alginate beads. They are extrusion and emulsification methods. These methods differ in the amount of shear the material undergoes and the size dispersity of the droplets produced.

2.3.1 Extrusion Methods

In the extrusion technique, often referred to as the drop method, solutions are extruded through a small tube or needle, permitting the droplets to fall freely into the hardening solution. The different types of extrusion methods are shown in Figure 2-3.

2.3.1.1 Extrusion Under Gravity

It is the simplest method and involves the dispensing of the liquid droplets from the tip of the tube under the force of the gravity. The break-up process consists of the onset of instability of the droplet at the tip of the tube followed by the stretching of the droplet and breakage of the drop under the needle tip. It leaves behind a portion of the pendant drop. The disadvantage of this technique is that it is too slow for commercial processes and that the droplets obtained are very large (greater than 1.5 mm) even from very small needles.

2.3.1.2 Extrusion Under Co-axial Liquid or Air Jet

It was Lane(1947) who initially proposed the application of an air jet around the needle to increase the force available to break-up a nascent drop from a suspending tip. With this co-axial extrusion technique, good droplets can be produced provided they are bigger than the needle tip used for their extrusion. However, when it is used to produce smaller droplet, the nascent drop may not be spherical and also the presence of the needle will perturb the drag force. Also, the needle will have a lesser impact on the droplet size since the diameter of the droplet contacting surface is less then the needle diameter. The airflow will create a depression, pinching and breaking of the droplet. This gives the system the disadvantage of producing broad droplet size distributions. Also, one discrete

drop is extruded at a time which makes it commercially unviable. Even with all these disadvantages, most researchers have used this system to produce alginate beads due to its simple procedure.

2.3.1.3 Drop Formation Under Electrostatic Potentials

Drop formation is greatly improved by replacing the drag force required to detach the droplets from the dispensing capillary tube with a high static potential between the capillary and the collecting solution. Alternatively, the electric potential may be applied between the capillary and a metal ring placed under the capillary. It is the electric force created by this setup which pulls the droplet from the needle tip. The continuous static voltage can also be replaced by very short electric pulses. The use of electric potential for the production of beads has been patented; however, no significant data exits in the literature.

2.3.1.4 Break-up Of Capillary Jet

Aerosol particles (less than 50 μ) have been made with low viscosity fluids using a vibrating orifice with a coaxial shearing fluid, using an air stream. The Vibrating Orifice Aerosol Generator (VOAG) is a commercial instrument manufactured by T.S.I., Inc.(Minneapolis, MN) based on this two-fluid oscillating orifice technique originally proposed by Berglund and Liu (1973).

Literature search shows that the two fluid vibrating orifice technique has not been used with viscous biopolymers like alginate solutions to make microgel beads (10-250μ). This is the area which has been extensively explored in this work.

2.3.2 Emulsification Process

In emulsification , droplets are not formed one by one, but rather in terms of millions. It involves the formation of a emulsion using cylindrical vessel with baffles and an impeller used for mixing. An emulsion may also be formed in other shear devices such as open-tube static mixers. Emulsification process creates a lot of shear and thus shear sensitive materials cannot be used in this process. Also, this technique gives a very broad range of particle size distributions. Typical standard deviations reported in literature range from 20% to 70 % of the mean.

2.3.3 Discussion

Numerous investigators have produced alginate beads for different research experiments and applications. Some prominent ones are listed below in Table 2.3 which lists the names of the investigator, year of research, diameter of alginate beads in microns, concentration of alginate solution used, and the method of production of alginate droplets which were subsequently crosslinked by divalent or trivalent ions. Tramper (1985), is the only researcher who used the method of vibration to produce alginate beads in which he immobilizes biocatalysts. In his work, he focuses more on biocatalysts rather than explaining or studying the process of alginate bead formation by stimulated jet break-up.

Table 2.3 LIST OF INVESTIGATORS WHO PRODUCED ALGINATE BEADS

Investigator	Year	Bead Diameter (microns)	Fluid	Apparatus
Cheetham, Blunt, and Bucke	1979	1900	2% Algin	Syringe
Rehg, Dorger, and Chau	1984	400-900	0.5%-1.5% Algin	Two fluid nozzle
Tramper	1985	1300-2500	Algin	Vibration
Goosen et. al.	1985	700	1.2% Algin	Two fluid nozzle
Rochefort, Rehg and Chau	1986	600	1% Algin	Two fluid nozzle
Gilson, Thomas, Hawkes	1990	2000-5000	1-6% Algin	Syringe
Goosen, Poncelet, and Vunjak	1994	170-550	1.5% Algin	Electrostatic droplet generator
Huguet, Groboillot, Neufeld, Poncelet, and Dellacherie	1994	1000	1.8% Algin	Syringe
Gilson and Thomas	1995	1000-6000	1-6% Algin	Two fluid nozzle

Figure 2.3 Different Methods of Producing Droplets

A. SIMPLE CAPILLARY

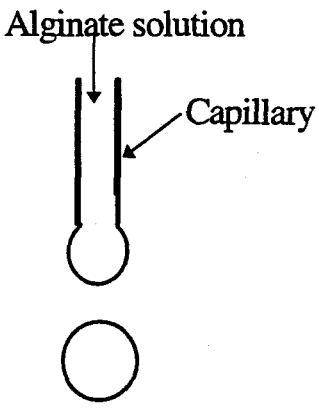

Gravity pulls down the droplet while surface tension gives it a spherical shape

Characteristics

1. Simplest method - very easy to use
2. Large droplets (>1 mm)formed even from small capillaries - cannot be used to produce small droplets.
3. Discrete droplets formed, one at a time.
4. Very little control over droplet size.
5. Commercially unviable.

B. C0AXIAL CAPILLARY

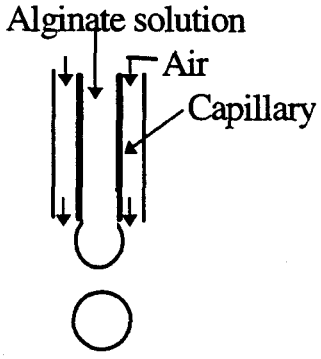

Coaxial fluid (usually air) helps provide an additional force to detach droplet from the capillary.

Characteristics

1. Relatively simple method - very easy to construct and use
2. Uniform droplets formed only when diameter of droplet is greater than capillary diameter.
3. Discrete droplets formed, one at a time.
4. Some control over droplet size with the coaxial fluid.
5. Very hard to form beads under 0.5 mm with uniform size.
6. Hard to extrude viscous solutions (like 2% alginate) from small diameter capillaries.
7. Good method for research applications.

Figure 2.3 (continued)

C. DROPLET FORMATION UNDER ELECTRIC POTENTIAL

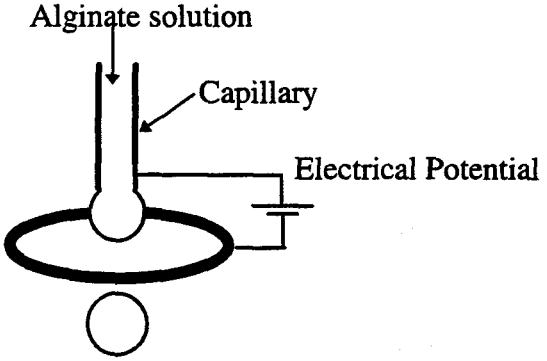

Electrostatic potential helps provide an additional drag force to detach droplet from the capillary.

Characteristics

1. Relatively complex system to construct and operate.
2. Uniform droplets formed only the applied potential is below a critical voltage.
3. Discrete droplets formed, one at a time.
4. Some control over droplet size with the variation of electric potential.
5. Very hard to form beads under 0.5 mm with uniform size.
6. Hard to extrude viscous solutions (like 2% alginate) from small diameter capillaries.
7. Commercially unviable.

D. BREAKUP OF LIQUID JET FROM CAPILLARY WITH VIBRATION

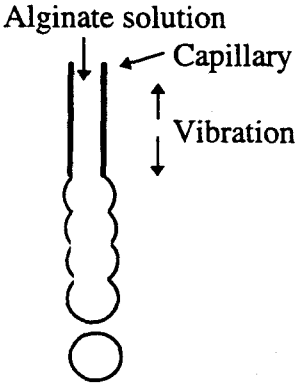

Overriding of the natural breakup of liquid jet with the help of an external vibrating source of constant frequency

Characteristics

1. Complex jet breakup process
2. Very Uniform droplets formed.
3. Large number of droplets produced.
4. Droplet size can be changed by varying frequency over a certain range.
5. Hard to extrude viscous solutions from small diameter capillaries.
6. Good method for research and commercial applications.

Figure 2.3 (continued)

E. BREAKUP OF LIQUID JET FROM ORIFICE WITH VIBRATION

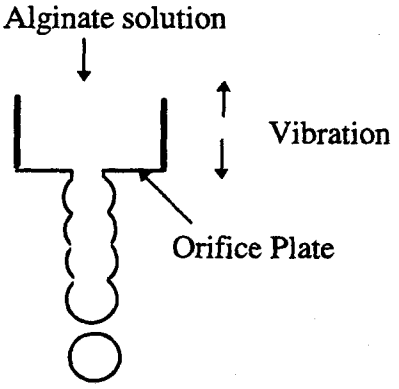

Overriding of the natural breakup of liquid jet with the help of an external vibrating source of constant frequency

Characteristics

1. Complex jet breakup process
2. Very Uniform droplets formed.
3. Large number of droplets produced.
4. Droplet size can be changed by varying frequency over a certain range.
5. Viscous polymer solutions can be easily extruded through small orifices due to low shear.
6. Small droplets can be produced.
7. Good method for research and commercial applications.

F. BREAKUP OF LIQUID JET FROM COAXIAL ORIFICE WITH VIBRATION

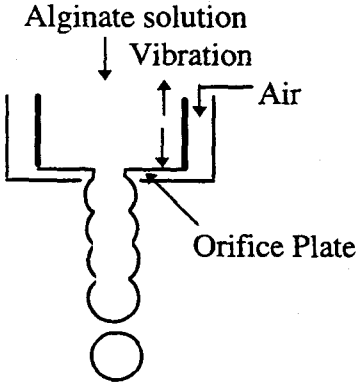

Overriding of the natural breakup of liquid jet with the help of an external vibrating source of constant frequency

Characteristics

1. Complex jet breakup process
2. Very Uniform droplets formed.
3. Large number of droplets produced.
4. Droplet size can be changed by varying frequency over a certain range.
5. Viscous polymer solutions can be easily extruded through small orifices due to low shear.
6. Very small droplets can be produced as coaxial air stream prevents droplet coagulation..
7. Good method for research and commercial applications especially aerosol production.

CHAPTER 3

3. POSSIBLE APPLICATIONS OF CALCIUM ALGINATE BEADS

Alginate beads, produced from an intracellular matrix polymer which exists naturally in marine brown algae and formed through the rapidly advancing technological processes of extrusion and emulsification described in Chapter 2 and in the present research, have diverse practical applications. In the biochemical industries, mammalian, plant, and insect cells have been immobilized and encapsulated in order to enhance productivity by increasing cell densities and product concentrations, a major area of concern in cell culture engineering.

Similarly, early stage biopharmaceutical companies and university research laboratories, despite the numerous questions (e.g. surface cell growth, membrane permeability and diffusion in animal cell encapsulation and immobilization), are investigating the use of polymer-encapsulated living cell transplants as potential therapies for human neurological and metabolic diseases such as Parkinson's, Alzheimer's, diabetes etc. With the potential U.S. market in these areas alone estimated by Goosen (1992) at more than $10 billion per year, naturally and regeneratively occurring polymers like alginate and gelatin are attractive candidate matrices for these techniques because of their accessibility and biodegradability (Schact, Vandichel, Lemahieu, De Rooze, & Vansteenkiste, 1993).

The use of polymer-based encapsulation technology also potentially avoids the controversial issue of grafting human fetal neural tissue (Aebischer, Goddard, & Tresco, 1992). In addition, biodegradable polymers are also clearly the materials of choice for parenteral sustained drug delivery. Considering the strengths and weaknesses briefly mentioned above, four applications of calcium alginate beads will be discussed in this chapter: encapsulation of animal cells, immobilization of enzymes, controlled drug release, and catalyst support in magnetically stabilized fluidized beds.

3.1 Encapsulation of Animal Cells

Despite the fundamental differences in applications of animal cells in medicine and biotechnology, Burgarski, Jovanovic, and Vunjak-Novakovic (1992) suggest that the requirements of both areas can be met by encapsulation of the cells. They further suggest that encapsulation can create an optimum environment that can be maintained for cell growth and product formation, or preservation of the cell morphology and functional response.

Properties of alginate beads meet the qualifying factors that an ideal polymer membrane system for tissue transplantation would require: nontoxic immobilization procedure, good control of membrane permeability and molecular weight cutoff, biocompatibility, optimum compliance with surrounding tissue, sterilizability, and indication of mechanical and chemical stability.

In addition, the encapsulating alginate membrane can be designed to exclude molecules beyond a given size. According to Bugarski et al. (1992), when the microencapsulated islets are used as implants, a membrane of about the same characteristics can provide maintenance of cell function and serve as an immunological barrier to the host immune system. This selectivity serves as an immune barrier by which tissue transplants can be successfully carried out in the absence of immune system suppression (Jaeger, Green, Tresco, Winn, & Aebisher, 1990).

Immobilization of animal cells using one of the currently available methods can mimic the *in vivo* environment of the cells' growth and function while protecting them from harsh surrounding conditions (Chang, 1988; Lim, 1983). Entrapment in alginate gel beads can provide a suitable confinement of cells within porous polymer and enable cell cultivation at high rates of cell growth and product formation (Lim & Sun, 1980).

According to Christenson, Dionne, and Lysaght (1992), these membranes can also provide adequate kinetics of response over a long period of time, alleviate symptoms in recognized animal models of disease, and allow retrieval of implanted tissue, which may be necessary in using this technology for human therapy.

Taken together, these characteristics support the process of encapsulation as a functional therapeutic modality in animal models of several common diseases. Discussed here are the two neurologically based diseases of Parkinson's and Alzheimer's and the metabolically based disease of diabetes.

3.1.1 Neurological Disorders

Neurotransmitters are small molecules in the 100-Da range that are normally released by specific neuronal cell-mediated contacts called synapses. The neurotransmitter release through synapses is responsible for the transmission of information within the nervous system (Aebischer et al., 1992). Whereas in some nervous system structures such as the cortex, the connection between the various neurons is highly specific, other brain structures are characterized by a highly divergent organization.

Deficiency of a specific neurotransmitter has been identified in various neurodegenerative diseases. Such diseases processes include Parkinson's (A lack of striatal dopamine following degeneration of the dopaminergic neurons of the substantia nigra which project to the striatum) and Alzheimer's.

3.1.1.1 Parkinson's Disease

Parkinson's disease is characterized by loss of dopamine-producing cells in the substantial nigra that project to the striatum, and its symptoms in experimental models may be alleviated by implants of dopamine-producing cells in the striatum (Winn et al., 1991). It has been suggested (Aebisher et al., 1992) that the transplantation of encapsulated, dopaminergic-releasing cells is a viable technique for the treatment of Parkinson's disease in humans. Encapsulated cell technology lends itself well to use for replacement of neurotransmitters, neurotrophic factors (Winn, Tan, Tresco, Sagen, & Aebischer, 1991; Winn, Tresco, Zielinski, Greene, Jaeger, & Aebisher, 1991). According

to Christenson, Dionne, and Lysaght (1992) PC12 cells, a rat cell line that releases L-dopa (Flanagan, Lavoie, Kaplan, Bell, Palmatier, Gentile, & Sanberg, 1991) and dopamine (Greene & Rein, 1977; Aebisher, Wahlberg, Tresco, & Winn, 1991) have been successfully encapsulated in microspheres (Winn et al., 1991) and macrocapsules (Aebisher et al., 1991).

The process for utilizing this technique would involve the delivery of neuroactive molecules through encapsulation technology . According to Aebisher et al., (1992) the value of this technique is founded on the following facts: a) PC 12 cells can survive encapsulation and neural transplantation procedures, b) encapsulated PC12 cells release dopamine *in vitro* both spontaneously and in response to chemical depolarization, c) well-preserved PC 12 cells can be observed in polymer capsules implanted in rats, guinea pigs, or nonhuman primates , PC 12 cells encapsulated in either thermoplastic-based systems or polyelectrolyte-based systems reduced rotational asymmetyry in experimental rat parkinsonism models, and d) microdialysis studies reveal that dopamine can be detected in the vicinity of cell-loaded capsules, whereas no dopamine was detected around empty polymer capsules, suggesting that dopamine is released from PC 12 cell-containing capsules *in vivo*.

Encapsulated PC12 cells alleviate the symptoms of Parkinson's disease in rodents (4 weeks) and primate (3 months) models of Parkinson's disease (Aebischer, Goddard, Timpson, Signore, Beuregard-Young & Rampone, 1990;Tresco, Winn, Zielinski, Jaeger, Greene, & Aebisher, 1991; Winn et al., 1991). Winn, Tan, and others (1991) also describe how microencapsulated bovine adrenal chromafin cells, a primary cell type that releases dopamine, epinephrine, and norepinephrine, have also shown efficacy in the rodent model of Parkinson's disease for up to 4 weeks. According to Christenson, Dionne, and Lysaght (1992), one benefit of macroencapsules over microspheres is that the entire implant containing the cells can be retrieved. In both the rodent and the primate models of Parkinson's disease in which encapsulated PC 12 cells showed efficacy, when the cells were removed, the Parkinsonian symptoms returned (primate, Aebischer, 1990; rodent, Tresco, et al, 1991). The explanted cells were alive and secreted dopamine in subsequent in vitro analyses. Microdialysis studies confirm that the encapsulated cell

implants secreted dopamine *in vivo* (Zeborn, Siebers, Zimmermann, Klenke, Bretzel, & Federlin, 1991).

The transplantation of autologous adrenal medullary cells in humans suffering from Parkinson's disease has also been reported to ameliorate the disease state (Goetz, Olanow, Koller, Penn, Cahill, Morantz, Stebbins, Tanner, Klwawans, Shannon, Comella, Witt, Cox, Waxman, & Gauger, 1989; Madrazo, Drucker-Colin, Diaz, Martinez-Mata, Torres, & Becerril, 1987). Thus, several forms of transplantation (and perhaps some day that of individual cells) represents a very promising avenue for the treatment of various neurological diseases where the deficiency of a specific molecule has been identified.

3.1.1.2 Alzheimer's Disease

A rodent model of Alzheimer's disease is induced by lesioning the fimbria-fornix in rats, leading to a decrease of choline acetyltransferase (chAT) expression in septal cells. The symptoms include deficits in learning and memory, similar to Alzheimer's disease in humans. Implantation of encapsulated rat fibroblasts genetically engineered to produce nerve growth factor prevented the decrease in chAT expression, as analyzed histologically 2 weeks after implantation (Hoffman, Breakefield, Shrot, & Aebisher, 1991). Histological analysis also showed that the capsules contained intact fibroblasts and that the host tissue reaction to the capsule was minimal.

For humans, it has been suggested (Knusel, Winslow, Rosentahl, Burton, Seid, Nikolics, & Hefti, (1991) that local delivery of these neurotrophic factors could be achieved by the transplantation of the polymer-encapsulated cells which release them (for nerve growth factor (NGF) and Brain-derived neurotrophic factor (BDNF)) in Alzheimer's cases, potentially also ciliary neurotrophic factor (CNTF) in amyotrophic lateral sclerosis or Lou Gehrig's disease (Aebischer, Goddard, & Tresco, 1992).

3.1.2 A Metabolic Disorder--Diabetes

The major obstacle to islet transplantation for treatment of insulin-dependent diabetes mellitus (IDDM) is the rejection of the transplanted tissue by human immune mechanisms (Bugarski et al., 1992). One way to overcome this problem is to introduce a semipermeable physical barrier between the transplanted islets and the host immune system.

Several methods have been developed to microencapsulate islets of Langerhans enabling them to remain viable and protected within a semipermeable membrane (Brunner & Schmidt, 1981; Goosen, O'Shea, Gharapetian, & Sheng, 1985; Lim & Sun, 1980). Lim and Sun (1980) successfully microencapsulated islets using an alginate-PLL procedure and demonstrated that the encapsulated islets could restore normoglycemia in diabetic rats when injected into the peritoneal cavity.

The use of biocompatible microcapsules which retain the transplanted cells in a non-immunogenic membrane and provide graft protection can potentially overcome the problem of immunological rejection (Brunner & Schmidt, 1981; Chang, 1988; Lim, 1983). And the ability of microcapsules to provide an immunological barrier to the implanted islets of Langerhans was demonstrated in conjunction with the normalization of blood glucose in rat allografts (Lim, 1983).

The microencapsulated islets of Langerhans, for instance, remain viable and preserve cell morphology and functional activities as well as the insulin response to glucose stimulation. Glucose and insulin pass freely through the membrane, while the components of the immune system are excluded due to their higher molecular weights (~150 kDA) (Bugarski et al., 1993).

Burgarski et al., (1992) also reported the limited success that has been achieved in experimental animals using hollow-fiber devices. Lacy (1995) expanded the implant approach by suspending the islets in gelled alginate within the hollow-fiber vessels. Implants put into the abdominal cavity or under the skin then maintained normal blood sugar levels in mice throughout a year of observation. The animals tolerated the implants well, generating little fibrous tissue around the outer surface of the fine plastic tubes.

3.2 Immobilization of Enzymes

Cells may be immobilized by attachment or confinement. In the first case, the cells adhere to a surface (Fuller & Bartlett, 1985) or one cell to another (Bitton & Marshall, 1980). Attachment surfaces include the interstices of fibrous materials, including hollow fibers (Shuler, 1981) or porous materials such as polyurethane foam (Bitton & Marshall, 1980). Cells can be attached by natural or induced self-adhesion, or by chemical bonding (Kolot, 1988). Poncelet De Smet, Poncelet, and Neufeld (1992) discussed how adsorption and attachment of cells to carrier surfaces, while inexpensive and simple, are dependent on the cell wall properties.

In the immobilization technique, confined cells are physically restrained within or by means of a solid or porous matrix, such as a stabilized gel. In the case of animal cell immobilization, these techniques are in an early stage of development, while widely used for immobilization of other cell types.

The different procedures and variety of materials provide a high degree of versatility in the selection of a suitable immobilization technique dependent on the particular application (Poncelet De Smet et al., 1992). For example, Santos, Marchal, Tramper, and Wijffels (1996) reported a model that had been developed to describe growth of nitrifying and denitryifying bacteria co-immobilized in double-layer gel beads.

Historically though, Mosback and Mosback (1966) reported the immobilization of cells by entrapment in cross-linked polymeric gels for continuous production of biochemicals by enzymatic conversion. Chibata, Yamada, Wada, Izuo, & Yamaguchi (1974) succeeded in industrializing the continuous reduction of L-aspartic acid, and later reported the production of L-malic acid and L-alanine with immobilized cells (Yamamoto, Tosa, & Sato, 1976). In 1979, Brodelius, Deus, Mosback, & Zenk extended the use of cell immobilization to the plant kingdom, for the production of secondary metabolites. In 1980, Nilsson and Mosback succeeded in immobilizing animal cells by adsorption on gelatin and chitosan beads and by entrapment in alginate and agarose.

More recently, King and Goosen (1992) have reported that materials such as polyamindes, polyacrylates, albumin, Eudragit RL, alginate, CM-cellulose, K-

carrageenan, and chitosan have been employed to immobilize cells. Among these, polymers such as alginate, CM-cellulose, K-carrageenan, and chitosan, which come from natural sources, are of particular interest because they are of low cost and naturally regenerable. From this group, alginate is one of the most popularly used gel matrix-forming materials (King & Goosen, 1992).

Particularly, the gelification of sodium alginate in presence of calcium ions has been utilized for the immobilization of drugs, biocatalysts and pesticides (Schacht, Vandichel, Lemahieu, De Rooze, & Vansteenkiste, 1993). Schacht et al., reported that when placed in water Ca-alginate gels release the enclosed active agent at a rate dependent on the water solubility of the agent. It has also been suggested that treatment of Ca-alginate gels with cationic polymers, e.g. polyamines such as poly (ethylene imine) (PEI) or polylysine, leads to formation of surface coated gels which have superior stability properties. This approach has been successfully applied for the immobilization of viable cells (Schacht et al., 1993). One of the most appropriate uses has been for the immobilization of enzymes.

Immobilized in the manner just described, enzymes have a number of qualities that make them more versatile than mobile enzymes. The chemical properties of an immobilized enzyme depend on the method of immobilization and the support (Brown, 1972; Capet-Antonini, Trimard, & Tamerasse, 1973; Flynn & Johnson, 1977; Herrin, Lawrence, & Kittrell 1972; Manecke, Gunzel, & Foster, 1970; Svenson & Andersson, 1977;). Immobilized enzymes are usually more stable to fluctuations in pH and temperature than their soluble counterparts. Further, when suspended in water, most of these insoluble enzyme derivatives are stable for months, and can be used many times as a catalyst.

It is also benefitial that the process of recycling immobilized enzymes reduces costs, whereas the soluble counterparts have continued to be quite expensive. Immobilization is still too expensive compared with that for soluble enzymes. This is primarily due to the fact that there are no commercially viable encapsulation or immobilization prcesses which can produce particles of controlled parameters. The

commercial use of immobilized glucoamylase on inorganic supports appears to have some advantages, and a number of inorganic supports have been investigated.

Considering the qualities producible in immobilized enzymes, there are a number of practical applications to be considered: conversion of starches to glucose, hydrolization of starch, immobilization of lactase, immobilization of penicillin acylase, and immmobilization of enzyme aminoacylase, as well as involvement with various forms of commercial processing of food and drugs.

To combat the poor quality of syrup produced by side reactions during acid hydrolysis of corn and other vegetable starches, immobilized glucose isomerase can be used for the production of an alternative sweetening agent, high fructose corn syrup (HF CS). Immobilization is also appropriate for converting lactose into glucose to be used as a food sweetener.

Immobilized lactase can also be used to hydrolyze lactose in milk. This is of particular benefit where there is a high incidence of lactose intolerance among particular population groups in areas of Asia, Africa, Latin America, and the U.S. Midwest. Reduction of lactose concentration in milk may encourage more widespread use.

Immobilized enzyme systems can also be used to produce the side chain of penicillins which is subsequently deacylated to produce 6-aminopenicillanic aid. The resultant 6-aminopenicillanic-acid, which is used to produce many antibiotics, is a product stable under a wide pH range since the catalyzed reation produces hydrogen ions and thus acidity.

The Aminoacylase enzyme is another industrial application for the immobilization process. In the case of Aminoacylase, L-amino acid can be separated from unreacted D-acylamino acid due to the different in solubility of the two compounds; and the D-acylamino acid is racemized and the enzyme treatment repeated. The use of immobilized aminoacylase improves this process since the enzyme does not have to be removed by a change in pH or heat treatments. It is also possible to regenerate the catalyst by adding fresh, soluble aminoacylase. Considerable savings have been realized form the use of immobilized amino-acylase by reducing labor and enzyme cost. In addition, the yield is higher and the product cleaner.

Additional commercial uses for enzymatic immobilization include processes associated with food and food products. The technological processes include the immobilization of cells when the cost of enzyme extraction and purification is prohibitive or when the enzyme molecule, removed from its native environment, is unstable and the immobilization of proteases is to be used to solubilize, texturize, and increase the digestibility of proteins.

Furthermore, immobilized pepsin, papain, and rennin can be used for the coagulation of skim milk in the manufacture of cheese as well as for the treatment of milk with immobilized trypsin (Hicks, 1974). This process enhances shelf life and prevents loss of flavor of such dairy products(Lee, Senyk, & Shipe, 1975).

The utilization of immobilized enzymes have also been investigated in the process of converting large quantities of cellulose in the biomass into glucose (Davis, 1974; Hudson, 1975). Glocose syrup could be produced in large volume from this source for use in fermentation to food and food products.

There are also a number of drug preparation based on fermentation process, where growing microbes supply the enzymes to convert the starting material. Fermentations are generally somewhat inefficient because of the large quantities of microbes that must be discarded and because nutrients and a ready carbon source must be available for microbial growth. Even the immobilization of whole cells reduces waste since the cells are usually not viable and thus do not require nutrients and a carbon source. If the proper enzyme or enzymes could be isolated and immobilized, the process could be performed cleanly, eliminating undesirable by-products. Many steroids can be transformed in this manner.

Maugh (1984) also notes the immobilization of heparinase as being considered for a potential medical application. Heparin is an anticoagulant used in conjunction with a heart-lung machine. Used during surgery, the patient's blood flows freely thought the machine and back. However, the presence of heparin in the patient can cause extensive internal bleeding. Passing the blood over immobilized heparinase before returning it to the patient would eliminate this problem. Similar systems could be developed to hydrolyze drugs in cases involving drug overdose.

Additional applications of immobilized enzymes have been suggested but cannot be proven practical without further research. For example, in the treatment of many diseases due to the deficiency of one or more enzymes, an immobilized enzyme could be positioned within an area of the body and be able to function over a long period of time. Treatment of a patient with an enzyme immobilized on a support rather than with the soluble enzyme may also reduce immunoresponse.

On a broader scale, research is being done on the use of immobilized enzymes in fuel cells and the utilization of solar energy. The use of enzymes in fuel cells should facilitate the preparation of stable cells based on reactions that would take place in the absence of an enzyme at elevated temperatures. These fuel cells can also be employed in the preparation of biochemicals. The conversion of solar energy into chemical energy by use of enzyme catalysts is actually somewhat similar to the natural process of photosynthesis.

3.3 Controlled Drug Release

Microcapsules and microspheres are very small particles (in the 1-500 μm size range) appropriate for use as carriers of drugs and other therapeutic agents. The term 'microcapsule' is commonly used for those systems having a definite coating or shell encapsulating the contents in the form of a particle. The term 'microsphere' describes a "monolithic spherical structure with the drug or therapeutic agent distributed throughout the matrix either as a molecular dispersion or as a dispersion of particles" (Whateley, 1992, p. 53).

Due to their methods of preparation and fliud properties, Microcapsules tend to be difficult to prepare in the lower end of the size range indicated above. Therefore, they are restricted in the routes of administration for which they are suitable. The drug carrier needs to be treated as a drug itself in terms of the safety, biocompatibility and lack of toxicity of the polymer and its degradation products.

Moreover, according to Zia, Needham, and Luzzi (1993), the system for a particular drug should, at the very least, not impugn the stability of that drug, and in the best of all possible worlds, should enhance the availability of the drug and protect the drug from attack by other materials. The delivery system should not lend any toxic product or potential toxic product or by-product to the dosage form.

In any case the delivery system may be biodegradable and should always be biocompatible and nonimmunogenic. The system should be engineeered and constructed so that drug is released at an appropriate rate, a rate that considers the kinetics of absorption, utilization and elimination. Biodegradable polymers like alginate are clearly the materials of choice for parenteral sustained drug delivery, and some of the drugs which require special drug delivery dosage forms include epidermal Growth Factor, Interferon gamma, Insulin Growth Factor, and Wound healing factor.

Whateley (1992) notes that microcapsules do, however, have wide application for the oral delivery of drugs for the following reasons:

(a) sustained release is possible; the coating acts as a barrier to drug release and various mechanisms of release are possible,

(b) taste masking (e.g. for an anti-malarial drug, chloroquine),

(c) protection of drug contents from moisture and/or oxygen,

(d) to allow the combination of incompatible constituents by the protection of one or more components by microencapsulation.

There are several applications for drug loaded biodegradable microspheres (Whateley, 1992), Two of these applications will be briefly discussed here: intra-arterial administration for tumor reduction and oral delivery of vaccines.

Regional chemotherapy is an attempt to increase the therapeutic index of the drug by increasing the concentration of the chemotherapy drug within the organ with the metastatic deposit. Delivery of microspheres loaded with the drug in this manner has a number of advantages. First, there is a reduction in side effects because system levels are low. Second, the embolic effect of the microspheres increases retention of the drug at the site of release. Third, the reduced oxygen levels which follow the release, may enhance the therapeutic efficacy of the drug.

In the case off vaccines, there is increasing evidence that small microspheres can be absorbed from the gastro-intestinal tract to a limited extent, probably via the Peyer's patches of the intestinal walls. Such an uptake can be adequate to generate an immune response and oral vaccines have been developed, according to Whateley (1992) for malaria,and staphylococcal enterotoxin B Toxoid.

3.4 Catalyst Support in Magnetically Stabilized Fluidized Beds

The feasibility and effectiveness of most biochemical, biomedical, catalytic, and non catalytic applications in multiphase processes (gas-liquid, gas-solid, liquid-solid, gas-liquid-solid) hinges on the efficiency and intensity of contact between phases. Interphase mass transfer is the rate limiting step in most liquid-solid catalytic, and non-catalytic reaction processes. Fluidized bed, spouted bed, packed bed, mowing packed bed, and trickle bed are some of the contacting schemes that are often used in multiphase operations. Their implementation is often specifically tailored toward particular applications. Fluidized beds, for example, are widely used contacting devices in biochemical and biomedical applications where liquid phase is laden with biological debris and/or exhibit non Newtonian characteristics.

Magnetically Stabilized Fluidized Bed (MSFB) is one of the most recent and novel chemical engineering development in the area of fluid-solid contacting operations. It combines some of the best characteristic of fluidized bed with excellent efficiency of the fixed bed in mass transfer, heat transfer, and chemical conversion. Aside from being an excellent liquid-solid contactor in usual operating environment MSFB can also successfully function under microgravity conditions. MSFB uses ferromagnetic material immobilized in a polymer matrix. Many researchers have used calcium alginate as the immobilizing carrier (Al-Mulhim, M., and Jovanovic, G. N.,(1994)). Thus, ferromagnetic material and catalysts or cells or enzymes are mixed in sodium alginate solution to form a slurry which is extruded into droplets. These are crosslinked with calcium ions to give a composite alginate bead. When operating a MSFB, these fluidized particles experience an additional drag force which is

created by an external magnetic field. The fluidized bed characteristics can be changed and tailored according to need by changing the intensity of the magnetic field.

3.5 Conclusion

It can be concluded that a process to form calcium alginate beads of controlled parameters has a very strong commercial potential. The possible applications of these polymer beads are innumerable. One of the major requirements of all these applications are that the alginate beads should be uniform in size. Uniformity of size lets the researchers model and predict the behaviour of a particular system. Diffusion, mass transfer and other properties which change with the size of the alginate beads can be easily modelled if the beads are monodisperse. Also, another major requirement is to be able to produce alginate beads of smaller size. Most of the researchers have used alginate beads of 0.5 mm to 2 mm. Smaller beads have lesser diffusion resistance and greater mass transfer coefficients. Also smaller beads help in reducing the size requirements. An important example is the encapsulation of islets of Langerhans in alginate beads. About 80,000 cells are needed by a healthy human individual, to avoid insulin deficiency and function normally. With the current use of 500 micron diameter beads to encapsulate these cells, it requires a lot of space to make an artificial pancreas. It should be noted here that the cell loading per bead is limited by diffusion and mass transfer. If these beads are reduced to about 50 microns in size, the volume of the artificial pancreas decreases by a factor of a 1000. Also the surface available for each cell increases thus increasing mass transfer.

In our study, we try to solve these problems by using a process to produce calcium alginate beads which are very uniform in size. The size of the beads can also be varied conviniently according to the requirement of each application.

CHAPTER 4

4. EXPERIMENTAL PROCEDURES

4.1 Alginate Bead Generators

This section describes the development, design and construction of oscillating capillary (orifice) apparatus to generate uniform droplets. The initial idea was to use a co-axial shearing fluid vibrating orifice to produce alginate droplets which could then be gelled with polyvalent ions. Due to the complexity of the system, it was thought that the phenomena of vibration and that of the co-axial shearing fluid should be separated and studied individually. A lot of work has already been done by previous investigators on co-axial shearing systems for producing alginate droplets, but little or no work has been done on a vibrating orifice system to produce uniform alginate droplets. With the elimination of the shearing fluid, a better understanding of the relationship between frequency of vibration, droplet diameter and the uniformity of the droplets can be obtained. Following this line of thought a simple droplet generator was developed which uses vibration only. this generator was then modified several times based on its operation and sensitivity.

4.1.1 Experimental Setup and Procedure

Although four different types of droplet generators are described in this study, the basic process of producing alginate beads remains the same. The experimental apparatus design is shown in Figure 4.1. It consists of a pressure vessel which contains the algin solution in which nitrogen pressure is used to feed the algin solution to the bead generator. The bead generator, could be any of the four types discussed later in this section. The signal from a function generator is amplified using an amplifier. The input signal is then fed to the vibrating device and is measured using a HP-1741A Oscilloscope. These vibrations cause the break-up of the liquid jet exiting the droplet

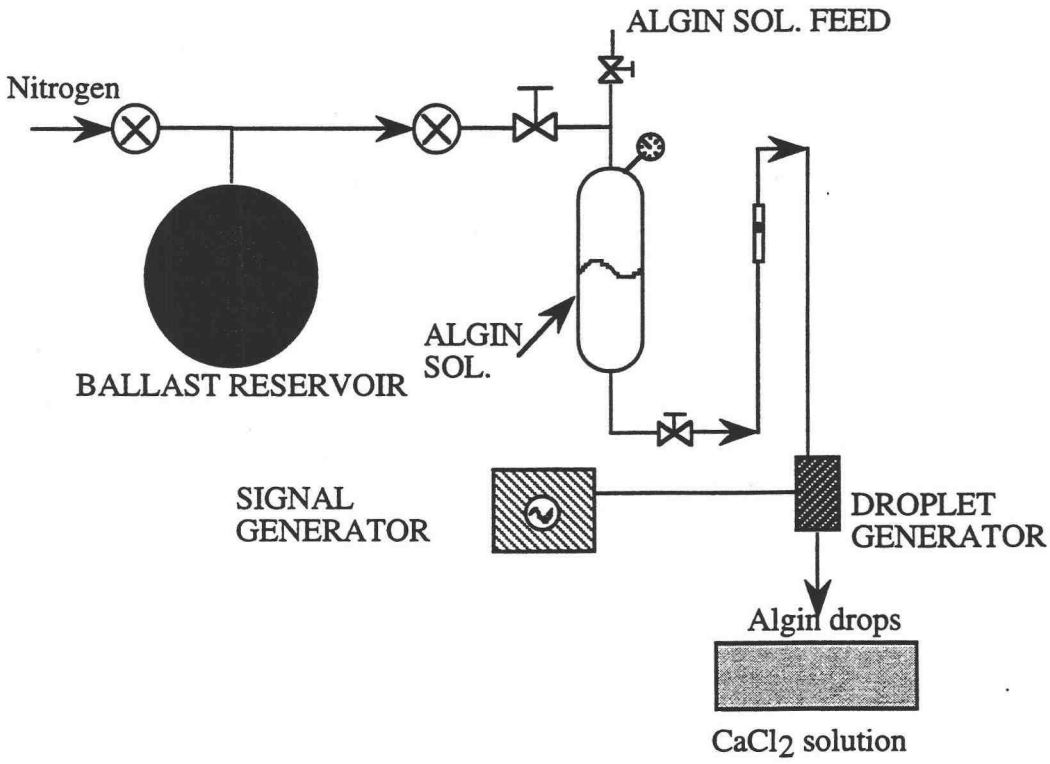

Figure 4.1 Schematic of process to generate algin beads

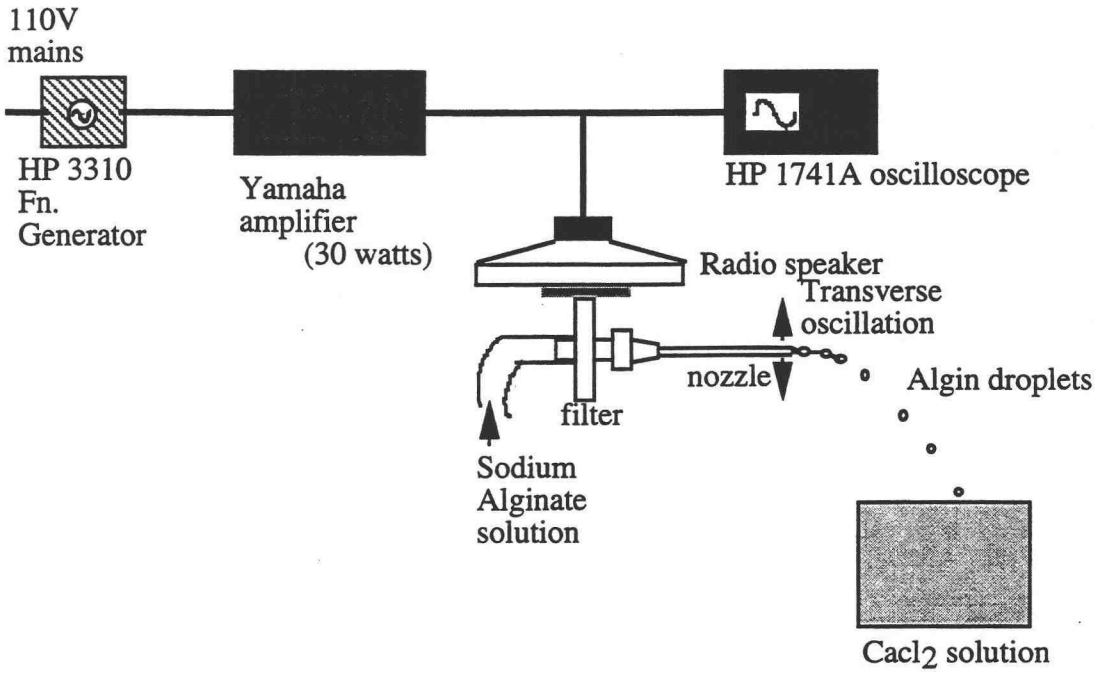

Figure 4.2 Transverse vibrating droplet generator

generator. The frequency can be fine-tuned to cause a uniform break-up of the liquid jet. The droplet formation (break-up) process can be observed by using a strobe light to visually freeze the motion. In this way, a qualitative analysis of the break-up process (single drop + satellite drops; extending liquid jet stream; etc.) can be made.

4.1.2 Transverse Vibrating Capillary Droplet Generator

In order to understand the effect of vibration necessary to stimulate the cylindrical liquid jet break-up, an apparatus was assembled which uses an audio speaker to transmit vibrations to the liquid cylinder. The design of the droplet generator is shown in Figure 4.2. It consists of a stainless steel in-line filter holder, hypodermic needle and an audio speaker. The signal from the HP-3310B Function Generator is amplified using a Yamaha 30 watt /channel amplifier. The input signal to the speaker is measured using a HP-1741A Oscilloscope. The vibrations from the speaker are transmitted to the filter holder and to the needle in such a way as to cause a deflection in the needle perpendicular to the flow direction. These vibrations cause the break-up of the liquid jet exiting the needle. The frequency can be fine-tuned to cause a uniform break-up of the liquid jet. This simple design allows the use of several different size needles to expand the range of droplet size as the needles are very easy to replace. Also, with this current experimental setup it can be visually determined if the droplets are uniform. The droplets which differ in sizes fall at different lengths from the needle. One of the biggest disadvantage lies in the difficulty of pushing viscous liquids through the needles.

4.1.3 Axial Vibrating Orifice Droplet Generator

The difficulty of pushing viscous liquids through needles was solved by adapting the previous apparatus to accept an orifice plate instead of needles. Also the vibration in this setup was in the axial direction rather than in the transverse direction. The design of

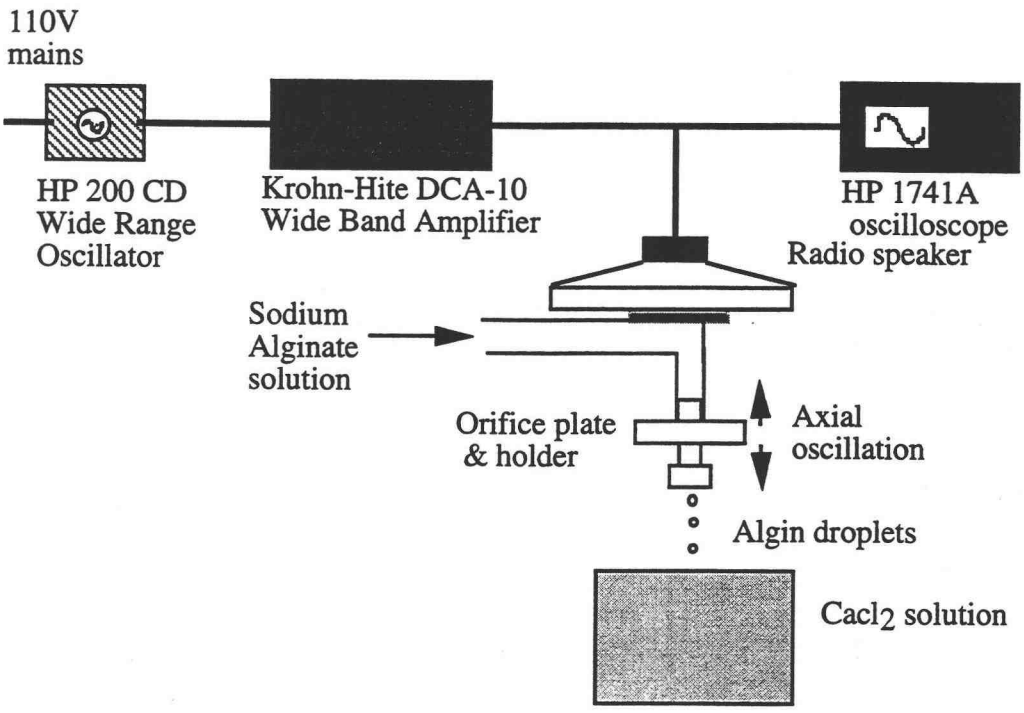

Figure 4.3 Axial vibrating droplet generator

the droplet generator is shown in Figure 4.3. It consists of a stainless steel in-line filter holder, stainless steel orifice plate & holder and an audio speaker. The signal from the HP 200 CD wide range oscillator is amplified using a Krohn-Hite DCA-10 wide band amplifier. The input signal to the speaker is measured using a HP-1741A Oscilloscope. The vibrations from the speaker are transmitted to the orifice plate holder in such a way as to cause deflection in the same direction as the flow of the liquid stream. These vibrations cause the break-up of the liquid jet exiting the orifice. The frequency can be fine-tuned to cause a uniform break-up of the liquid jet. The adaptation of the orifice plate helped in forming liquid jet from highly viscous alginate solutions. Also, the use of a different function generator and amplifier gave more control over the range of the amplitude of vibration.

4.1.4 Axial Vibrating Diaphragm Droplet Generator

It should be noted that in the previous two types of generators, vibration was transmitted to the whole apparatus. Sometimes this resulted in the dampening of certain frequencies. This problem was overcome by designing an axial vibrating diaphragm droplet generator. As the name suggests, it consists of a stainless steel assembly which has a diaphragm covering a cavity. The cavity is fed with alginate solution and the inlet pressure of this solution helps in forming a liquid jet at the orifice in the middle. The diaphragm is vibrated with a audio-magnetic coil. The diaphragm then passes the vibrations through the algin solution in the cavity to the exiting jet. These vibrations cause the break-up of the liquid jet. The design of the droplet generator is shown in Figure 4.4. A variety of polymer films were tested as the material of the diaphragm. Of these, Kapton worked best. Kapton polyimide film possesses a unique combination of properties which make it very suitable for this operation. It is synthesized by polymerizing an aromatic dianhydride and an aromatic diamine. The film has excellent chemical resistance. In our experiments we used the Kapton HN film which had a nominal thickness of 200 gauge. This was able to withstand the pressure of the fluid in

the cavity and the repetitive vibrations. Also the transmittance of vibrations from the diaphragm to the liquid jet was very good as there was less damping of vibration which occured in the previous droplet generators where the full apparatus assembly was vibrated. This was possible by making the fluid cavity very large in diameter and small in depth. Different size orifice plugs can be used in this apparatus. This provided a great deal of flexibility in the operation of this generator.

4.1.5 Two Fluid Vibrating Piezoceramic Droplet Generator

When production of alginate droplets smaller than 100 microns is needed, the frequency range requirements far exceed those provided by an audio speaker. These high frequency vibrations can be achieved using a piezoceramic crystal. Also a dispersion fluid is needed to disperse the droplets which otherwise would coagulate with each other to produce non-uniform droplets. The design of this droplet generator is shown in Figure 4.5. Basically, the liquid polymer is fed at a known rate through an orifice held in place in a stainless steel cup by a Teflon O-ring. The cup is bonded to a piezoelectric transducer which, when excited by the correct ultrasonic frequency F, causes the cylindrical liquid jet to become unstable and disintegrate into droplets. The detachment of the droplets is facilitated by a co-axial shearing fluid (dispersion fluid) which may be either gas or liquid.

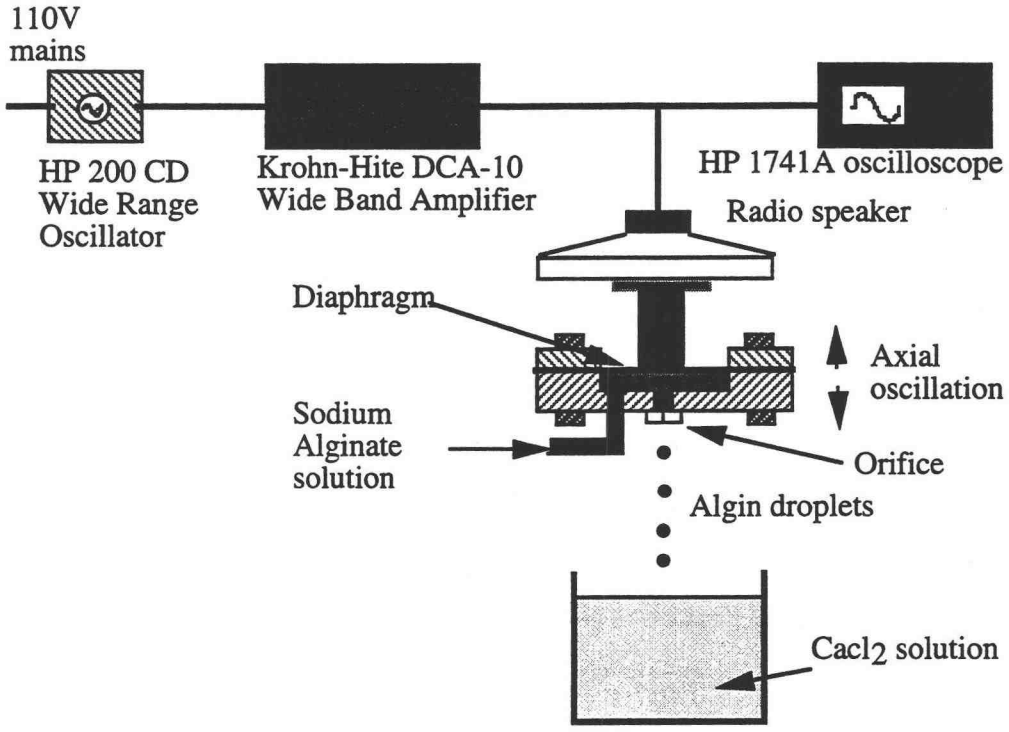

Figure 4.4 Axial vibrating diaphragm droplet generator

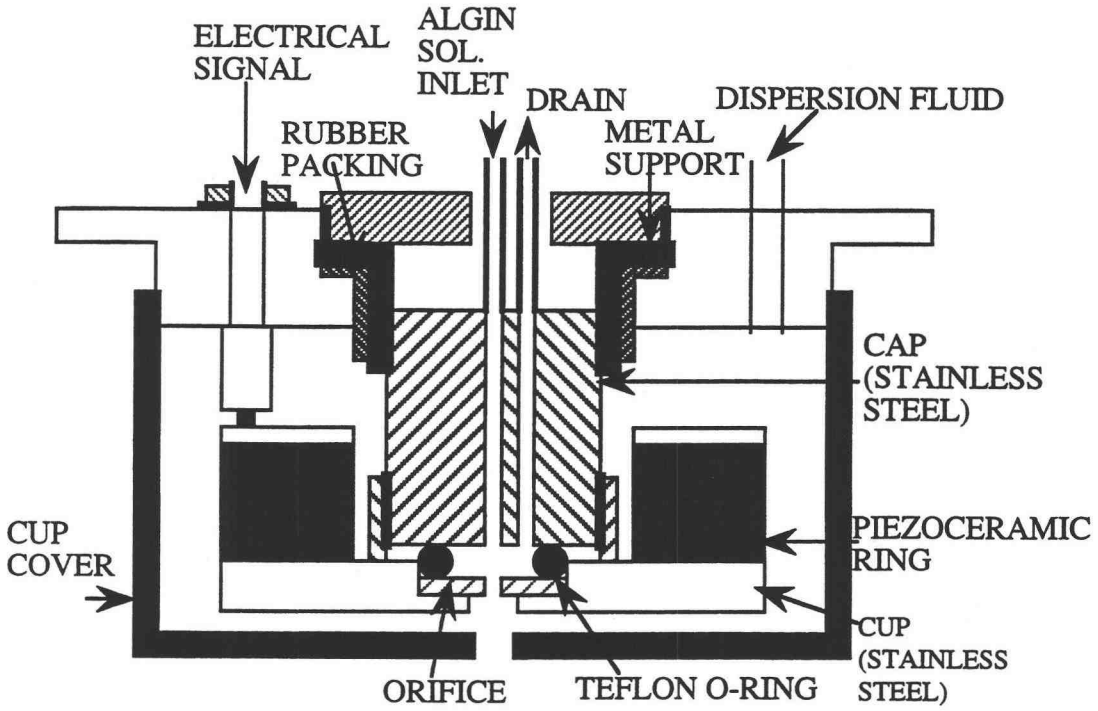

Figure 4.5 Two fluid axial vibrating piezoceramic droplet generator

4.2 Experimental Procedures

4.2.1 Sodium Alginate Solutions

Keltone LV (by Kelco Co.) was the sodium alginate used throughout the bead formation experiments. The suffix LV stands for "Low Viscosity" meaning that this particular algin solution has a lower viscosity at the same concentration, than its HV (high viscosity) counterpart. All solutions were made by dissolving a known amount of Keltone LV in distilled water. When dissolved in distilled water, alginates form smooth solutions having long flow properties which are dependent on both physical and chemical variables.

Keltone LV is hydrophilic in nature. A single granule of this material will wet immediately when put in water and will dissolve very rapidly. But when a mass of granules is put into water without agitation sufficient for complete dispersion, clumps of granules will be formed. The surfaces of these clumps solvate, forming a layer which prevents wetting of the interior of the clump. Thus time for solution in this case depends on the rate of solution from the exterior surface of the clump. This usually takes a very long time depending on the size of the clump. Thus uniform dispersion (separation of individual granules) is the key to the rapid preparation of Keltone LV solutions. Various methods of mixing can be used to prepare algin solutions. In our experiments we used the concept of high-shear mixing. Very good dispersion is obtained with a high-shear mixer which gives a good vortex. For low concentrations of Keltone LV, a magnetic stirrer usually suffices. But for higher concentrations, an air driven stirrer was used. The agitator should be placed off center to obtain maximum turbulence at the lower portion of the vortex. The Keltone LV powder is slowly sifted onto the upper portion of the vortex so that it falls as individual granules which are then wetted rapidly as they travel to the center of the vortex. For higher concentration solutions, the addition of the powdered Keltone LV should be complete before thickening destroys the vortex.

In our experiments 1%, 1.5% and 2% (w/v) Keltone LV solutions were formed. For example, in the case of 1% (w/v) Keltone LV solution, 10 grams of Keltone LV powder was weighed out and then added to stirred distilled water. Also, a few drops of formalin (40% solution of formaldehyde in water) were added to stop any microbial growth when these solutions are stored over a long period of time. Stirring time for all the solutions was at least three hours to ensure complete mixing for obtaining a homogenous solution.

4.2.2 Experimental Procedure for the formation of alginate droplets.

The design and operating principle of the three droplet generators used in this work has been explained in section 4.1. Except for the difference in construction of the three droplet generators, the operation procedure for each of them is very simple and similar. The Keltone LV solutions are prefiltered through a 5 micron filter. This is very important as it eliminates any particles which may clog up the orifice of the droplet generator. The prefiltered solution is then fed to a stainless steel pressure vessel where it is pressurized to 100psi. The pressurized solution then passed through an inline needle valve. The needle valve which has an inbuilt micrometer, helps in controlling the flow rate of the solution being fed to the droplet generator. This pressurized feed solution passes through the orifice in the droplet generator and forms a jet. The jet is then superimposed with vibration of different frequencies. A typical experimental run consisted of keeping the flow rate constant and varying the frequency to obtain uniform droplets. The size of these droplets varied as the frequency of vibration was changed. Then the flow rate was increased or decreased and held constant, while frequency was varied again. The minimum flowrate used was that required to form a jet while the maximum flowrate used was the flow rate above which the beads became splattered and non-uniform. The frequency range explored was the range of frequencies which when individually superimposed on the liquid jet gave uniform droplets.

4.2.3 Bead Collection Technique

The alginate droplets were allowed to fall into a beaker of 0.1 M calcium chloride solution. The calcium ions in the solution crosslink the alginate droplets to form gel beads. At high jet flow rates, the calcium chloride solution was stirred to form a vortex and the droplets from the jet were collected along the surface of the vortex. This reduced the deformation of the beads which occur when the alginate droplet hits the surface of the calcium chloride solution at high velocity. A jet of alginate solution may break-up into a satellite and a bigger droplet or uniform droplets. It is noticed that two droplets may merge after a certain distance from the orifice. All the samples were collected above this merging point. Each sample consisted of 1000 to 2000 beads.

4.2.4 Bead Sizing Technique

The accurate measurement of beads is very important to correlate the size of the beads to various operating conditions and solution characteristics. In our technique, a minimum of 50 beads obtained randomly from a sample were photographed using an optical microscope. The objective used was either 4x or 10x. The eyepiece was either a 2.5x or 4x. The camera was mounted on the microscope using a T-mount. A 400 ASA black & white film was used to take the photographs. The film negatives were developed in the dark room using standard developing techniques. These negatives were then scanned using a HP Scanner. All the scans were enlarged 600 times. Then each alginate bead was measured using a high precision ruler.

A similar procedure was also carried out using a 1 mm micrometer slide. This was used to calibrate and measure the actual bead sizes. These were in agreement with the bead sizes calculated by taking the magnifications and enlargement into account.

4.3 Rheological Measurements

As reported earlier, sodium alginate was the polymer used in all the experiments with droplet generator to form droplets which were crosslinked subsequently with calcium ion in calcium chloride solution. The droplet formation involves the formation of a jet through an orifice and superposition of vibration in order to control the break-up the jet. Both of these fluid flow phenomena depend on the properties of the liquid used to form the droplets. Specifically, the viscoelastic properties of the liquid play a major role in determining the break-up dynamics of the jet. Therefore, it is very essential to determine the viscoelastic behavior of the liquid. This was accomplished by using the rotational Bohlin Constant Stress Rheometer (Model CS-50) and Clark High Shear Capillary Viscometer.

4.3.1 Introduction

Rheology is the science of deformation and flow of material. It deals with the response of material when subjected to forces over different time periods. The response of the fluid is dependent on the molecular structure, molecular weight, and molecular arrangements. It is known that ideal gases behave differently from non-ideal gases, while gases behave differently from liquids, and purely viscous fluids behave differently from viscoelastic or elastic liquids.

Based on the response to deformation, fluids can be classified in two broad categories, namely Newtonian and non-Newtonian. Fluids having linear response to stress (σ) are called Newtonian fluids. These fluids are related by the Newton's law

$$\sigma = \eta \dot{\gamma} \tag{4.1}$$

where η is the viscosity and $\dot{\gamma}$ is the shear rate. Fluids which do not follow the Newton's law are called non-Newtonian and these fluids are described by different stress-shear equations.

Polymer solutions like sodium alginate (Keltone) in DIW are fluids which exhibit a behavior between that of a purely viscous fluid and a purely elastic solid. This intermediate behavior is descried as viscoelastic (for more information see Ferry, 1980). Viscoelastic materials exhibit elastic and viscous (damping) response to a deformation. The elastic component is in-phase with the stress imposed while the viscous (damping) component is out-of-phase.

Understanding the rheology of the material is an essential prerequisite for using it in any application and processing. The rheological properties of any material can be studied using a rheometer. There are two main types of rheometers, capillary and rotational. For this research a rotational rheometer, Bohlin Constant Stress Rheometer (Model CS-50) and a capillary rheometer, Clark High Shear Capillary Viscometer were used to study the rheological properties of the alginate solutions and its gels. The Bohlin CS-50 Rheometer was used to perform low shear rate and dynamic experiments while the Clark High Shear Capillary Viscometer was used to measure fluid properties at high shear rates.

A controlled stress viscometry test is commonly used to study the viscosity - shear rate relationships. It provides very important information on how the viscosity changes with changing shear rate. In the droplet generator the alginate solution is pressurized through an orifice to form a jet. As, the solution passes through the orifice, it experiences shear. With increasing jet velocity, the shear rate increases and therefore the apparent viscosity changes. Thus knowledge about viscosity - shear rate relationships is helpful in understanding the fluid flow dynamics.

A dynamic oscillatory test is used to study the linear viscoelastic properties of a polymer solution. When the stress to strain ratio is time dependent only and does not depend on the magnitude of the stress, then a polymer is in a linear viscoelastic region. This is possible when the deformation rate is infinitesimal [Ferry, 1980]. This test involves the measurement of the elastic and viscous moduli of the polymer solution or gel as it undergoes oscillatory shear. Such a test provides a good understanding of the viscoelastic properties of the material under consideration.

4.3.2 Controlled Stress Viscometry

In controlled stress viscometry test, a sample of fluid within the measuring system is sheared between two rigid boundaries under the action of an applied shear stress, σ. This produces a distribution of fluid velocity tangential to the walls of the measuring system which varies across the gap. This principle of controlled stress viscometry is shown in Figure 4.6.

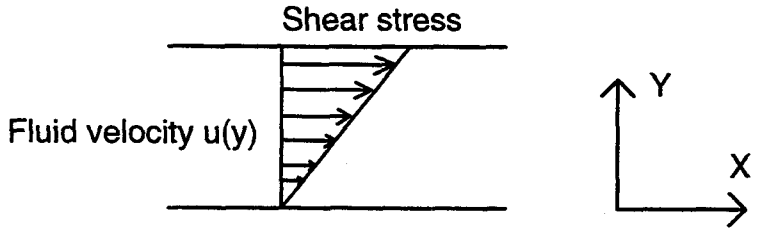

Figure 4.6 Newtonian sample under shear

The rate of change of velocity u in the y direction is called the shear rate, $\dot{\gamma}$ and is defined as follows

$$\dot{\gamma} = du/dy \tag{4.2}$$

The Newtonian viscosity of the fluid η can then be calculated from the following equation

$$\eta = \sigma/\dot{\gamma} \tag{4.3}$$

The controlled stress rheometer imposes a known torque T on the measuring shaft and detects the rate of change of angular deflection, $\dot{\theta}$. These quantities are related to the

shear stress, σ and the shear rate, $\dot{\gamma}$ via the measuring system constants C_1 and C_2 which take the different measuring system geometries into account.

$$\sigma = C_1 T \tag{4.4}$$

$$\dot{\gamma} = C_2 \dot{\theta} \tag{4.5}$$

Most of the geometries utilize narrow gaps thus ensuring a reasonably constant shear rate across the gap. Averaged values are used in geometries where some variation of stress or shear rate exists.

4.3.3 Dynamic Oscillatory Shear Testing

In a dynamic oscillation experiment, the sample placed between the measuring geometries is subjected to a harmonic shear stress (σ) with controllable amplitude $\sigma_{21}{}^{o}$ and angular frequency ω. The shear stress is described by

$$\sigma_{21} = \sigma_{21}{}^{o} \cos\omega t \tag{4.6}$$

The resulting harmonic strain is written as

$$\gamma_{21} = \gamma_{21}{}^{o} \sin\omega t \tag{4.7}$$

where, $\gamma_{21}{}^{o}$ is the amplitude of the strain response (which is measured by the Bohlin CS-50 Rheometer). The strain , is in-phase with the stress for a purely elastic material and 90° out-of-phase for a purely viscous material. So, for viscoelastic material, the phase angle of the strain lies between those two. Obtaining the value of shear rate by differentiating the above equation we get,

$$\dot{\gamma}_{21} = \omega\gamma_{21}{}^{o} \cos\omega t \tag{4.8}$$

As non-Newtonian fluids do not follow the Newton's law of viscosity, a constitutive equation has to be used to derive an expression for the relation between stress and shear rate. the constitutive equation is expressed as follows:

$$\sigma_{21}(t) = \int_{-\infty}^{t} G(t-t')\dot{\gamma}_{21}(t')dt' \tag{4.9}$$

Substituting equation (4.38) in equation (4.39), and denoting (t-t') by (s) we obtain,

$$\sigma_{21}(t) = \int_0^{\infty} G(s)\omega\gamma_{21}{}^{o}\cos\left[\omega(t-s)\right]ds \tag{4.10}$$

Expanding the cosine term in the above equation gives,

$$\sigma_{21}(t) = \gamma_{21}{}^{o}\left[\omega\int_0^{\infty} G(s)\sin\omega s ds)\right]\sin\omega t + \gamma_{21}{}^{o}\left[\omega\int_0^{\infty} G(s)\cos\omega s ds)\right]\cos\omega t \tag{4.11}$$

The term in the first parenthesis is in-phase with $\gamma_{21}{}^{o}$ and is defined as the storage or elastic modulus and is denoted by G'. The term in the second parentheses is out-of-phase with $\gamma_{21}{}^{o}$ and is defined as the viscous or loss modulus and is denoted by G". Thus the above equation can be written as follows:

$$\sigma_{21}(t) = \gamma_{21}{}^{o}(G'\sin\omega t + G''\cos\omega t) \tag{4.12}$$

Also, equation (4.3.6) may be written in the following form using trigonometric identities.

$$\sigma_{21} = \sigma_{21}{}^{o}\sin(\omega t + \delta) = \sigma_{21}{}^{o}\cos\delta\sin\omega t + \sigma_{21}{}^{o}\sin\delta\cos\omega t \tag{4.13}$$

where δ is the phase lag which is a characteristic of viscoelastic behavior.

Comparing the above two equations we get

$$G' = \left[\frac{\sigma_{21}{}^{o}}{\gamma_{21}{}^{o}}\right]\cos\delta \tag{4.14}$$

$$G'' = \left[\frac{\sigma_{21}{}^{o}}{\gamma_{21}{}^{o}}\right]\sin\delta \tag{4.15}$$

whence

$$\delta = \tan^{-1}\left[\frac{G''}{G'}\right] \tag{4.16}$$

It is often convenient to adopt complex notation by using the following complex forms for the stress and strain respectively:

$$\sigma^* = \sigma_{21}{}^{o} e^{i\omega t} \tag{4.17}$$

So the complex modulus is given by :

$$\frac{\sigma^*}{\gamma_{21}{}^{o}} = G^* = G' + iG'' \tag{4.18}$$

and magnitude of G* is :

$$\left|G^*\right| = \frac{\sigma_{21}{}^{o}}{\gamma_{21}{}^{o}} = \sqrt{(G')^2 + (G'')^2} \tag{4.19}$$

Thus G' and G" are given as:

$$G' = \left|G^*\right| \cos\delta \tag{4.20}$$

$$G'' = \left|G^*\right| \sin\delta \tag{4.21}$$

Finally, the complex dynamic viscosity is related to the components of the complex dynamic modulus and the frequency by

$$\eta^* = \eta' + i\eta'' = \frac{G''}{\omega} - i\frac{G'}{\omega} \tag{4.22}$$

In terms of the Bohlin CS-50 Rheometer measurement principles, G' and G" are calculated from the applied torque (T_D^*). According to the Bohlin User's manual, the general equations for G' and G" account for the moment of inertia (I) and for different measuring systems as given below.

$$G' = \left[\frac{C_1}{C_2}\right] \frac{\left|T_D{}^*\right| \cos\varphi + I\omega^2 \left|\theta^*\right|}{\left|\theta^*\right|} \tag{4.23}$$

$$G'' = \left[\frac{C_1}{C_2}\right] \frac{\left|T_D{}^*\right| \sin\varphi}{\left|\theta^*\right|} \tag{4.24}$$

where C_1 and C_2 are constants pertaining to each type of measuring system which are built into the Bohlin software , θ^* is the complex angular deflection of the sample, and φ is the phase lag between sample measuring shaft and the drag cub shaft. Both are measurable quantities.

4.3.4 Bohlin Constant Stress Rheometer

The Bohlin CS-50 is a rotational rheometer that works on the principle of controlled stress. It means that the instrument controls the amount of shear stress put on the sample and then correspondingly calculates other properties by measuring the extent of displacement the sample undergoes. The CS-50 consists of a drag cup motor, an angular position transducer, air bearings, sensors and various measurement geometries. The array of measurement geometries include parallel plates, cone & plate, and bob & couette (co-axial cylinders). This rheometer can perform a very wide range of fluid measurements for different kinds of fluids like oils, polymer solutions, gels etc. In addition, this instrument has the capability of controlling the sample temperature very well in the range of -20°C to 250°C. Data acquisition and measurement control are done by computer which is programmed with the Bohlin software CS 4.84. This software provides the capability of doing a great variety of rheological tests like stress viscometry, oscillation, constant rate, yield stress etc. During measurements, the computer collects the data, performs an interactive plot, and generates a table of all the measurement parameters. Also, the data can be converted to ASCII files which can be used in spreadsheets to do further data analysis. The principle components of the CS-50 are shown in Figure 4.7a and the various measurement geometries are illustrated in Figure 4.7b.

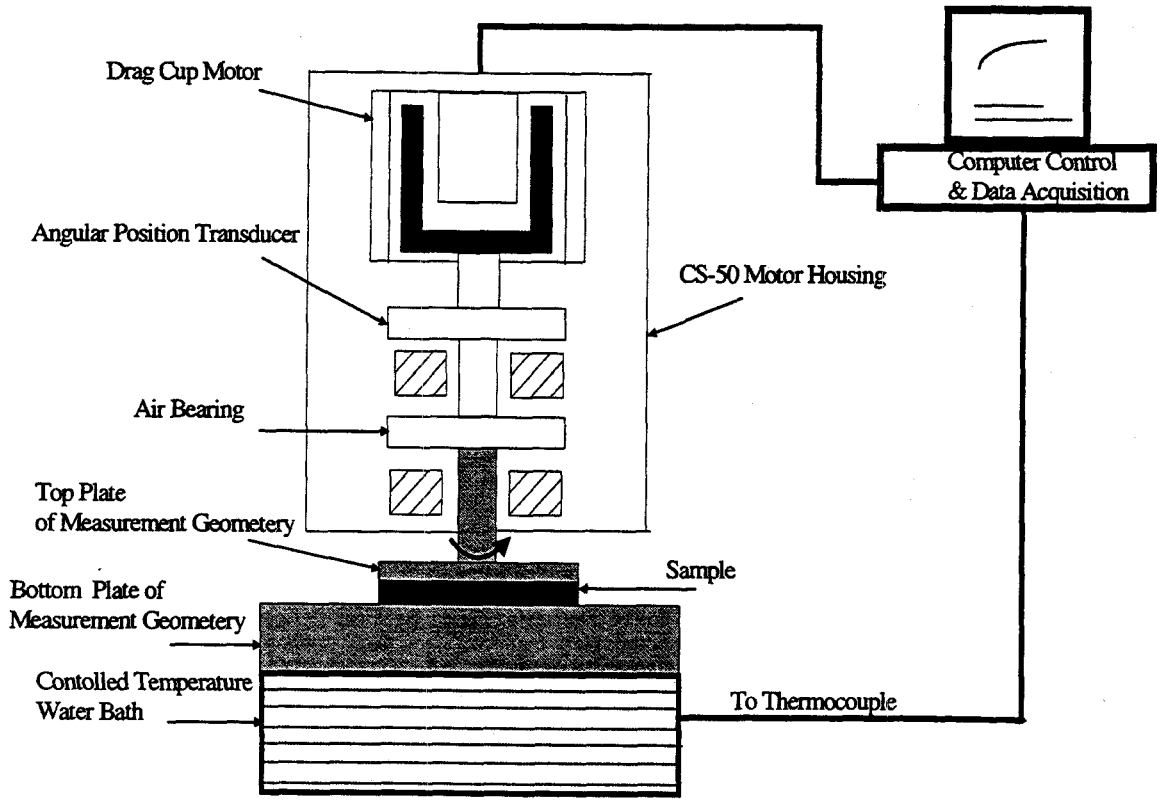

Figure 4.7a Schematic of Bohlin Constant Stress CS-50 Rheometer

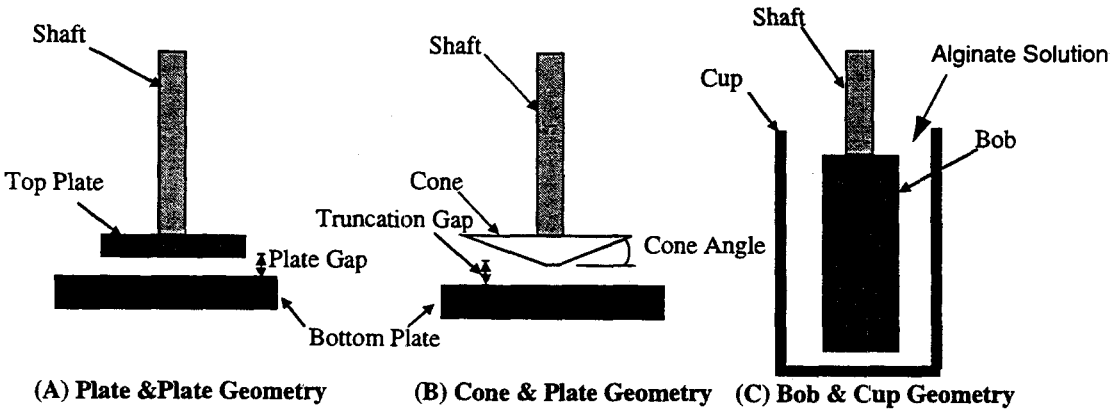

Figure 4.7b Measuring Geometries of Bohlin CS-50

The CS-50 was calibrated extensively with viscous (i.e., 100-5000 cp oils) and viscoelastic (i.e., NBS 1490 and PDMS) standards. When using the CP 4/40 (cone and plate geometry with diameter of 40 mm and cone angle of 4 degrees), the gap was set at 0.15 mm. When using the C 25 (couette) geometry, the instrument gap was first zeroed using a parallel plate or a cone & plate geometry. The gap change with temperature due to thermal expansion of the measuring geometry was 0.001 mm/°C. All the rheological tests in our work were done at room temperature.

4.3.5 Clark High Shear Capillary Viscometer

Clark High Shear Capillary Viscometer was available at Hewlett Packard (Corvallis) in their ink laboratory. This viscometer was constructed at HP and is based on the plans of a high shear capillary machine built by Ross Clark of Kelco Corp in San Diego and designed by Eric Matthys of UCSB and Ross Clark. This machine was built primarily for laminar flow viscosity measurements, but can be adapted for turbulence studies also. A schematic is shown on Figure 4.8 which outlines the principal components of the machine.

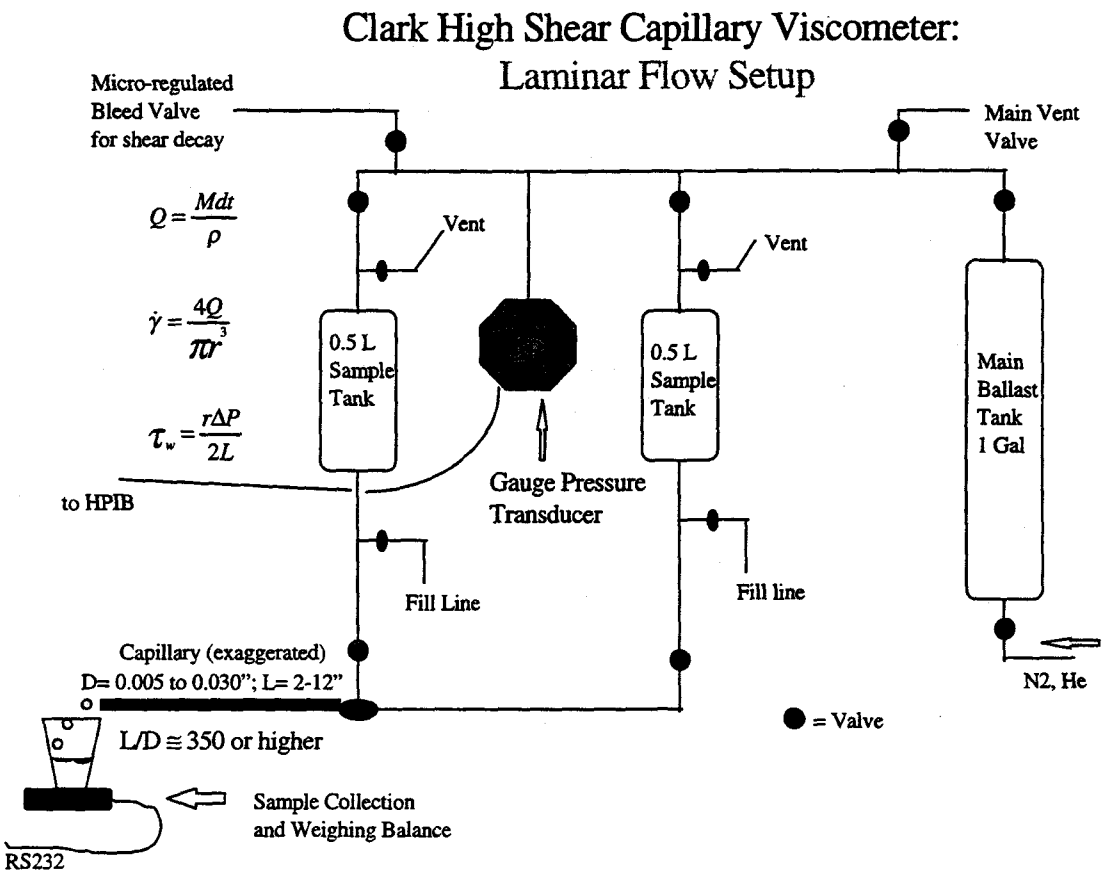

Figure 4.8 Schematic of Clark High Shear Capillary Viscometer

In concept, a high shear capillary viscometer is a very simple instrument. Driving force which is measurable, is provided by a pressurized tank of nitrogen or helium with a pressure transducer attached to it. The other components are mainly capillaries of known radii and lengths, and a way to measure the flow rate at the end of the capillary. It is impossible to obtain a perfectly round and smooth capillary, for instance, or to design a system that does not have constrictions in any of the tubing, etc. It is therefore necessary to add correction terms. A simple shear experiment consists of loading a sample, establishing a pressure head according to the capillary and shear rate wanted (from 1 psi to 1200 psi), starting flow at highest pressure, then slowly bleeding pressure (and therefore decreasing shear rate) until required shear data are collected.

In order to calculate viscosity, two quantities need to be determined, which are stress and shear rate:

$\eta = \tau_w / \gamma_{dt}$ where τ_w = stress at the wall of the capillary

and γ_{dt} = shear rate at the wall of the capillary

The measured dP is directly related to the stress:

$\tau_w = r\, dP / 2L$ where dP = pressure drop across capillary

L = length of the capillary

r = radius of capillary

The volumetric flow rate, another measured variable, is determined easily by weighing the output flow in a weigh balance as a function of time and dividing by the density of the fluid being tested:

$Q = M_{dt} / \rho$ where M_{dt} = change in mass per unit time

and ρ = density of the fluid

The shear rate is then: $\gamma_{dt} = 4Q/\pi r^3$

Note that higher shear rates can be achieved with smaller capillary tubes because of the r^3 factor.

One further derivable parameter is the Reynolds Number, Re, which is the ratio of inertial to viscous forces:

$Re = \rho v d/\mu$ where d = diameter of capillary

μ = apparent viscosity of fluid

v= velocity = $Q/ \pi r^2$ of fluid

Because of the velocity term, higher Re numbers are achievable with larger diameter capillaries.

Under a well controlled flow field, turbulence is achieved between Re = 2100 - 2300. Re numbers below 2100 classifies the flow as laminar and above 2500 as turbulent. Capillaries made from HPLC (high pressure liquid chromatography) tubing with diameters from 0.005" to 0.030" and lengths up to 11" were available. Pressure capabilities are up to 2000 psi, but for safety reasons the the experiments were not run over 1500 psi. All calibration is performed against water. All of the above derivations assumed laminar flow conditions.

4.3.6 Sodium Alginate

Alginate is a polysaccharide isolated from brown algae, where its function is skeletal. It forms strong gels with divalent cation like Ca^{2+}, giving both strength and flexibility to the algal tissue. Chemically, alginate is a linear copolymer of two uronic acids: D-mannuronic acid (M) and L-guluronic acid (G) linked together by b 1,4 and a1,4 glycosidic bonds respectively. The two monomers are arranged in homopolymeric blocks, M-blocks and G-blocks as well as in copolymeric, regularly alternating MG-blocks. The structures of D-mannuronic acid (M) and L-guluronic acid (G) are given in Figure 4.9 and Figure 4.10 respectively.

The following information was obtained from Kelco Co. brochure. Alginic acid traces its history back to 1884, when E. C. C. Stanford, the great pioneer in seaweed research, suggested a number of methods for chemical utilization of seaweeds including destructive distillation and a "Lixivation" process. One of the by-products of the "Lixivation" process for the production of potash was crude alginic acid. Krefting (1896) was the first one to prepare a pure alginic acid, and then many of the properties of the salts of this acid were determined. Commercial production began in 1929 by Kelco Company.

Algin, the polysaccharide extracted from the brown seaweeds, *Phaeophyceae*, has only recently been chemically identified. The first report on its structure was made in 1930 by Nelson and Cretcher, who claimed it was a D-mannuronic acid connected by b 1,4 linkages (Hirst et al. 1939). Fischer and Dorfel (1955), determined that L-guluronic acid was also present as a major component of alginic acid by using paper chromatography. Also, Vincent (1960) and Hirst, Percival, and Wold (1964) showed that at least some of the alginic acid molecules contained both mannuronic acid and guluronic acid by use of partial acid hydrolysis to isolate oligomers containing both uronic acids.

With the improvements in the techniques for the hydrolysis, separation, and analysis of alginic acid, the composition of alginic acid from different sources were accurately determined. Mild acid hydrolysis showed the presence of three kinds of polymer segments in alginic acid from various brown algae (Haug et al. 1966, 1967a, and 1967b). Out of the three kinds of polymer segments, one segment consists essentially of D-mannuronic acid units; a second unit consists essentially of L-guluronic acid units; and the third segment consists of alternating L-guluronic acid and D-mannuronic acid residues. These are illustrated in Figure 4.11. Haug and co-workers (1966 and 1967a) also determined the proportions of the three polymer segments in alginic acid samples from different sources using partial acid hydrolysis and separating the alternating and the homopolymeric segments. P.M.R. spectroscopy was also used by Penman and Sanderson (1972) to determine the proportions of the three polymer segments present.

The differences in properties and functionality of alginates isolated from different species of brown algae can be accounted by the differences in composition and fine structure. The theoretical equivalent weight of alginic acid is 176, but bound water within the molecule results in values close to 194. Dissociation constant depends on the ratio of mannuronic acid to guluronic acid and was reported by Haug (1964) as follows:

ACID	pKa
Mannuronic acid	3.38
Guluronic acid	3.65

Polymannuronic acid (Figure 4.12) chain has similar structure to that found in cellulose and other b 1,4 linked hexosans. The mannuronic acid is in the C1 conformation and, therefore diequitorially linked. Polymannuronic acid is a flat ribbon-like molecule the conformation of which appears to be stabilized by the formation of an intra-molecular hydrogen bond between the hydroxyl group on Carbon 3 of one unit and the ring oxygen atom of the next unit in the chain. Hydrogen bonds also exist between chains in parallel and antiparallel chains thus forming sheets.

On the other hand, the shape of polyguluronic acid (Figure 4.13) is quite different as it has a buckled, ribbon-like molecule in which the guluronic acid unit is in 1C conformation and, therefore it is di-axially linked. Hydrogen bonding exists between the hydroxyl group on carbon 2 of one unit and the oxygen atom of the carboxyl group in adjacent unit. The interchain bonding is more complex than its counterpart as it involves water molecules such that the water molecule functions twice as a hydrogen bond doner and twice as an acceptor (Atkins et al. 1971).

An important feature is the strong correlation between physical properties of the polymer and the proportions and the sequential arrangements of the two uronic acids. While viscosity depends mainly on molecular size, the affinity for ions and the gel forming properties are related to the content of guluronic acid. When two guluronic acid residues are adjacent in the polymer, they form a binding site for calcium ions, and accordingly the content of G-blocks is the main structural feature contributing to gel strength and stability of the gel.

Alginate isolated from different algae or different tissues can both vary in monomer composition and block arrangement. Low content of guluronic acid is found in alginate from Ascophyllum nodosum and Macrocystis pyrifera (35%-42% G), while the stipes of the kelp Laminaria hyperborea contains an alginate with a G-content of 65-75 %. This alginate is a very strong gel former.

Rheological Experiments on Sodium alginate

Rheology is the study of the internal response of materials to forces and between the extremes of the conceptual views of the Newtonian fluid and the Hookean solid lie materials of great interest; algin being one of them. The Bohlin CS-50 Rheometer was used to study the rheological properties of sodium alginate. For all the experiments, either cone and plate (CP 40) or cup and bob geometries (C25) were used. Oscillation and Stress Viscometry tests were performed on 1%, 1.5% and 2% Keltone LV in DIW.

4.3.7 Calcium Alginate

Sodium alginate forms strong gels with divalent and trivalent cations and this gelling property of algin is widely used, especially in the food and medicine industry. In food industry, it is used in instant puddings, cooked puddings, chiffons, pies & pastry fillings, dessert gels, structured foods etc. On the other hand, alginate gel is used widely for its controlled drug release feature as both topical application and oral capsules. In order to get the best out of any application, we need to understand the gel formation (crosslinking) and the properties of the gels. In this paper, an effort has been made to study the crosslinking of Keltone LV (sodium alginate) with Ca^{2+} ions.

Alginate gels resemble a solid in retaining their shape and resisting stress even though water constitutes more than 99% of the gel. The structure of alginate gel is shown in Figure 4.15. Circular dichroism studies have shown that the calcium ions react preferentially with the polyguluronic acid segment. In this interaction the polyguluronate segments associate into aggregates with the interstices into which calcium ions fit. This is called the "Egg box model" (Figure 4.14) and is described by Grant *et al. (1973)* and Morris *(1986)*.

As no permanent bond exists between the algin molecule and the calcium ions, the calcium ions can migrate between algin molecules. In this dynamic system, the presence of other ions will affect the properties of the gel. A monovalent ion, like sodium

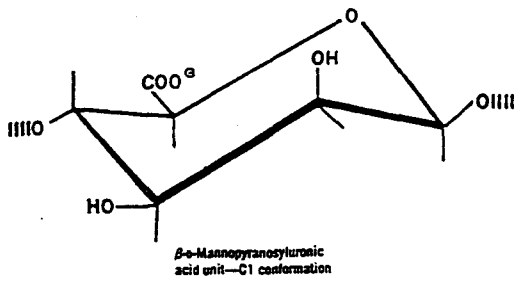

FIGURE 4.9 CONFORMATION OF MANNURONIC ACID.

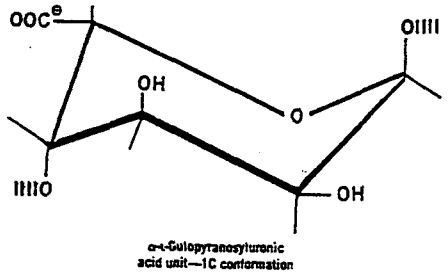

FIGURE 4.10 CONFORMATION OF GULURONIC ACID.

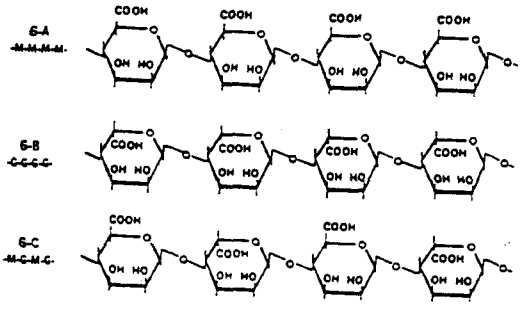

FIGURE 4.11 STRUCTURE OF THE THREE POLYMER SEGMENTS CONTAINED IN ALGINIC ACID.

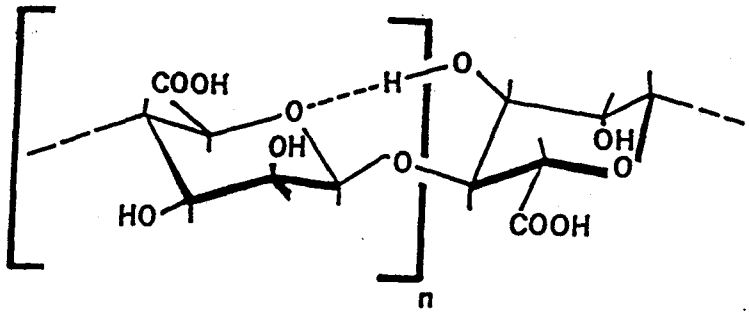

FIGURE 4.12 REPEATING UNIT OF POLYMANNURONIC ACID.

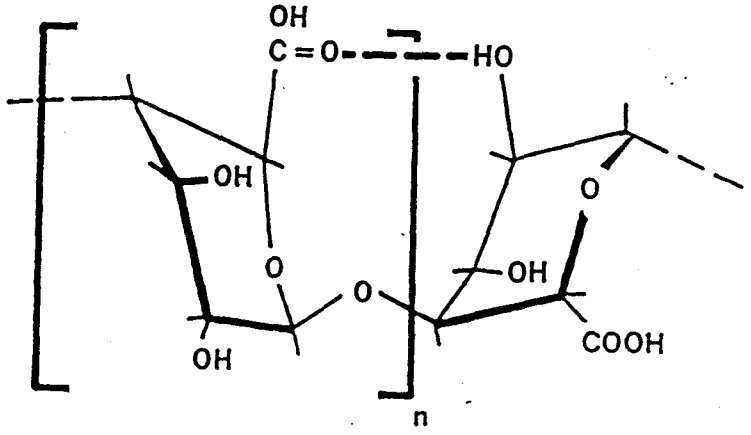

FIGURE 4.13 REPEATING UNIT OF POLYGULURONIC ACID.

ion will decrease the strength of the gel and a trivalent ion, like aluminum will make the gel more rigid.

Salient features of the Chemical System used in experiment:

SODIUM ALGINATE-- Keltone LV (provided by Kelco)

Concentration = 0.1 - 2 % (w/v).

DIVALENT ION-- Ca^{2+} (Calcium chloride)

Concentration = 0.01-1 M.

forms STRONG divalent complexes.

SOLVENT-- a) Water (distilled)

b) Water (distilled) + 5.84 g/l NaCl (0.1M NaCl)

GOOD solvent for sodium alginate

SOLUTION--

ISO-VOLUMETRIC : Keltone LV solution. + $CaCl_2$ solution.

pH that of the system (not adjusted).

Method:

Two groups of algin solutions (0.1-2%) were prepared; one using only distilled water as the solvent and the other using a 0.1M NaCl solution. Also solutions of calcium chloride (0.01-1M) were prepared.

4.3.7.1 For Phase Diagram experiment:

The algin solution was mixed iso-volumetrically with calcium chloride solutions (0.01-1M), in test-tubes and then allowed to gel. The various concentrations of the algin and calcium chloride used in studying the gelation are given in Table 4.1 & Table 4.2. The gelation process was observed at various time intervals and the gels were categorized visually after 48 hours. The categories of classification are as follows:

a) Gel- homogenous (H); rigid.

b) Gel- H, semi-rigid or apple sauce (APS).

c) Gel/Sol- inhomogenous (IH); globs + sol.

d) Sol/Gel- visible microgels (M).

e) Sol- clear and no visible microgels.

Table 4.1 Keltone LV in distilled water.

S.no.	$CaCl_2$ conc. (M)	Keltone LV (%)	S.no.	$CaCl_2$ conc. (M)	Keltone LV (%)
1.	0.01	0.1	14.	0.1	1.5
2.	0.01	0.5	15.	0.1	2
3.	0.01	1	16.	0.5	0.1
4.	0.01	1.5	17.	0.5	0.5
5.	0.01	2	18.	0.5	1
6.	0.05	0.1	19.	0.5	1.5
7.	0.05	0.5	20.	0.5	2
8.	0.05	1	21.	1.0	0.1
9.	0.05	1.5	22.	1.0	0.5
10.	0.05	2	23.	1.0	1
11.	0.1	0.1	24.	1.0	1.5
12.	0.1	0.5	25.	1.0	2
13.	0.1	1			

Table 4.2 **Keltone LV in 0.1 M NaCl.**

S.no.	$CaCl_2$ conc. (M)	Keltone LV (%)	S.no.	$CaCl_2$ conc. (M)	Keltone LV (%)
1.	0.01	0.1	14.	0.1	1.5
2.	0.01	0.5	15.	0.1	2
3.	0.01	1	16.	0.5	0.1
4.	0.01	1.5	17.	0.5	0.5
5.	0.01	2	18.	0.5	1
6.	0.05	0.1	19.	0.5	1.5
7.	0.05	0.5	20.	0.5	2
8.	0.05	1	21.	1.0	0.1
9.	0.05	1.5	22.	1.0	0.5
10.	0.05	2	23.	1.0	1
11.	0.1	0.1	24.	1.0	1.5
12.	0.1	0.5	25.	1.0	2
13.	0.1	1			

4.3.7.2 For Rheology experiment:

The Bohlin CS-50 Rheometer was used to study the rheological properties of algin and gels. For all the experiments, cup and bob geometries (C25) were used. The gel samples were prepared in-situ i.e. the algin and calcium chloride solutions were poured into the couette & mixed and the gel allowed to form.

Oscillation tests (frequency sweep) were performed on 2% Keltone LV (0.1 M NaCl) + 0.01M $CaCl_2$ gel after every half hour starting at the mixing of solutions in the couvette (time = 0 hour). An extensive time-sweep test was then carried out at a frequency of 1 Hz in which the measurement was taken after every 30 seconds till the values of viscous modulus and elastic modulus became constant. Similar tests were carried out on 1.5% Keltone LV (0.1 M NaCl) + 0.01M $CaCl_2$ Gel and 1.5% Keltone LV (0 M NaCl) + 0.01M $CaCl_2$ Gel.

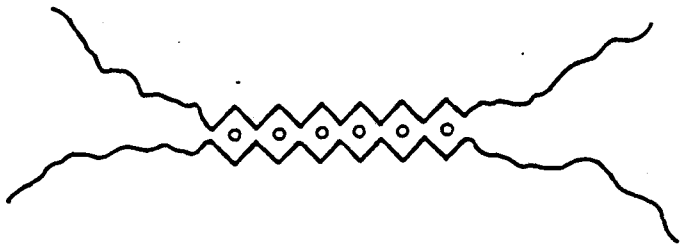

FIGURE 4.14 THE "EGG BOX MODEL".

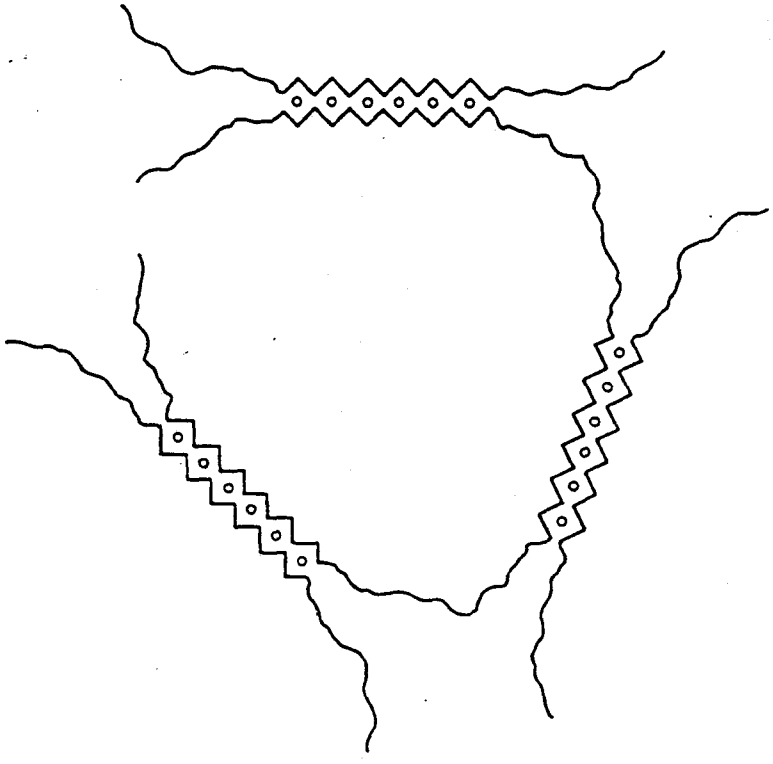

FIGURE 4.15 STRUCTURE OF CALCIUM ALGINATE.

CHAPTER 5
5. RESULTS

5.1 Introduction

The results of the operation of the bead generators and rheological studies of alginate solution and its crosslinking will be discussed in the following sections. The experimental data that are not explicitly contained in this chapter have been placed in the appendix. The operation of the bead generators will be discussed first to establish their operating range in term of bead sizes. The extensive rheological studies on algin solutions will then be summarized followed by the rheological investigation of crosslinking of algin solution with divalent calcium ion in absence and presence of other monovalent ions like sodium.

5.2 Results of Bead Generators

5.2.1 Transverse Vibrating Capillary Droplet Generator

This was the first generator which was assembled in an attempt to produce beads and in order to understand the effect of vibration necessary to stimulate the cylindrical liquid jet break-up for algin solutions. The construction of the bead generator is explained in Section 4.1.2 of Chapter 4 and the diagram of the droplet generator is shown in Figure 4.2. Its simple design allows the use of several different size needles to expand the range of droplet size as the needles are very easy to replace. The results of the initial experiments on this setup are summarized in Table 5.1. Solutions with different concentrations of Keltone algin (0.5% LV, 1%LV, 3%LV, 1%HV, 3%HV) were passed through vibrating needles of different sizes.

Table 5.1 Performance of Transverse Vibrating Capillary Droplet Generator

Run	Algin solution (Keltone)	Needle size i.d. mm (Gage)	Flow rate (ml/min)	Freq. (Hz)	Min/Max size of beads (microns)	Mean dia of beads (microns)	Comments (Type of distribution)
1	0.5%LV	0.1524 (30)	5.6	20-2300	--------	-----	Beads not formed
2	1%LV	0.292 (24)	15.4	100	300-800	636	normal
				200	200-800	600	skewed
				500	200-600	300,600	bimodal
				700	100-600	286	skewed
				2900	100-600	300, 500	bimodal
3	1%LV	0.1905 (27)	6	470	100-700	333	normal
				1000	200-600	320	skewed
				1000	200-500	316	normal
				5000	100-700	303	skewed
4	3%LV	0.292 (24)	12	300	800-1100	956	skewed
				330	800-900	860	normal
5	3%LV	0.1905 (27)	10.4	100	500-900	600,800	bimodal
				475	400-800	623	skewed
				550	400-800	500,800	bimodal
6	1%HV	0.292 (24)	10.4	100	400-600	0.533	normal
				370	400-800	400,600	bimodal
				500	400-700	520	bimodal
7	1%HV	0.1905 (27)	8	330	300-500	406	normal
				1000	200-600	406	skewed
8	3%HV	0.292 (24)	-----	-----		-----	No Jet Break-up

The experiments on this apparatus indicated that it is possible to fine tune the frequency of vibration to produce uniform droplets. It should be noted here that the droplets coming out of the nozzle are very uniform but they deform when they hit the calcium chloride solution surface. The diameter of the beads was measured using a low power optical microscope with a scale which could measure a minimum distance of 0.1 mm. This is rather a crude method of bead diameter measurement, which is reflected in the breadth of the distribution curves. It is our feeling from observing the break-up process that the distribution may actually be "narrower" than they appear to be from the present data and the crude measuring technique. Thus, the skewness and breadth of the curves can be explained on the basis of both the deformation of the droplets and the crudeness of the method of diameter measurement. The bimodal distribution curves can be explained by the fact that at some frequencies the liquid jet breaks up into a larger drop and a relatively smaller droplet (satellite droplets).

One of the biggest disadvantage lies in the difficulty of pushing viscous liquids through the needles. With the increase in concentration of Keltone solution, this difficulty increases. It is very hard to push algin solutions through smaller diameter needles (greater than 27 gage) with a large L/D, so an orifice technique will most likely be a better setup.

For a given fluid and needle, the size of droplets decreases at higher resonant frequencies. Even with the available nozzles, at certain frequencies the liquid jet breaks up into a uniform size big droplet and a uniform size satellite droplet. The size of the satellite droplets are much less than 100μm, and they can be captured separately.

It is seen that the elasticity of the algin solution at higher concentrations causes the liquid jet coming out of the nozzle under vibration to form thin fluid strands joining bigger drops (Figure B-4, Appendix B). It is also seen that the greater the elastic modulus G' , the greater is the time taken for the liquid jet to break-off into droplets and for the droplets to break from each other. This effect was experimentally observed in 1%LV, 3%LV, 1%HV as the elasticity as measured from G'(w) increased proportionately.

The vibrations were not able to break-up the jet when 3% Keltone HV was used. As it was observed that Keltone HV solutions with their relatively higher viscosity were harder to push through the needles to form a jet. Thus. it was decided that all the remaining work be done with 1-2% Keltone LV solutions.

5.2.2 Axial Vibrating Orifice Droplet Generator

The difficulty of pushing viscous liquids through needles was solved by adapting the previous apparatus to accept an orifice plate instead of needles. Also the vibration was in the axial direction rather than in the transverse direction. The design of the droplet generator is discussed in Section 4.1.3 and the diagram is given in Figure 4.3. As the previous setup had some problems in vibration like damping etc., a different signal generator and amplifier were used. The signal from the HP 200 CD wide range oscillator is amplified using a Krohn-Hite DCA-10 wide band amplifier. The use of these gave more control over the range of the amplitude of vibration. The orifice plate helped in forming liquid jet from highly viscous alginate solutions more easily than needles due to lesser pressure drop. Initial runs on this setup were done using 202.8 micron orifice and 2% Keltone LV solution in DIW. Some of these results are presented in Appendix A. Figure A-1 (AppendixA) shows the photograph of a bimodal distribution in which a main bead is 630 microns in size and a satellite bead of 210 microns is produced. Figure A-2 shows a monodisperse sample in which the bead size of 460 microns is produced. Figure A-3 shows a bimodal distribution in which two beads of 480 microns and 620 microns are produced. Further systematic study was done using an orifice of 100 micron diameter in an attempt to produce smaller beads. Good initial runs resulting in monodisperse beads are tabulated below in Table 5.2.

Table 5.2 Performance of Axial Vibrating Orifice Droplet Generator

Experimental data for Monodisperse bead samples								
Test no.	Orifice size (microns)	$CaCl_2$ conc.	Keltone LV Conc.% (w/v)	Flow Rate (ml/min)	Freq. (Hz)	Bead diameter (microns)	Sample no.	Comments
9	100	0.1M	1	2	270	430±20	D-36	Monodisperse
9	100	0.1M	1	2	340	400±25	D-37	Monodisperse
9	100	0.1M	1	2	440	350±15	D-38	Monodisperse
10	100	0.1M	1	2	360	390±20	D-39	Monodisperse
15	100	0.1M	1	2	170	460±25	E-10	Monodisperse
15	100	0.1M	1	2	210	450±10	E-11	Monodisperse
15	100	0.1M	1	2	400	360±30	E-12	Monodisperse
15	100	0.1M	1	2	1130	350±25	E-13	Monodisperse
5	100	0.1M	1.5	2	550	350±20	D-18	Monodisperse
7	100	0.1M	1.5	2.4	350	380±15	D-21	Monodisperse
8a	100	0.1M	1.5	2.5	260	470±25	D-26	Monodisperse
8a	100	0.1M	1.5	2.5	460	380±15	D-27	Monodisperse
8b	100	0.1M	1.5	3.5	2700	230±10	D-35	Monodisperse

5.2.3 Axial Vibrating Diaphragm Droplet Generator

In the experiments with the previous droplet generators, the disturbance vibrations were transmitted to the whole apparatus assembly before being transmitted to the liquid jet. This resulted in the dampening of certain frequencies which produced unpredictable bead sizes at those frequencies. This problem was overcome by designing an axial vibrating diaphragm droplet generator. In this droplet generator a diaphragm is vibrated which then passes the vibrations through the algin solution in the cavity to the exiting jet. These vibrations cause the break-up of the liquid jet. The design of the droplet generator is shown in Figure 4.4 and the design is explained in Section 4.1.4 in Chapter 4. The size

of the alginate beads produced under different conditions was measured and correlated to the operating conditions of the bead generator. According to theory, the size of the droplets produced by vibration for low viscosity Newtonian liquids is given by the following equation

$$Dp = \left[\frac{6Q}{\pi F}\right]^{\frac{1}{3}} \qquad \text{(eq. 5.1)}$$

Taking logarithm of both sides we get,

$$Log(Dp) = \frac{1}{3} Log\left[\frac{6Q}{\pi F}\right] \qquad \text{(eq. 5.2)}$$

That means that if the log terms are plotted on a graph, a line having a slope of 0.3333 and passing through the origin will be obtained.

The alginate bead data obtained from the experiments was plotted (Figure 5.1) in the form represented by equation 5.2. It should be noted here that D_p was taken as the actual size of the crosslinked calcium alginate bead and not the size of the droplet formed by the break-up of the alginate solution jet. From Figure 5.1, it can be seen that for a fixed operating condition, the size of the calcium alginate bead increases as the concentration of the alginate solution (Keltone LV) increases from 1% to 2%. Also, it is seen that for a fixed concentration of alginate solution, the size of the beads increases as the ratio of flow rate to the frequency of vibration, (Q/F) increases. Thus the beads become bigger as the flowrate increases or the frequency of vibration decreases which supports the predictions from theory.

The experimental data has been compared to that predicted by theory for low viscosity Newtonian fluids in Figure 5.2, where the theoretical line represents equation 5.2. It is noticed from this graph that most of the data lies below the theoretical line, which is reverse of what was expected.

An error analysis was made by estimating the experimental error in measurement of flowrate, frequency of vibration and measurement of size. This is graphically represented for 1% Keltone LV solution in Figure 5.4 with the help of error bars. The percent error for 1.5% and 2% Keltone LV solutions is same as that calculated for 1% Keltone LV solutions and therefore is not shown here.

The size of the crosslinked calcium alginate beads produced are actually smaller than the droplets produced from the nozzle. This is due to the shrinkage of the droplet as it undergoes gelation with the divalent calcium ions. The alginate molecular chains are drawn together by the calcium ion which forms both inter-molecular and intra-molecular bonds. This crosslinking tends to decrease the volume of the droplet thus causing shrinkage in size. The amount of shrinkage depends on the source of alginate, concentration of alginate solution, concentration of calcium ions in calcium chloride solution, time of crosslinking, pH of solutions and temperature. Figure B-7 (Appendix B) shows the photograph of an alginate droplet as it is falling through air. While Figure B-8 (Appendix B), shows the crosslinked beads (from the same jet break-up as Figure B-7) after 5 minutes of crosslinking in calcium chloride solution. It can be clearly seen that the droplets shrink in size when they crosslink to form a gel.

The results of the gel bead shrinking experiments are presented in Appendix D. Figures D-1, D-2 and D-3 show the total percentage decrease in bead diameter with gelling time for 1%, 1.5%, and 2% Keltone LV solutions. Here gelling time is refered to the time the alginate beads are allowed to sit in calcium chloride bath. These graphs show that the percentage decrease increases from 22 % to 25 % as the concentration of Keltone LV is increased. From Figures D-4 and D-6, it can be seen that with all other variables remaining constant, the smaller beads shrink faster initially than larger beads. Also comparing Figures D-5 and D-6, it is seen that the initial rate of shrinking is greater as the concentration of alginate increases, but after sometime it becomes less. This is probably due to the greater diffusion resistance experienced by calcium ions as the concentration of alginate solution increases.

The bead size data were corrected for 25% contraction in size due to crosslinking, and plotted as shown in Figure 5.3. Out here 25% contraction just represents an approximate value, so that the effect of contraction on the bead size data may be seen. Now the theoretical line passes through the 1.5% Keltone LV data and that 1% Keltone LV data still lies below the theoretical line. The difference in the shift of the data by incorporating the coagulation factor correction can be seen by comparing the data for the corrected and uncorrected 1% Keltone LV data.

A detailed study is currently underway to study this complex phenomenon and investigate the effect of other variables on the shrinkage of alginate droplets as they undergo gelation with divalent calcium ion.

The data presented in this section is given as a function of crosslinked calcium alginate bead diameters. Thus it gives only a relative idea of the droplet diameters formed by the break-up of alginate solution jets. Photographs of the alginate solution jet break-up process and some samples of monodisperse calcium alginate beads produced with the help of this bead generator are given Appendix B. Figures B-1 and B-2 are samples of crosslinked alginate beads produced in different runs, under the same operating conditions. This shows that this bead generator has very good reproducibility to give same size beads when operated under similar conditions. Figure B-3, shows that the size of the beads increase as compared to Figure B-1, when the frequency of vibration is lowered, other conditions remaining same. Increasing jet velocity also has the same effect. Thus, a wide range of beads can be produced by changing frequency of vibration and jet velocity. Figure B-4 is a photograph of strand formation during the break-up of alginate solution jets. The tendency to form strands between two droplets increases with increase in alginate concentration. Comparing Figures B-4 and B-5, we can see that satellite formation occurs as the amplitude of vibration is increased over a certain critical value, other conditions remaining constant. Figure B-6 illustrates the alginate jet break-up at high frequency and large amplitudes. Figure B-10 is the photograph of the beads produced if no assisted vibration is used to cause jet break-up. As seen, beads with large size dispersion are produced. Also the beads are much larger and less spherical than those produced by stimulated jet break-up process.

Figure 5.1 Performance of Axial Vibrating Diaphragm Droplet Generator
Experimental Conditions: Keltone LV 1%0.1M Calcium Chloride,
100 micron orifice, 2-3 ml/min flowrates

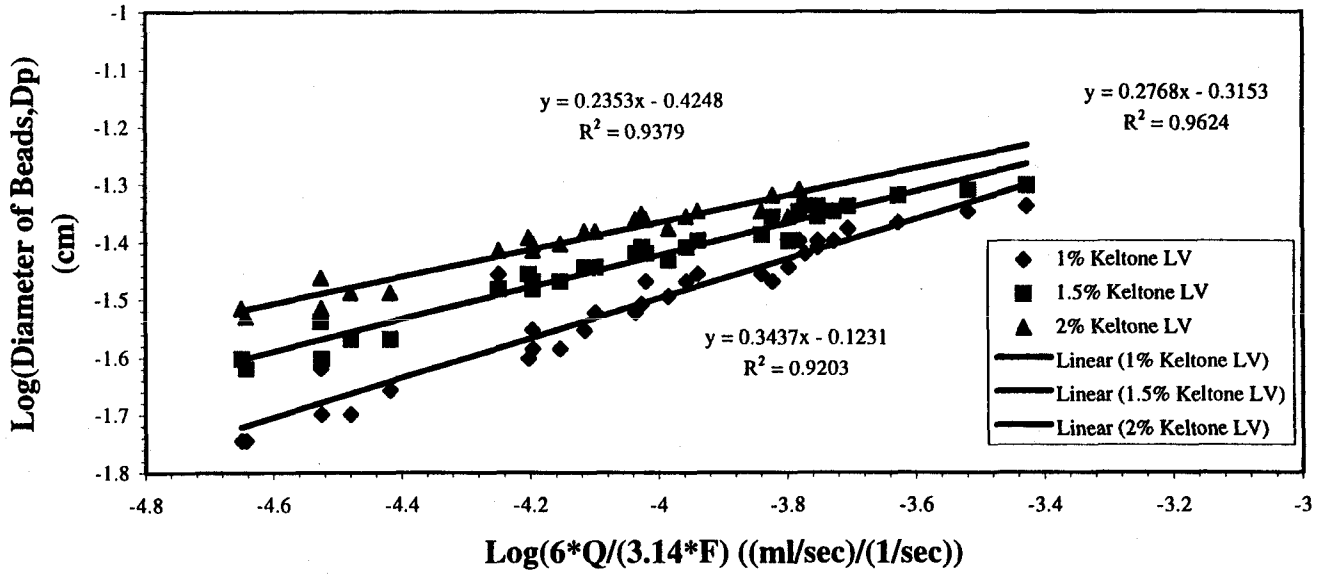

Figure 5.2 Performance of Axial Vibrating Diaphragm Droplet Generator
Experimental Conditions: 0.1M Calcium Chloride, 100 micron orifice,
2-3 ml/min flowrates

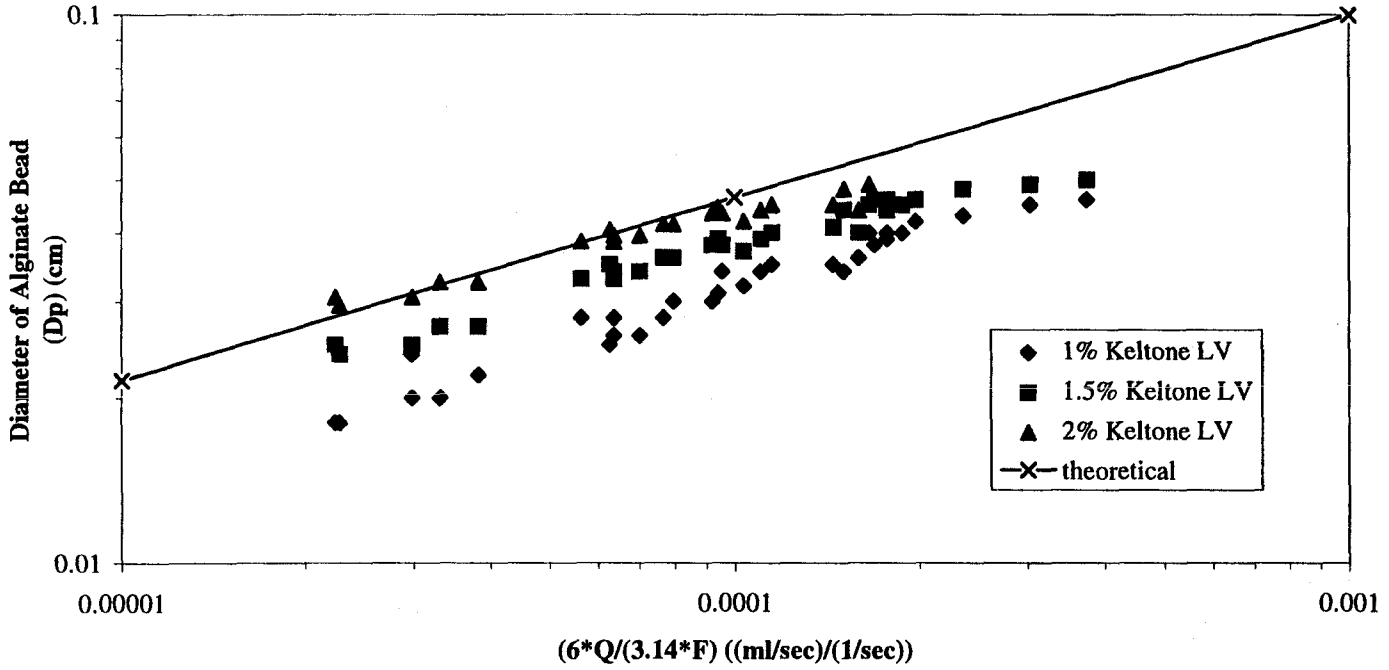

Figure 5.3 Performance of Axial Vibrating Diaphragm Droplet Generator
Experimental Conditions: 0.1M Calcium Chloride, 100 micron orifice,
2-3 ml/min flowrates
Data Corrected For 25% Contraction

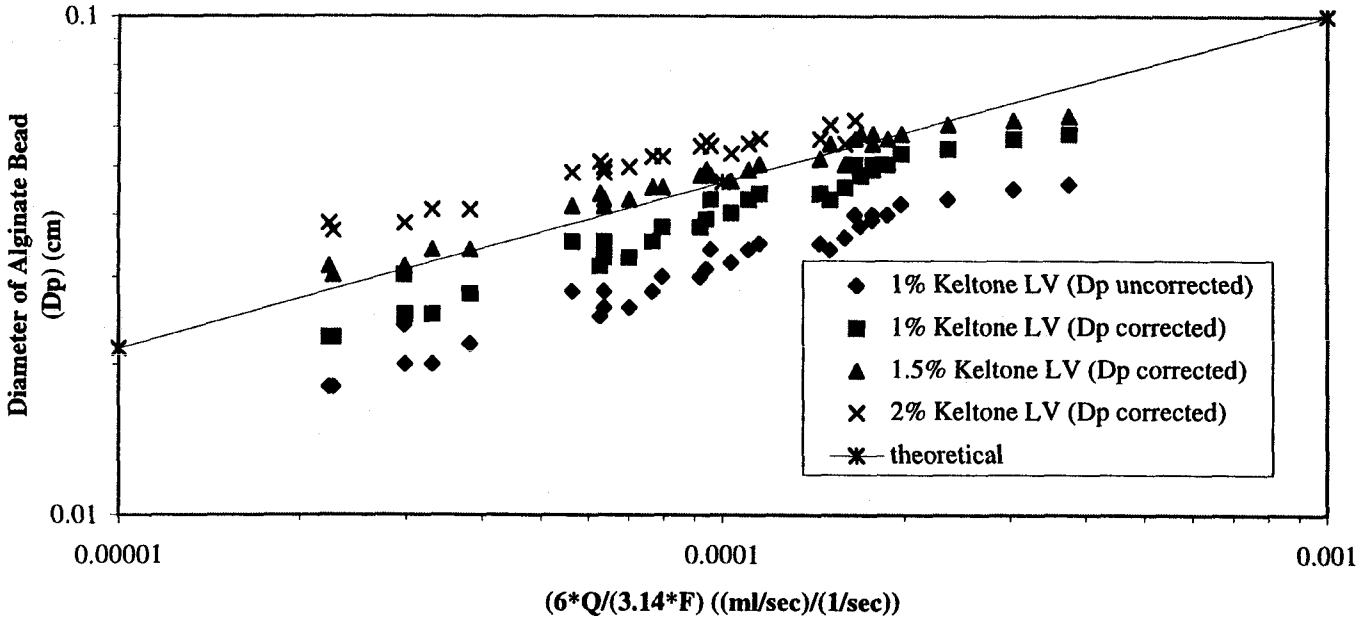

Figure 5.4 Performance of Axial Vibrating Diaphragm Droplet Generator
Experimental Conditions: 0.1M Calcium Chloride, 100 micron orifice, 2-3 ml/min flowrates
Error Analysis

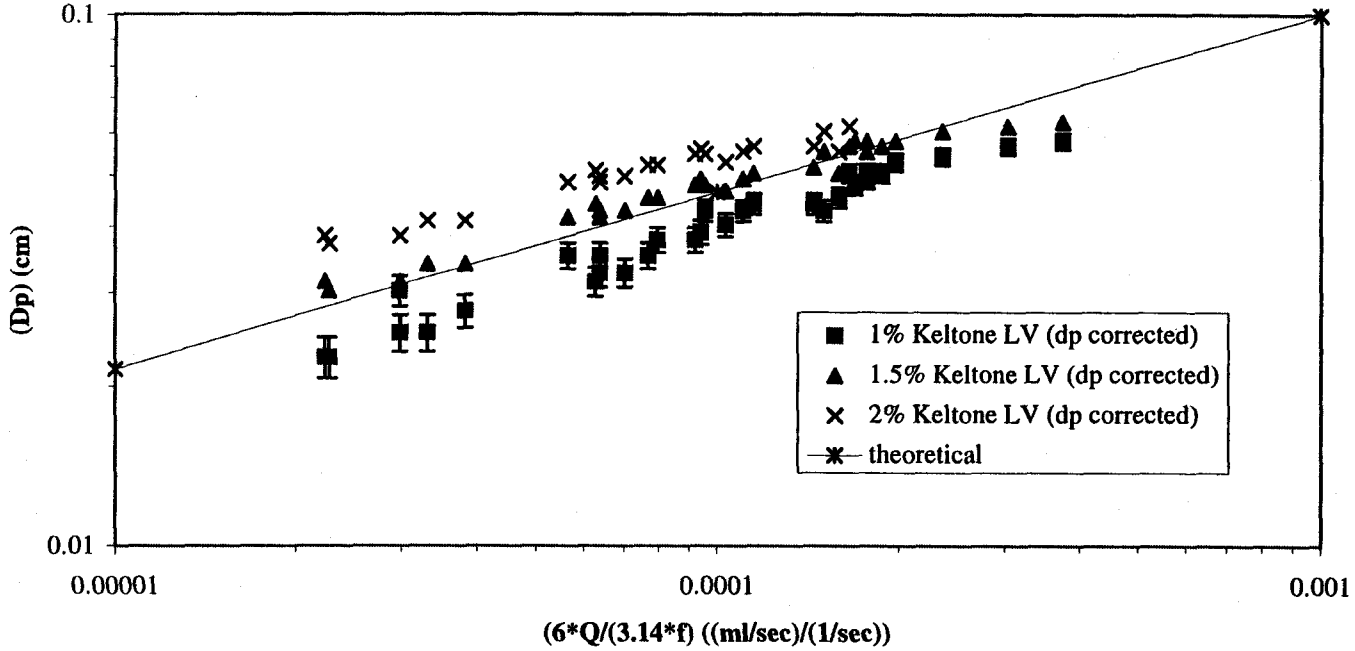

5.2.4 Two Fluid Vibrating Piezoceramic Droplet Generator

This apparatus is currently being tested. It is useful to produce alginate beads which are 100 microns and less. The results will be presented in a future work.

5.3 Results of the Rheological Study on Sodium Alginate Solutions

The results of the rheological testing on 1%, 1.5%, 2% Keltone LV solutions in DIW are presented in this section. The stress viscometry test indicates that the polymer is a psuedoplastic or shear thinning fluid. The stressviscometry test result of 1% Keltone LV is given in Figure 5.5 and that for 1.5% & 2% Keltone LV are given in Figures 5.6 & 5.7 respectively. From these graphs it is seen that the fluid becomes more shear thinning as the concentration of Keltone LV increases. It should be noted that all these solutions have a relatively wide zero shear viscosity plateau i.e. the linear viscoelastic region. Above a shear rate of 1000 sec^{-1} these solutions show a drastic shear thinning behavior till about a shear rate of 300, 000 sec^{-1} . After this upper Newtonian plateau is seen. Oscillation tests on these solutions are given in Figures 5.8- 5.10. These show that algin is a viscoelastic fluid with its viscous modulus, G" dominating over the elastic modulus, G'.

5.4 Results on the Gelation of Calcium Alginate

5.4.1 Results of Gel Phase Experiment

The phase diagrams for calcium alginate gels was obtained by plotting Algin concentration vs. Calcium chloride concentration. The phase diagrams are given in Figures 5.11 & 5.12.. The critical concentration for gelation, C^*_{gel} is shown as a dashed line on the plots. This concentration represents the critical concentrations of the alginate

Figure 5.5: Stress Viscometry Test
1% Keltone LV
Viscosity vs. Shear Rate

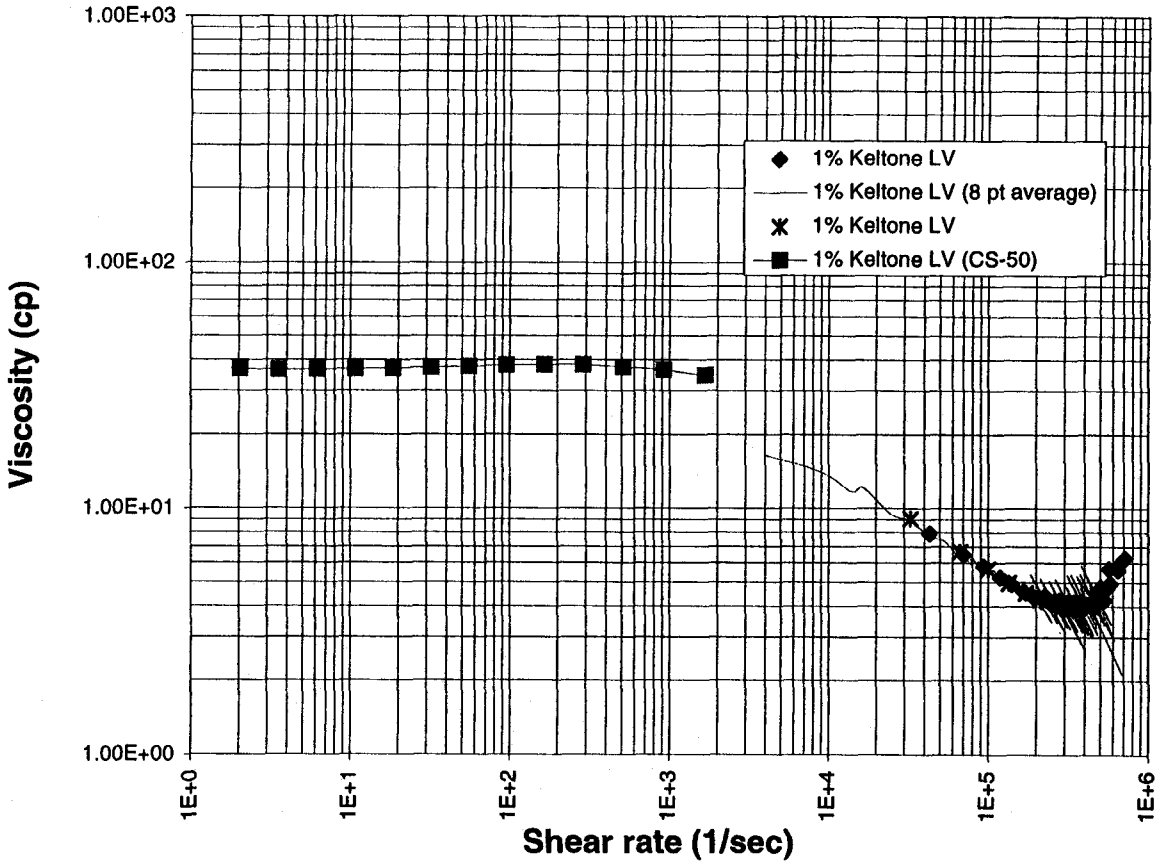

Figure 5.6: Stress Viscometry Test
1.5% Keltone LV
Viscosity vs. Shear Rate

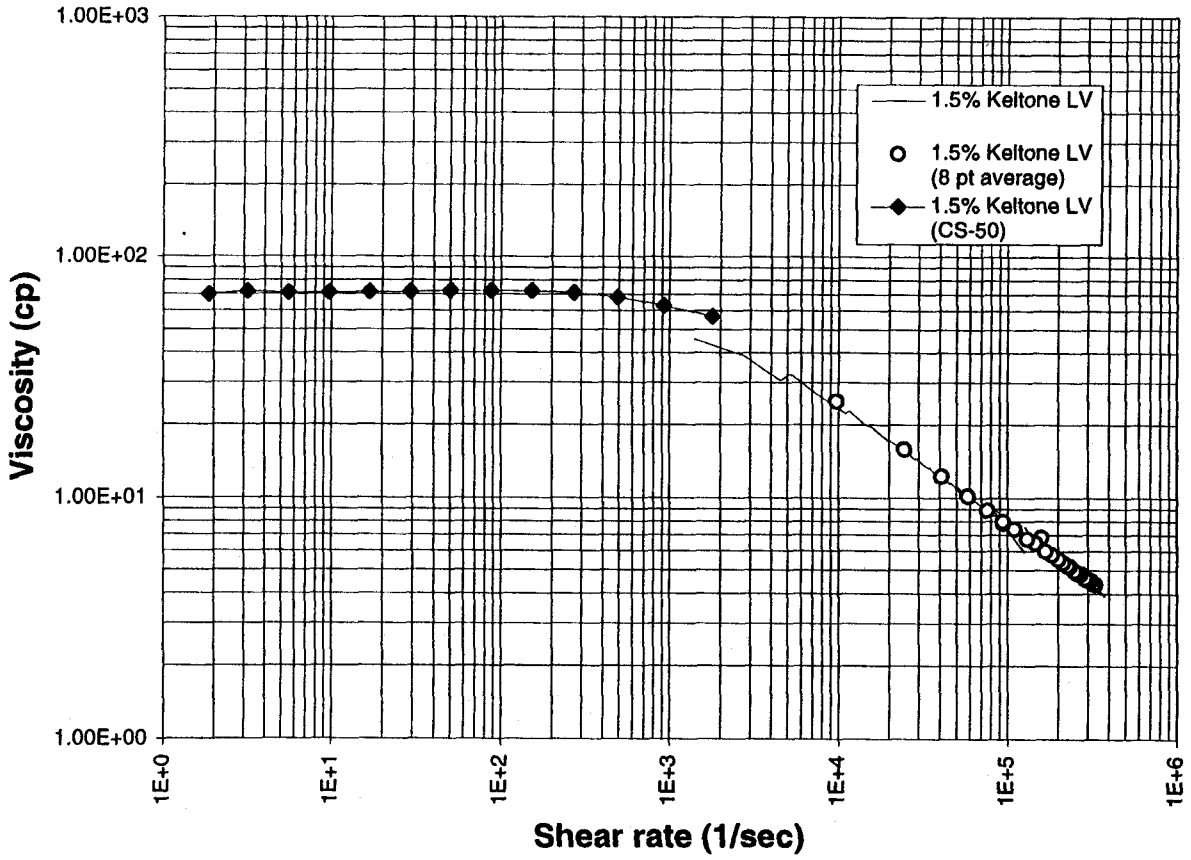

Figure 5.7: Stress Viscometry Test
2% Keltone LV
Viscosity vs. Shear Rate

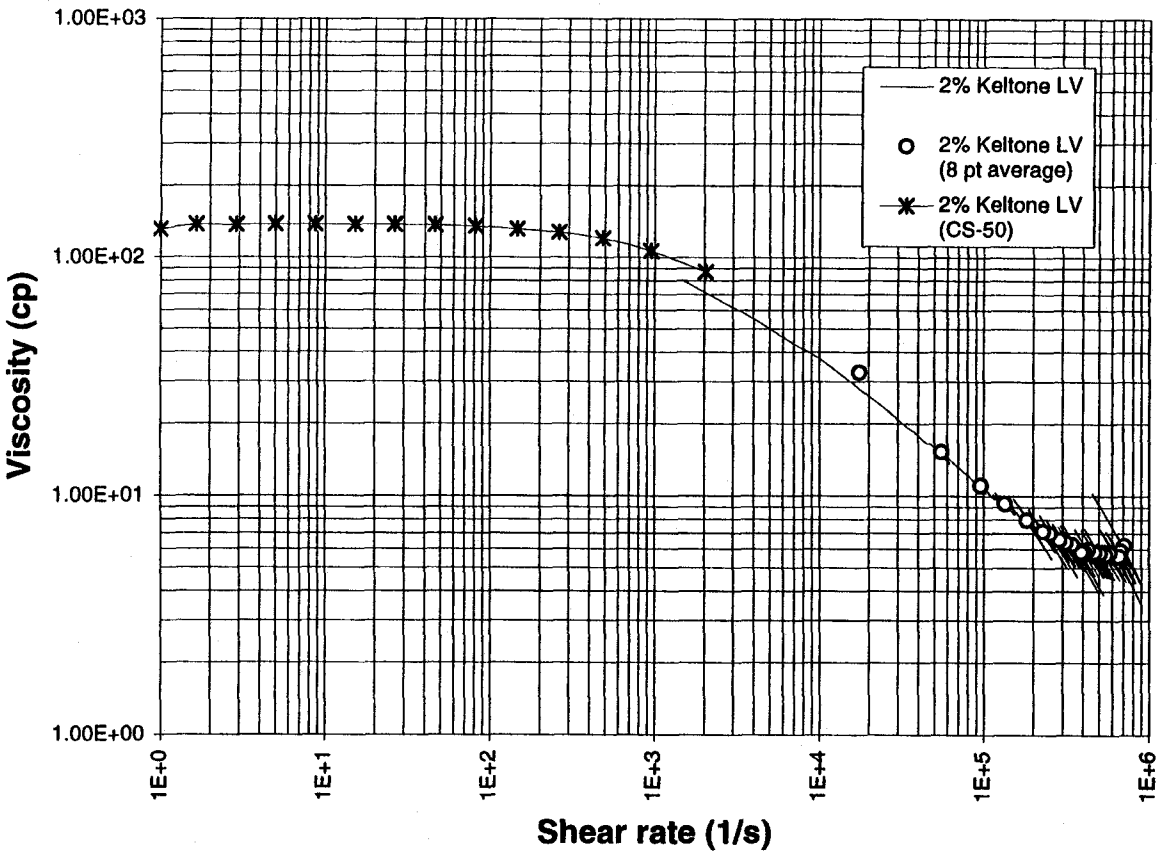

Figure 5.8: Oscillation Test (CS-50)
1% Keltone in DIW, C 25 Geometry

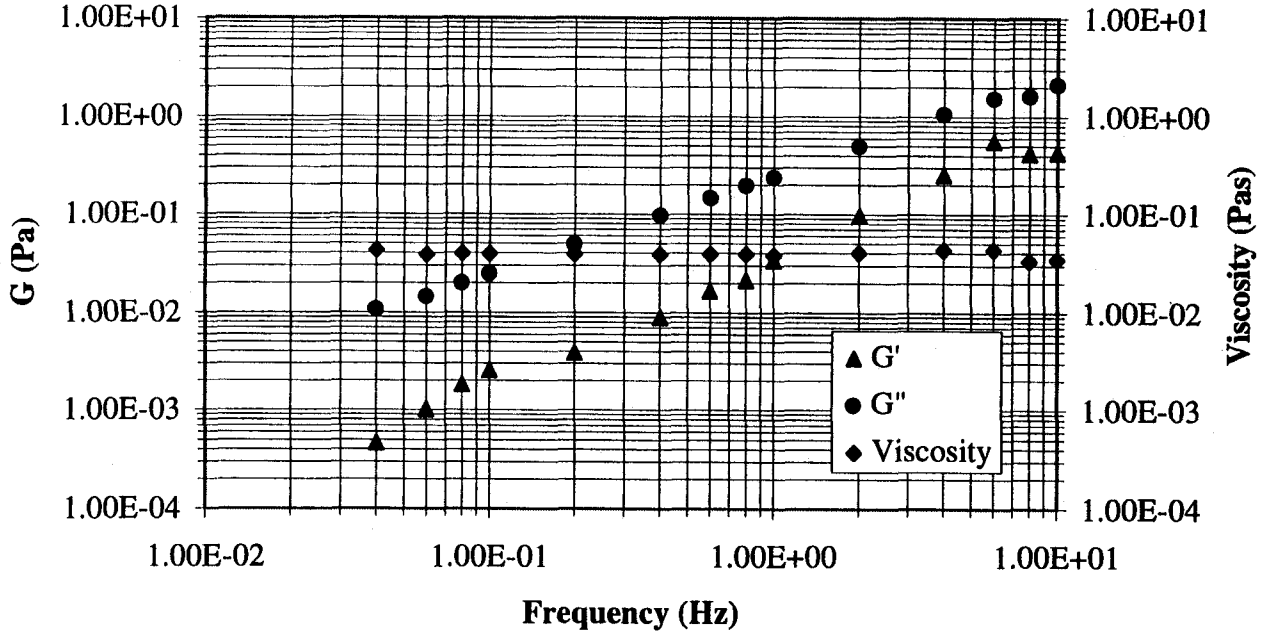

Figure 5.9: Oscillation Test (CS-50)
1.5% Keltone in DIW, C 25 Geometry

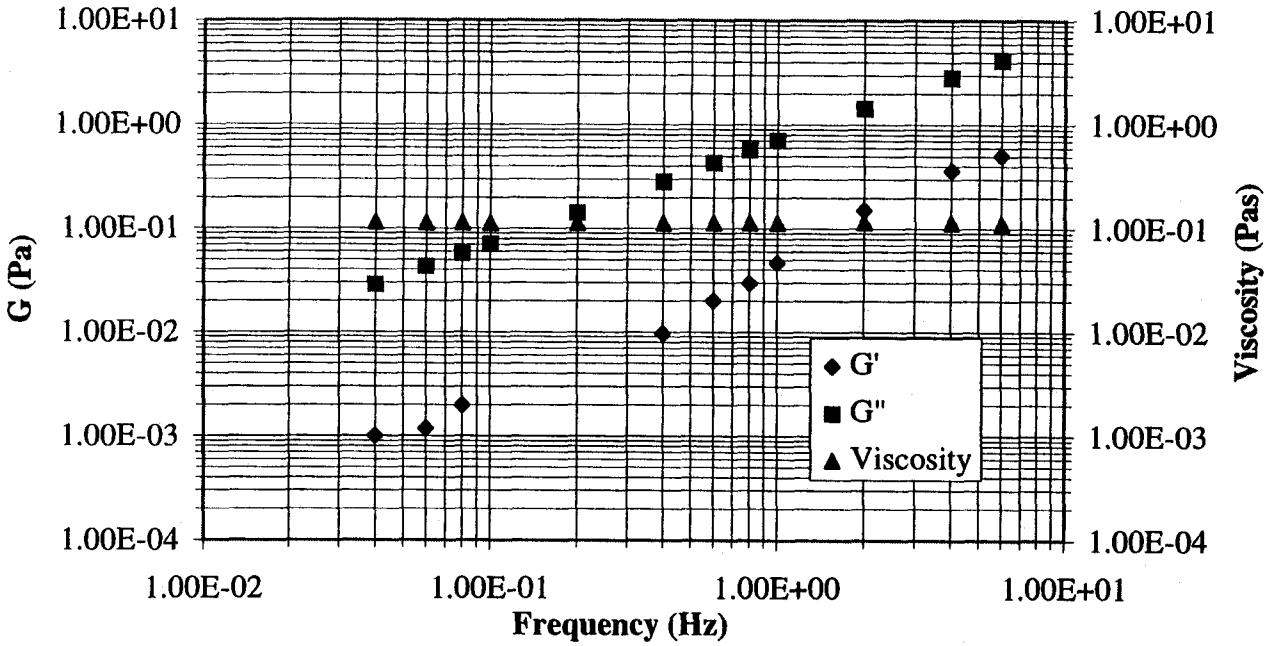

Figure 5.10: Oscillation Test (CS-50)
2% Keltone in DIW, C 25 Geometry

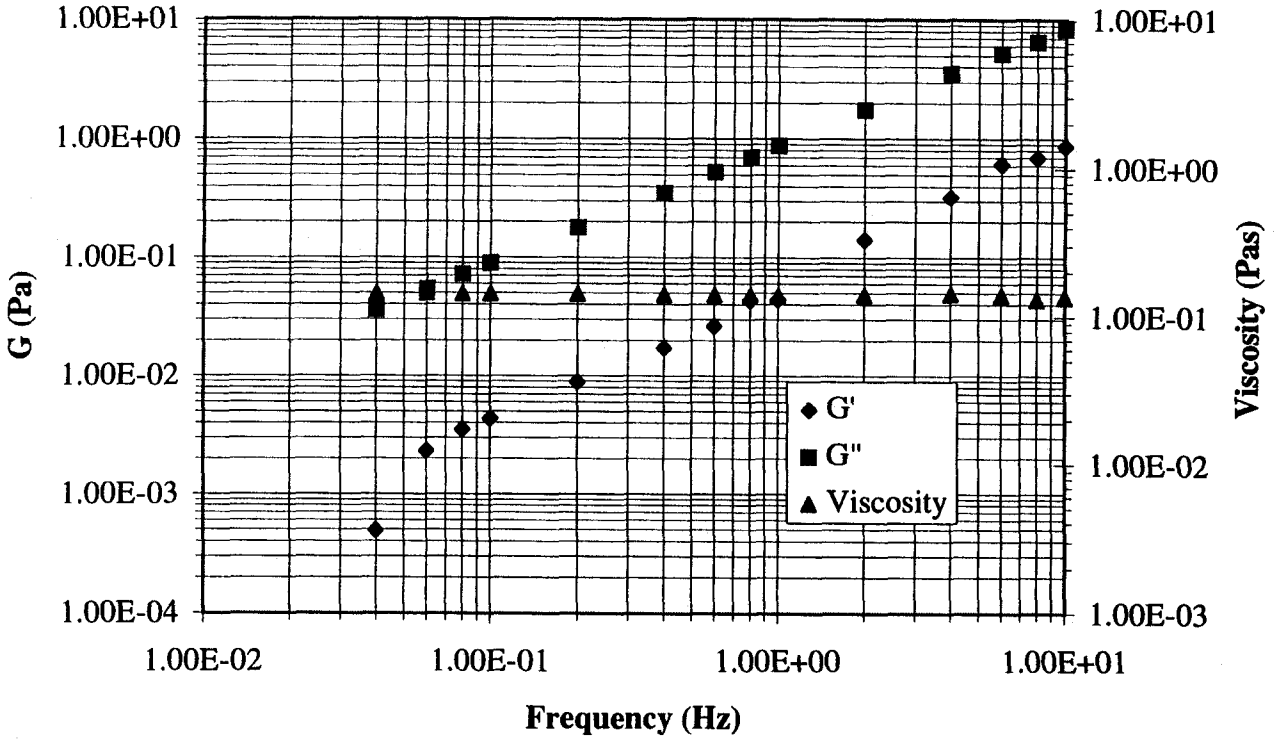

solution and calcium chloride solutions required to for a gel. Figure 5.11., gives the phase diagram for calcium alginate gel with no NaCl present in the alginate solutions while Figure 5.12, is the phase diagram of calcium alginate when 0.1 M NaCl is present in the alginate solution. It can be seen from the two phase diagrams that the presence of NaCl has an observable effect at low concentrations of both algin and calcium chloride concentrations. Also notable is the fact that there are only three specific concentrations at which the gel is homogenous and rigid. From these phase diagrams, it was concluded to use a calcium chloride concentration of 0.1 Molar for all bead generation experiments.

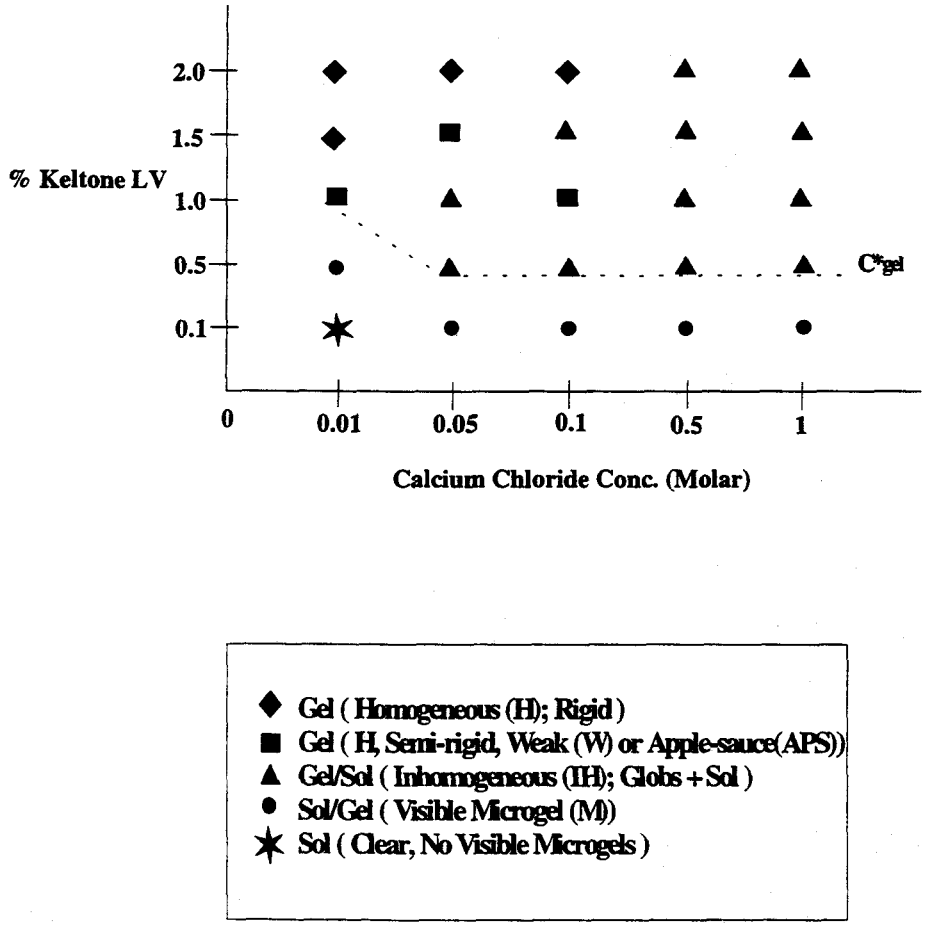

Figure 5.11 : Calcium Alginate (Keltone LV) Gel (No NaCl) Phase Diagram

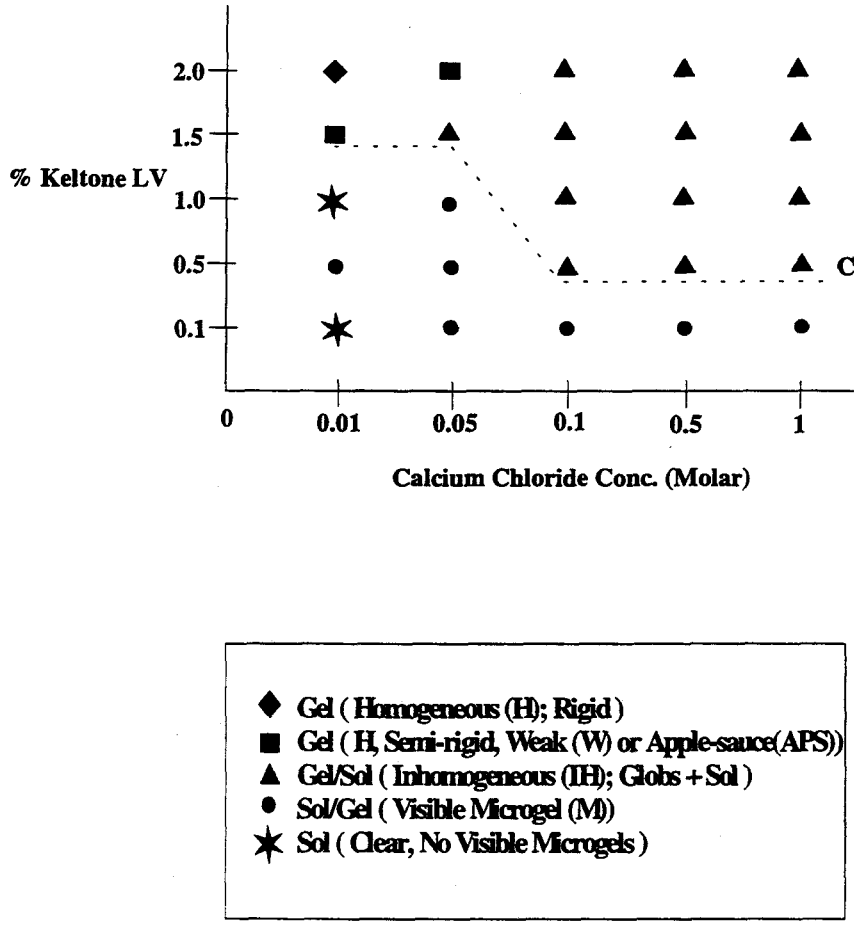

Figure 5.12 : Calcium Alginate (Keltone LV) Gel (in 0.1M NaCl) Phase Diagram

5.4.2 Rheological Results

The time sweep curves for 1.5% Keltone LV and 0.01M $CaCl_2$ Gels (with and without 0.1M NaCl) are given in Figures 5.13 & 5.14. It is clearly seen from the curves, that the gel from algin having NaCl in it has a much lower elastic modulus, G' and is about the same as the viscous modulus, G". On the other hand algin gel which has no NaCl present has a much higher G' as compared to G". This shows that the gels having NaCl in them are weak and more fluid like unlike the stronger, solid like gels formed in

Figure 5.13: Gelation of 1.5% Keltone LV in DIW with 0.01M Calcium Chloride

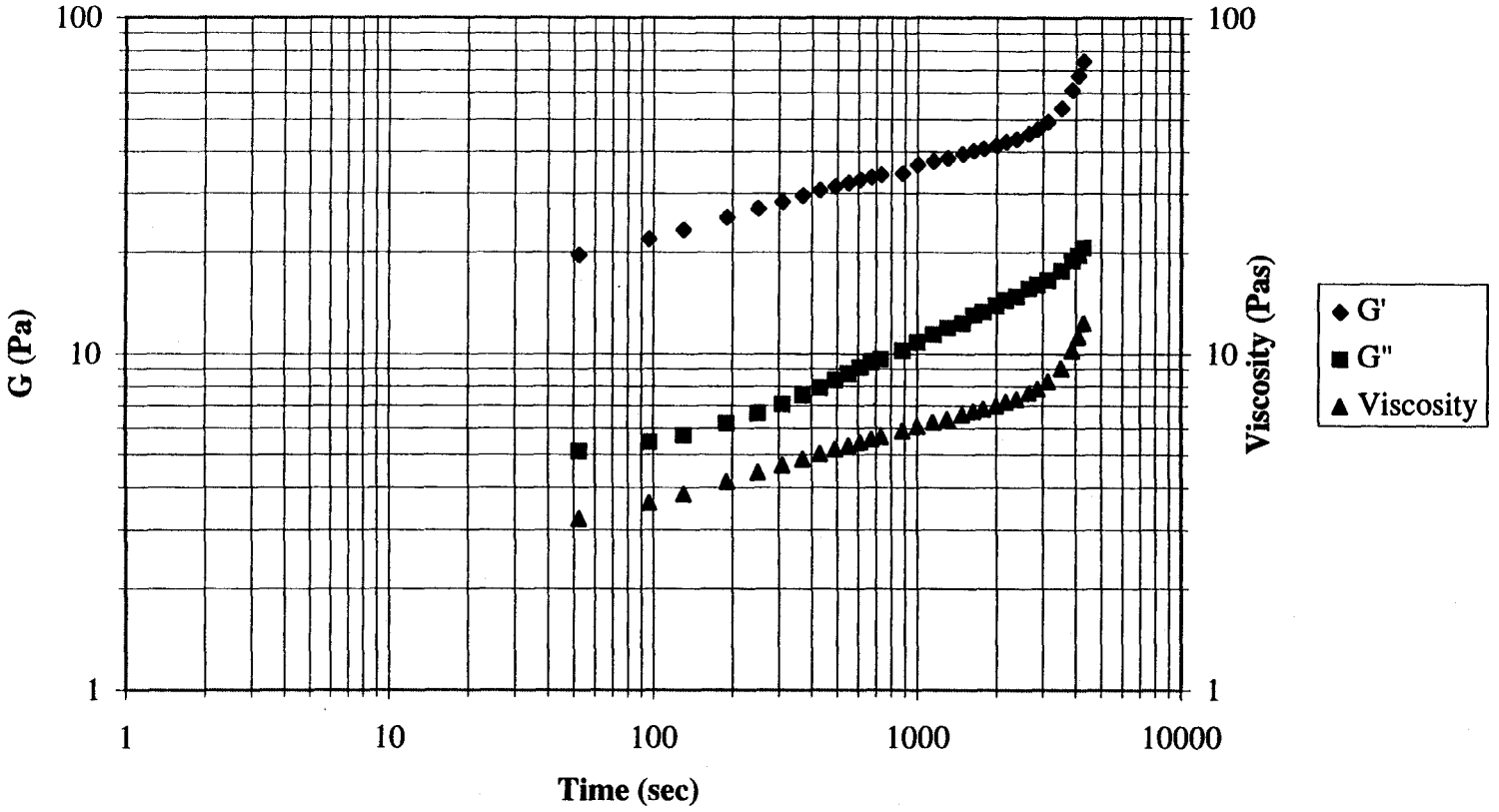

Figure 5.14: Gelation of 1.5% Keltone LV in 0.1M NaCl with 0.01M Calcium Chloride

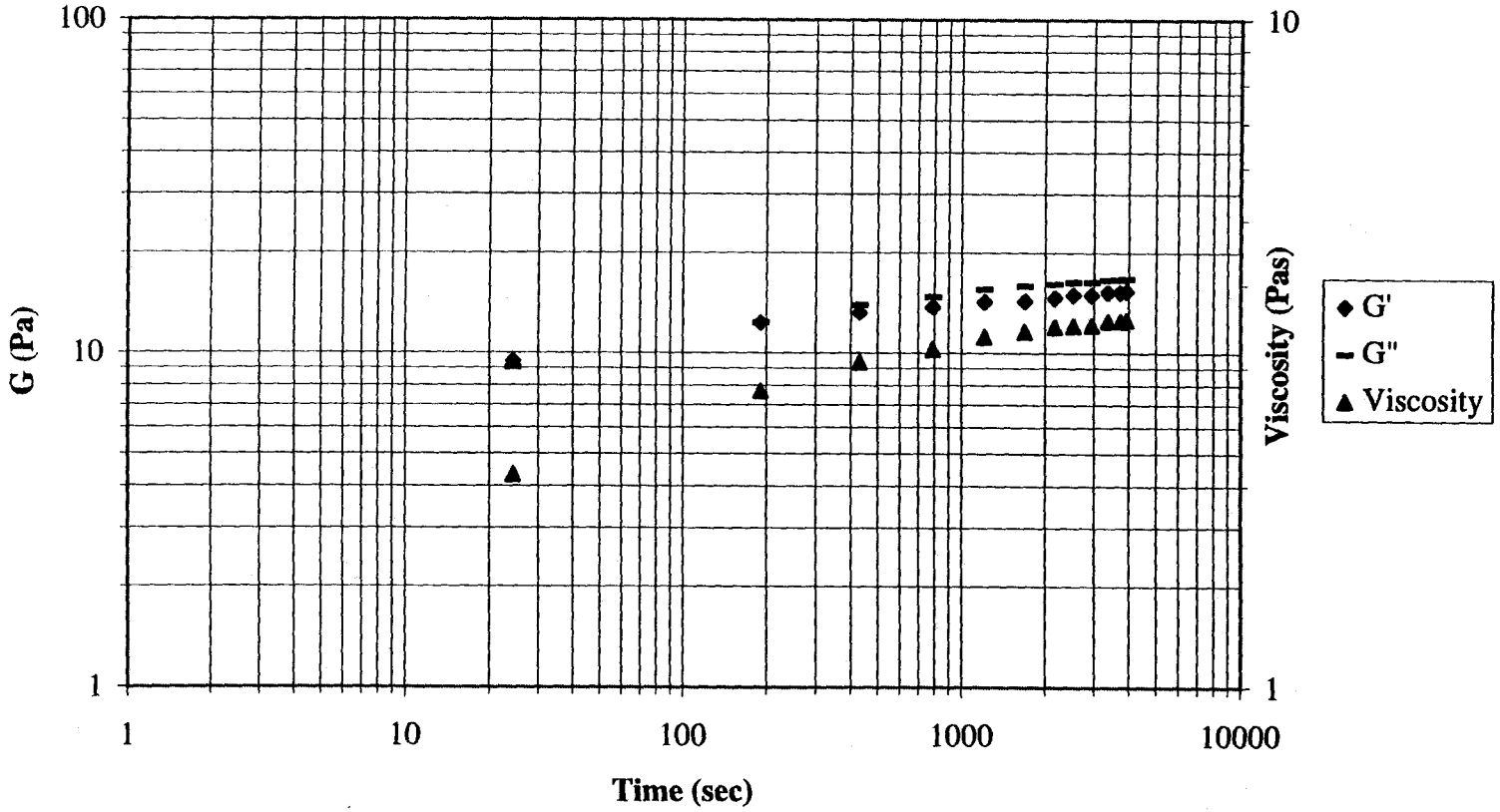

Figure 5.15: Gelation of 2% Keltone LV in 0.1M NaCl with 0.01M Calcium Chloride

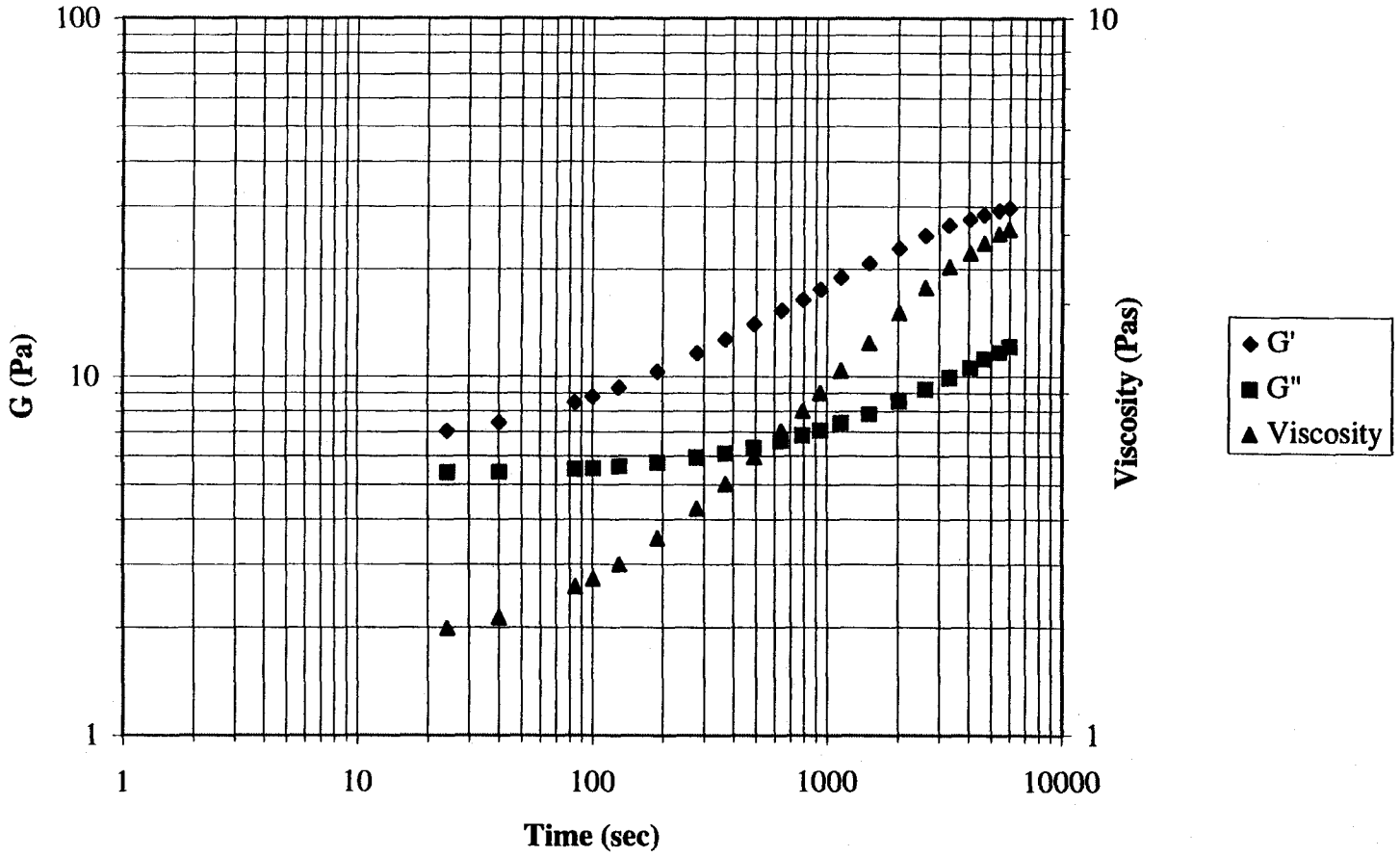

absence of NaCl. This is also reflected by the phase angles. This can be explained by the fact that the monovalent sodium ion is not capable of crosslinking two alginate chain molecules like a divalent calcium ion can do. When present, the sodium ion competes for the bonding spaces, on which otherwise calcium ion would have bonded. It is visualized that when the sodium ion concentration exceeds a certain limit, then its effect on the properties of the gel becomes important. Also gelation takes a longer time when sodium ions are present and the crosslinking of the gel does not increase after a 1000 sec as seen in the absence of sodium chloride.

Results of dynamic experiment on gelation of 2% Keltone LV (0.1 M NaCl) and 0.01M $CaCl_2$ are given in Figure 5.15.

5.5 Conclusions and Recommendations

From our study, it can be concluded that it is possible to produce monodisperse alginate droplets by stimulated jet break-up process. The apparatus is relatively simple to build and can be easily converted to a commercial scale. The bead size can be changed by changing the frequency of vibration and the velocity of the jet. 1%, 1.5%, and 2% Keltone LV solutions can be used to form good spherical monodisperse beads between 160 - 700 microns using the current apparatus. Increasing frequency of vibration or decreasing flowrate of alginate solutions cause the beads to increase in size. The bead size can be predetermined if the operating conditions and the concentration of alginate solutions are known. The bead size tends to become bigger as the concentration of alginate solution is increased. For the same operating conditions, the alginate droplets produced are bigger in size than those formed using Newtonian fluids. Although these alginate droplets are bigger, they start shrinking in size as they crosslink. Some of the preliminary experiments on bead shrinkage show that the beads can shrink by 25% in 5 hours. The beads should be allowed to crosslink for at least 24 hours for them to reach an equilibrium and not change significantly in size.

A detailed study on crosslinking of alginate bead is strongly recommended to determine the affect of different variables like alginate source, alginate concentration in the solution, concentration of sodium ion in sodium alginate solution, type of crosslinking ion (divalent, trivalent etc.), concentration of crosslinking ion, time of gelation, size of alginate solution droplet and temperature.

Also, the phenomenon of stimulated jet break-up should be used to produce sub-100 micron alginate beads with the help of vibrations by piezoceramic crystal. Certain difficulties like orifice clogging etc., can be overcome with a good design of the system.

Further study involving encapsulation and immobilization of biological material needs to be carried out. This will be an area of future research to better understand the process and take it to the commercial front.

Bibliography

Aebischer, P., M. Goddard, R. Timpson, A. Signore, Young A. Beuregard and C. Rampoine, "Polymer encapsulated PC12 cells transplanted in MPTP lesioned primates", *Soc. Neruosci Abstr.*, 16, pg. 963, (1990).

Aebischer, P., L. Wahlberg, P. A. Tesco & S. R. Winn, "Macroencapsulation of dopamine-secreting cells by coextrusion with an organic polymer solution", *Biomaterials*, 12, pg. 50, (1991).

Aebischer, P., M. Goddard, & P. A. Tresco, "Cell encapsulation for the nervous system," In M. F. A. Goosen (Ed.), Fundamentals of animal cell encapsulation and immobilization, Boca Raton, FL: CRC Press, (1992).

Al-Mulhim, M., and G. N. Jovanovic, "Fluidization Regimes, Structure and Porosity of Magnetically Stabilized Liquid-Solid Fluidized Bed", *AIChE Annual Meeting*, paper No: 157d, November 14-18, 1994, San Francisco, (1994).

Araki, N. and A. Masuda, "Production of Droplets of Uniform Size by Vibration", *ICLASS 78*, 8-1, pg. 173-180, (1978).

Atkinson, W. R. and A. H. Miller, "Versatile technique for the Production of Uniform Drops at a Constant Rate and Ejection Velocity", *Rev. Sci. Inst.*, 36, pg. 846-857, (1965).

Barr, E. B., R. L. Carpenter and G. L. Newton, "Improved Liquid Feed System for the Berglund -Liu Vibrating Orifice Mondisperse Aerosol Generation", *Environ. Sci. Technol.*, 18, pg. 721-723, (1984).

Basset, A. B., "Waves and Jets in a Viscous Liquid", *American Journ. Math.*, 16, pg. 93, (1894).

Berglund, R. N. and Benjamin Y. H. Liu, "Generation Of Monodisperse Aerosol Standards", *Environmental Science And Technology*, 7(No.2), (1973).

Bitten, C., & K. C. Marshall, "Adsorption of microorganisms to surfaces", John Wiley & Sons, New York, (1980).

Blaisot, J., M. Ledoux, D. Ducret and J. Vendel, "A New Monosized Drop Generator: Monitoring of Isolated Drop and Drop Packet", *J. Aerosol Sci.*, 25(Suppl. 1), pg. s231-s232, (1994).

Brodelius, P., B. Deus, K. Mosbach, & M. H. Zenk, "Immobilized plant cells for the production and transformation of natural products", *FEBS Lett.*, 103, pg. 93, (1979).

Brown, H. D., *Biochim. Biophys. Acta* , 279, pg. 356, (1972).

Brunner, G., & F. W. Schmidt (eds)., Artificial Liver Support, Springer-Verlag, Berlin, (1981).

Bogy, D. B., "Wave Propagation and Instability in a Circular Semi-infinite Liquid Jet Harmonically Forced at the Nozzle", *J. Appl. Mech*,. 45, pg. 469-474, (1978).

Bousefield, D. W., G. Marrucci, and M. M. Denn, "Dynamics Of Liquid Filament Breakup", *Proc. IX Intl. Congress on Rheology, Mexico*, pg. 239-245, (1984).

Burgarski, B, G. Jovanovic, & G. Vunjak-Novakovic, "Bioreactor systems based on microencapsulated animal cell cultures", In M. F. A. Goosen (Ed.), Fundamentals of animal cell encapsulation and immobilization, Boca Raton, FL: CRC Press, (1992).

Capet-Antonini, F. C., M. Trimard, & S. Tamerasse, *Thromb. Res.*, 2, pg. 479, (1973).

Chang, T. M. S., Methods in Enzymology, Vol 137, Mosbach, K. Ed., Academic Press, New York. (Part D), (1988).

Charauau, J., P. Tierce and M. Birocheau, "The Ultrasonic Generation of Droplets for the Production of Submicron Size Particles", *J. Aerosol Sci.*, 25(Suppl. 1), pg. s233-s234, (1994).

Chibata, I., S. Yamada, M. Wada, N. Izuo, & T. Yamaguchi, "Cultivation of Aerobic Microorganisms," U.S. Patent 3, 850, 753. ,(1974).

Cheetham, P. S. J., K. W. Blunt and C. Bucke, "Physical Studies on Cell Immobilization Using calcium Alginate Gels", *Biotech. and Bioeng.*, 21, pg. 2155-2168, (1979).

Christenson, L., Dionne, K. E., & Lysaght, M. J., "Biomedical applications of immobilized cells", In M. F. A. Goosen (Ed.), Fundamentals of animal cell encapsulation and immobilization, Boca Raton, FL: CRC Press, (1992).

Crane L., S. Birch, and P. D. McCormack, "The Effect of Mechanical Vibration on the Break-up of a Cylinderical Water Jet in Air", *Brit. J. Appl. Phys.,* 15, pg. 743, (1964).

Dabora, E. K., "Production of Monodisperse Sprays", Rev. Sci. Inst., 38(4), pg. 502-506, (1966).

Davis, J. C. (1974), Chem. Eng., 81, 52, (Aug 19, 1974).

Denn, M. M. and Rene'e Van De Griend, "Co-Current Axisymmetric Flow In Complex Geometries: Experiments", *JNNFM* , 32, pg. 229-252, (1989).

Dimmock, N. A., "Production of Uniform Droplets", *Nature*, 166, pg. 686-687, (1950).

Ferry, J. D., "Viscoelastic Properties of Polymers", 2nd Edition, John Wiley Inc., (1970).

Flanagan, T. R., M. P. Lavoie, F. A. Kaplan, W. J. Bell, M. A. Palmatier, F. T. Gentile, & P. R. Sanberg, "An encapsulated PC12 cell line releases levodopa constitutively *in vitro", Soc. Neurosci. Abstr.,* 17, pg. 569, (1991).

Flynn, A. & D. B. Johnson, *International Journal of Biochm.* 8, pg. 507, (1977).

Fuller, K. W., & D. J. Bartlett, *Annu. Proc. Phytochem Soc. Eur.*, 26, pg. 229, (1985).

Gavis, J., "Contribution of Surface Tension to Expansion and Contraction of Capillary Jets", *Physics of Fluids*, 7, pg. 1097, (1964)

Gilson, C. D., A. Thomas and F. R. Hawkes, "Gelling Mechanism of Alginate Beads with and without Immobilized Yeast", *Process Biochem. International*, pg 104-108, June (1990).

Gilson, C. D. and A. Thomas, "Calcium Alginate Bead Manufacture: With and Without Immobilized yeast. Drp Formation at a Two-Fluid Nozzle", *J. Chem. Tech. Biotechnol.*, 62, pg. 227-232, (1995).

Goedde, E. F., and M. C. Yuen, "Experiments on Liquid Jet Instability, *J. Fluid Mech.*, 40(3), pg. 495-511, (1970).

Goetz, C. G., C. W. Olanow, W. C. Koller, R. D. Penn, D. Cahill, R. Morantz, G. Stebbins, C. M. Tanner, H. L. Klawans, K. M. Shannon, C. L. Comella, T. Witt, C. Cox, M. Waxman, & L. Gauger, "Multicenter study of autologous adrenal medullary trnsplantation to the corpus striatum in patients with advanced Parkinson's disease", *N. Engl. J. Med.*, 320, 337, (1989).

Goosen, M. F. A., Geraldine M. O'Shea, Hrire M. Gharapetian and Sheng Chou, "Optimization Of Microencapsulation Parameters: Semipermeable Microcapsules As A Bioartificial Pancreas", *Biotech. and Bioengg.*, 27, pg. 146-150, (1985).

Goren, S. L., "The Shape of a Thread of Liquid Undergoing Break-up", *J. of Colloid Sci.*, 19, pg. 81-86, (1964)

Goren, S. L. and S. Wronski, "The Shape of Low-speed Capillary Jets of newtonian Liquids", *J. Fluid Mech.*, 25, pg. 185, (1966).

Goren, S. L. and M. Gottlieb, "Surface-tension-driven breakup of viscoelastic liquid threads", *J. Fluid Mech.*, 120, pg.245-266, (1982).

Greene, L. A., & G. Rein, "Release, storage, and uptake of catecholamines by a clonal cell line of nerve growth factor (NGF) responsive pheochromocytoma cells", *Brain Res.,* 129, 247, (1977).

Haas, F. C., "Stability of Droplets Suddenly Exposed to a High Velocity Gas Stream", *A.I.C.H.E. Journal,* 10(6), pg. 920-924, (1970).

Haas, P. A., "Formation of Liquid Drops with Uniform and Controlled Diameters at Rates of 1000 to100000 Drops Per Minute", *AICHE Journal,* vol. 21(No.2), pg.383-385, (1975).

Harmon, D. B., "Drop Sizes from low speed jets", *J. of Franklin Inst.,* 259, pg. 519, (1955).

Hendricks, C. D. and J. B. Y. Tsui, "Production of Uniform Droplets by Means of an Ion Drag Pump", *Rev. Sci. Instrum.,* 39, pg. 1088, (1968).

Herring, W. M., Lawrence, R. L., & Kittrell, J. R., *Biotechnol. Bioeng.* 14, pg.. 975, (1972).

Hicks, C. L., *J. Dairy Sci.,* 58, 177, (1974).

Hoffman, D., X. Breakefield, P. Short, & P. Aebischer, "Transplantation of polymer encapsulated NGF-releasing cells prevents lesion-induced reduction ChAT expression by septal cells", *Soc. Neuroschi. Abst.,* 17, 570, (1991).

Hudson, B. J. F., *Chemical Ind.,* 20, 1059, (1975).

Huguet, H. L. , A. Groboillot, R. J. Neufeld, D. Poncelet and E. Dellacherie, "Hemoglobin Encapsulation in Chitosan/Calcium Alginate Beads", *J. of Applied Polymer Science,* 51, pg. 1427-1432, (1994).

Jaeger, C. B., L. A. Green, P. A. Tresco, S. R. Winn, & P. Aeb ischer, "Polymer encapsulated dopaminergic cell lines as alternative grafts", *Progress in Brain Research,* Vol 82, 41, (1990).

Karsa & R. A. Stephenson, (Eds)., "Encapsulation and Controlled Release", Manchester, UK: The Royal Society of Chemistry.

King, G. A., & M. F. A. Goosen, "Cell immobilization technology: An overview", In M. F. A. Goosen (Ed.), Fundamentals of animal cell encapsulation and immobilization. Boca Raton, FL: CRC Press, (1992).

Knusel, B., J. W. Winslow, A. Rosental, L. Burotn, D. P. Seid, K. Nikolics, & F. Hefti, "Promotion of central cholinergic and dopaminergic neuron differentiation by brain-derived neurotrophic factor but not neurotrophin 3", *Proc. Natl. Acad. Sci. U. S. A.*, 88, 961,(1991).

Kolot, F. B., "Immobilized Microbial systems: Principles, Techniques and Industrial Applications", Robert E. Krieger, Malabar, FL, (1988).

Kurabayashi, T. and T. Karasawa, "Production of Uniform Droplets by Non-Circular Nozzles", *The 2nd International Conference on Liquid Atomization and Spray Systems*, June 20-24, (1982).

Lacy, P. E., "Treat diabetes with transplanted cells", *Scientific American*, (1995).

Lee, E. C. , Senyk, G. F. & Shipe, W. F., *J. Dairy. Sci.*, 58, 473, (1975).

Lim, F., & A. M. Sun, *Science,* 210, 908, (1980).

Lim, F., "Biomedical applications of microencapsulation", CRC Press, Boca Raton, FL 137, (1983).

Lin, H. B., J. D. Eversole and A. J.Campillo, "Vibrating Orifice Droplet Generator For Precision Optical Studies," *Rev. Sci. Instrum.*, 62(3), pg 1018-1023, (1990).

Lindblad, N. R. and J. M. Schneider, "Production of Uniform-sized Liquid Drops", *J. Sci Instrum.*, 42, pg. 635, (1965).

Liu, Y. H., D. Y. H. Pui and Xian-Qing Wang, "Drop Size Measurement Of Liquid Aerosols", *Atmos. Environ.*, 16(No.3), pg. 563-567, (1982).

Madrazo, I., Colin R. Drucker, V. Diaz, Mata J. Martinez, C. Torres & J. Becerril, "Open microsurigcal autograft of adrenal medulla to the right caduate nucleus in two patients with intractable Parkinson's disease", *N. Engl. J. Med.*, 316, 831, (1987).

Magarvey, R. H. and B. W. Taylor, "Apparatus for the Production of Large water Drops", *Rev. Sci. Instrum.*, 27(11), pg 944-947, (1956).

Manecke, G. , G. Gunzel, & H. J. Forster, *J. Polym. Sci. Part* , 30, 607, (1970).

Maugh, T. H., *Science*, 223, 474, (1984).

Merrington, A. C. and E. G. Richardson, "The Break-up of Liquid Jets", *Proc. Phys. Soc.*, 59, pg. 1, (1947).

Middleman, S. and J. Gavis, "Expansion and Contraction of Capillary Jets of Newtonian Liquids", *The Physics of Fluids,* 4(3), pg. 355, (1961).

Mosbach, K., & R. Mosbach, "Entrapment of enzymes and microorganisms in synthetic cross-linked polymers and their application in column techniques", *Acta Chem. Scand,* 20, 2807, (1966).

Musarra, S., and R. Keunings, "Co-current Axisymmetric Flow In Complex Geometries: Numerical Solution", JNNFM, 32, pg.253-268, (1989).

Nilsson, K., & K. Mosbach, "Preparation of immobilized animal cells", *FEBS Lett.*, 118(1), 145, (1980).

Poncelet De Smet, B., D. Poncelet, & R. Neufeld, "Emerging techniques, materials, and applications in cell immobilization", In M. F. A. Goosen (Ed.), Fundamentals of animal cell encapsulation and immobilization. Boca Raton, FL: CRC Press, (1992).

Potter K., T. A. Carpenter, and L. D. Hall, "Mapping of the spatial variation in alginate concentration in calcium alginate gels by magnetic resonance imaging (MRI).", *Carbohydrate Research,* 246, pg. 43-49, (1993).

Potter K., B. J. Balcom, T. A. Carpenter, and L. D. Hall, "The gelation of sodium alginate with calcium ions studied by magnetic resonance imaging (MRI)", *Carbohydrate Research,* 257, pg. 117-126, (1994).

Rayleigh, Lord, "On the Instability of Jets", *Proc. London Math. Soc.,* 10, pg. 4, (1878).

Rayleigh, Lord, "On the Capillary Phenomena of Jets", *Proc. Roy. Soc. (London),* 29, pg. 71, (1879).

Rayleigh, Lord, "On the Instability of a Cylinder of Viscous Liquid under Capillary Force", *Phil. Mag.* S.5, 34(207), pg. 145, (1892).

Rehg, T. , C. Dorger, and P. C. Chau, "Application Of An Atomizer In Producing Small Alginate Gel Beads For Cell Immobilization", *Biotech. Letters*, 8, pg.115.

Rochefort,W. E., T. Rehg and P. C. Chau, "Trivalent Cation Stabilization Of Alginate Gel For Cell Immobilzation", *Biotechnology Letters* , 8(No. 2), pg.115-120, (1986).

Ryley, D. J. and M. R. Wood, "The Construction and Operating Characteristics of a New Vibrating Capillary Atomizer", *J. Sci. Instrum.*, 40, pg. 303, (1963).

Saki, T. and N. Hoshino, "Production of Uniform Droplets by Logitudinal Vibration of Audio Frequency", *J. of Chemical Engineering of Japan*, 13(4), pg. 263-268, (1980).

Schact, E., J. C. Vandichel, A. Lemahieu, N. De Rooze, & S. Vansteenkiste, "The use of gelatin and alginate for the immobilization of bioactive agents", In D. R. Karsa & R. A. Stephenson, (Eds)., Encapsulation and Controlled Release. Manchester, UK: The Royal Society of Chemistry, (1993).

Schneider, J. M., and C. D. Hendricks, "Source of Uniform-Sized Liquid Droplets", *The Review Of Scientific Instruments*, 35(No.10), pg. 1349-1350, (1964).

Schummer, P. and K. H. Tebel, "A New Elongational Rheometer For Polymer Solutions", *JNNFM*,12, pg.331-347, (1983).

Schummer, P. and K. H. Tebel, "Design And Operation Of The Free Jet Elongational Rheometer", *Rheol. Acta.*, 21, pg. 514-516, (1982).

Schummer, P. and H. G. Thelen, "The Relaxation times Of Polymer Solutions Investigated In Extensional Flow", *Proc. IX Intl. Congress on Rheology, Mexico*, (1984).

Shuler, M. L., "Production of secondary metabolites from plant tissue culture: Problems and prospects", *Ann. N.Y. Acad. Sci.*, 369, 65 (1981).

Slamovich, E. B. and F. F. Lange, "Spherical Zirconia Particles Via Electrostatic Atomization: Fabrication And Sintering Characteristics", *Mat. Res. Soc. Symp. Proc.*, 121, (1988).

Smidsrod O., S. T. Moe, G. Skjak-Braek, and A. Elgsaeter, "Swelling of covalently crosslinked alginate gels: influence of ionic solutes and non-polar solvents.", *Macromolecules*, Vol. 26, No. 14, pg. 3589-3597, (1993).

Smidsrod O., S. T. Moe, G. Skjak-Braek, and Draget K.I., "Temperature dependence of the elastic modulus of alginate gels.", *Carbohydrate Polymers*, Vol. 19, pg. 279-284 (1992).

Smidsrod O., S. T. Moe, G. Skjak-Braek, and Ichijo H., "Calcium alginate fibers: influence of alginate source and gel structure on fiber strength.", *J. of Applied Polymer Science*, Vol. 51, pg. 1771-1775, (1994).

Sterling, A. M. and C. A. Sleicher, "The Instability of Capillary Jets", *J. Fluid Mech.*, 68(3), pg. 477-495, (1975).

Strom, Lars, "The Generation of Monodisperse Aerosols by Means of a Disintegrated Jet of Liquid", *The Review Of Scientific Instruments*, 40(No.6), pg. 778-782, (1969).

Svenson, A., & Andersson, *Anal. Biochem.* 83, 739, (1977).

Teng, H., C. M. Kinoshita and S. M. Masutani, "Prediction of Droplet Size from the Break-up of Cylinderical Liquid Jets", *Int. J. Multiphase Flow*, 21(1), pg. 129-136, (1995).

Tramper, J., "Immobilizing Biocatalysts For Use In Synthesis", *Trends in Biotechnology,* 3(No.2), (1985).

Tresco, P. A., S. R. Winn, B. Zielinski, C. B. Jaeger, L. A. Greene, & P. Aebischer, "Reversal of behavioral recovery following the removal of polymer encapsulated", *Soc. Neuroschi. Abstr,* 17, 1077, (1991).

Wang Z., Q. Zhang, M. Konno, and S. Saito, "Sol-gel transition of alginate solution by the addition of various divalent cations: a rheological study", *Biopolymers*, Vol. 34, pg. 737-746, (1994).

Warnica, W. D., M. V. Reenen, M. Renksizbulut and A. B. Strong, "Charge Synchronization for a Piezoelectric Droplet Generator", *Rev. Sci. Instrum.*, 64(8), pg. 2334-2339, (1993).

Wang Z., Q. Zhang, M. Konno, and S. Saito, "Sol-gel transition of alginate solution by the addition of various divalent cations: C-NMR spectroscopic study", *Biopolymers*, Vol. 33, pg. 703-711, (1993).

Wang Z., Q. Zhang, M. Konno, and S. Saito, "Sol-gel transition of alginate solution by additions of various divalent cations: critical behavior of relative viscosity", *Chemical Physics Letters*, Vol. 186, pg. 463-466, (1991).

Wedding, J. B. and J. J. Stukel, "Operational Limits of Vibrating Orifice Aerosol Generator", *Environmental Science & Technology*, 8(5), pg. 456-457, (1974).

Wedding, J. B., "Operational Characteristics of the Vibrating Orifice Aerosol Generator", *Environmental Science & Technology*, 9(7), pg. 673-674, (1975).

Whateley, T. L., "Biodegradable Microspheres for Controlled Drug Delivery", In D. R. Karsa & R. A. Stephenson, (Eds)., Encapsulation and Controlled Release. Manchester, UK: The Royal Society of Chemistry, (1993).

Winn, S. R., S. A. Tan, P. A. Tresco, J. Sagen, & P. Aebischer, "Striatal transplantation of bovin chromaffin cell-load microcapsules reduces experimental Parkinsonism in rats", *Soc Neurosci. Abstr.*, 17, 1077, (1991).

Winn, S. R., P. A. Tresco, B. Zielinski, L. A. Greene, C. B. Jaeger, & P. Aebischer, "Behavioral recovery following intrastriatal implanttion of microencapsulated PC 12 cells", *Exp. Neruol.*, 113, 322, (1991).

Yamamoto, K., T. Tosa, & T. Sato, "Continuous production of L-malic acid by immobilized *Brevibacterium ammoniagenes* cells", *Eur. J. Appl. Microbiol.*, 3, 169, (1976).

Zekorn, T., U. Siebers, U. Zimmermann, C. Klenke, R. G. Bretzel, & K. Federlin, "Successful xenotransplantation of islets in 2 strains of diabetic mice by use of Ba2+ alginate-microcapsules", *Diabetes*, 40, (Suppl 1), 285A, (1991).

Zia, H., T. E. Needham, & L. A. Luzzi, "Why infusion and not microcapsules or other controlled release methods?", In D. R. Karsa and R.A. Stephenson's Encapsulation and Controlled Release, Cambridge, U.K.: The Royal Society of Chemistry, (1993).

APPENDICES

APPENDIX A

Figure A-1 Bimodal Distribution
Satellite Formation
2% Keltone LV, Orifice 202.8 microns,
Flow rate 7 ml/min, Frequency 250Hz.

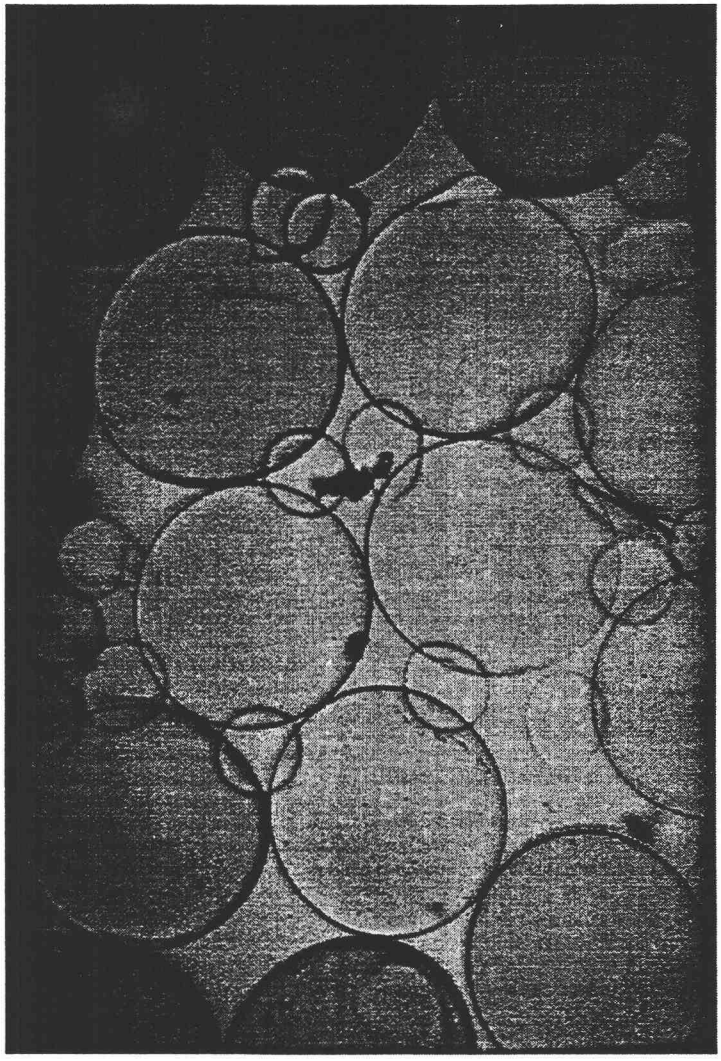

Figure A-2 Monodisperse Distribution
2% Keltone LV, Orifice 202.8 microns,
Flow rate 7 ml/min, Frequency 550Hz.

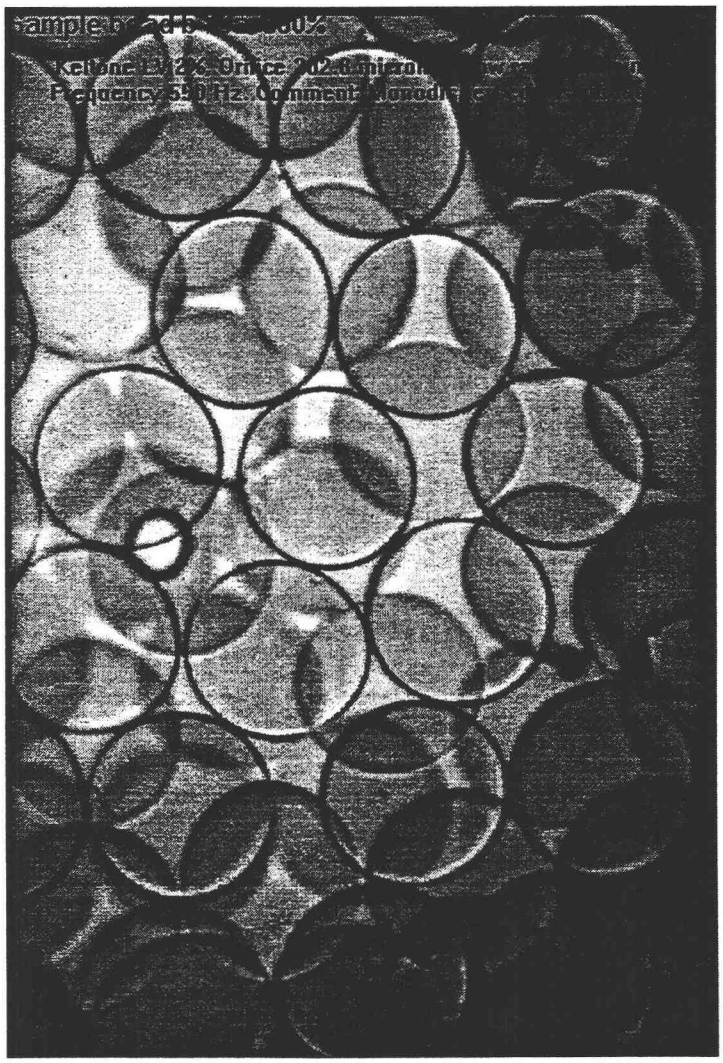

Figure A-3 Bimodal Distribution
2% Keltone LV, Orifice 202.8 microns,
Flow rate 7 ml/min, Frequency 250Hz.

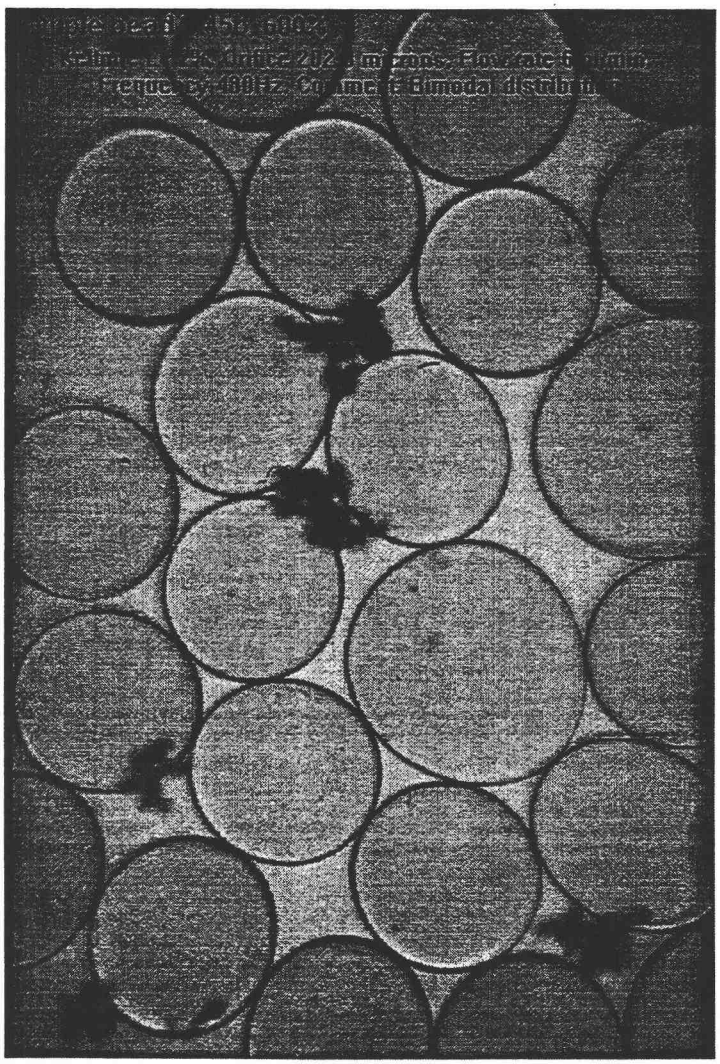

APPENDIX B

Figure B-1 Calcium Alginate Beads Produced From Axial Vibrating Diaphragm Droplet Generator

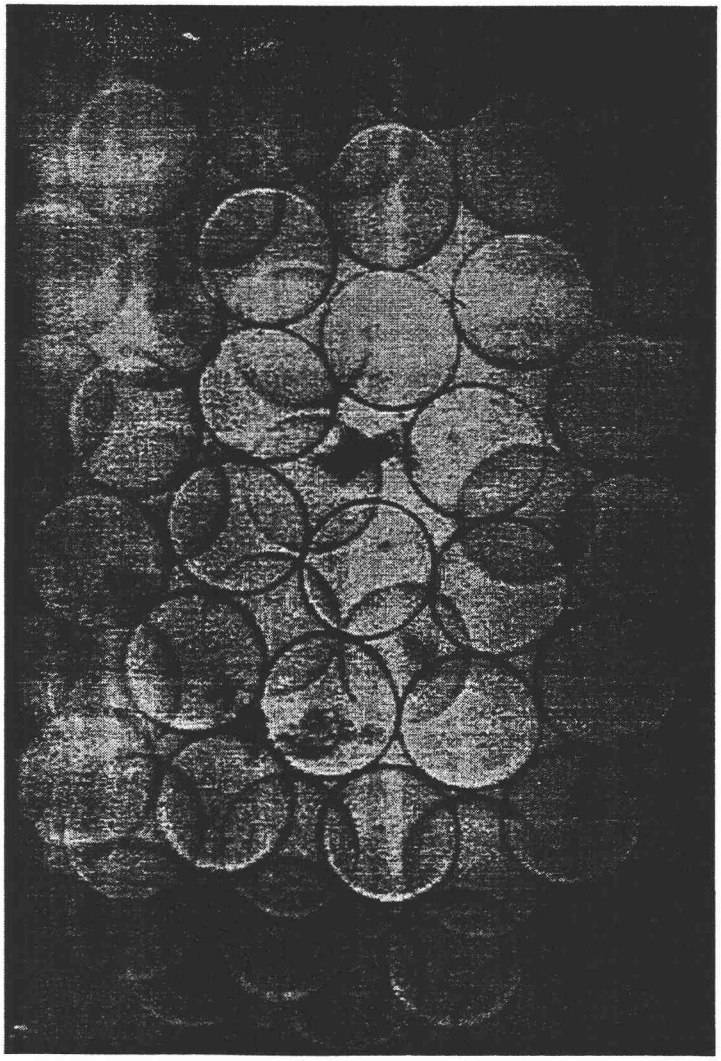

Figure B-2 Calcium Alginate Beads Produced From Axial Vibrating Diaphragm Droplet Generator

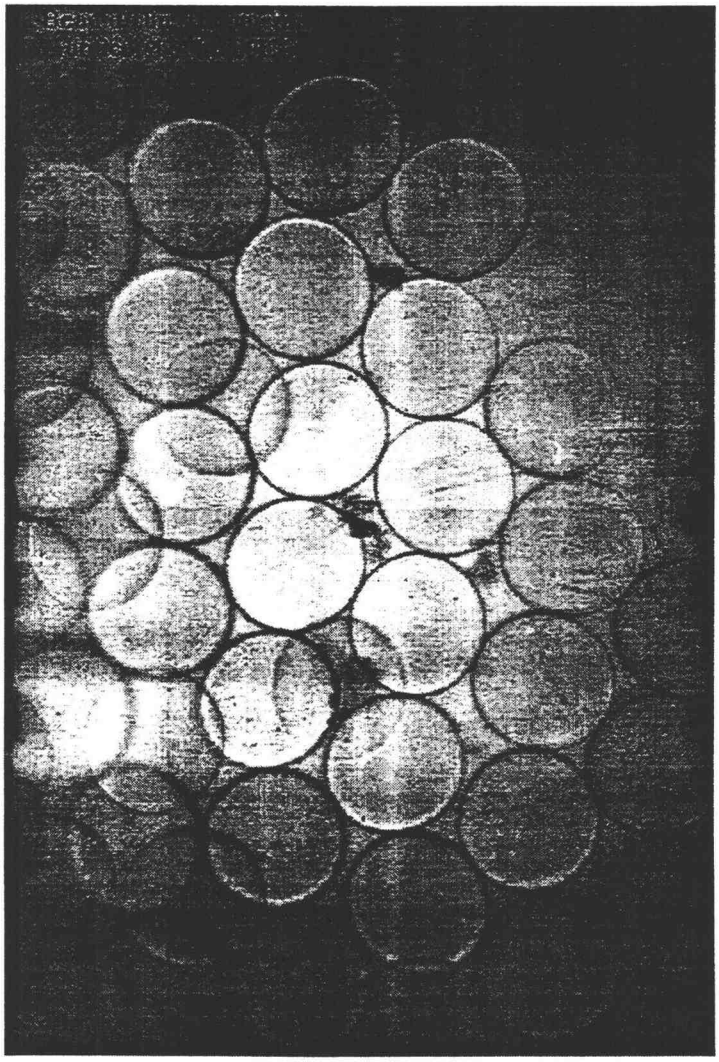

Figure B-3 **Calcium Alginate Beads Produced From Axial Vibrating Diaphragm Droplet Generator**

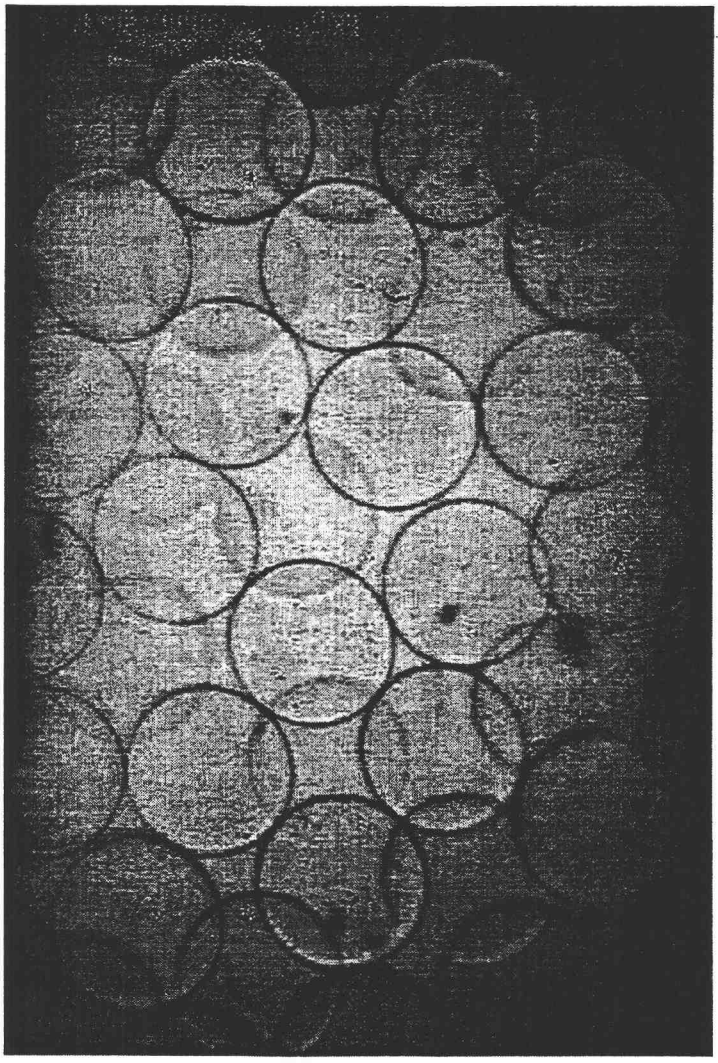

Figure B-4 Alginate Jet Breakup
Long Wavelengths, Minimum Amplitude

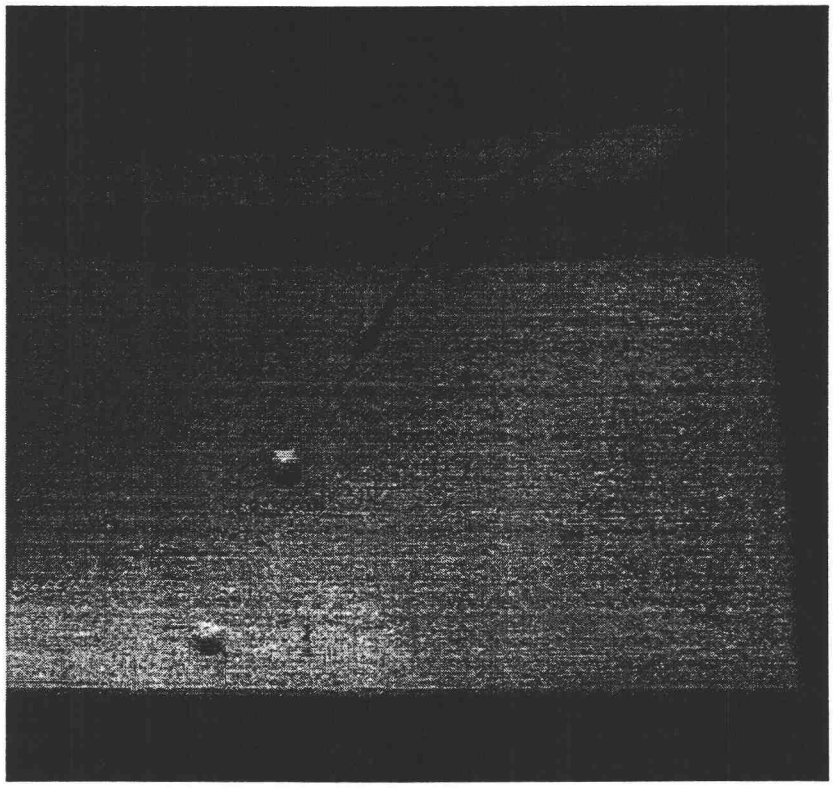

Figure B-5 Alginate Jet Breakup
Long Wavelengths, Large Amplitude
Satellite Formation

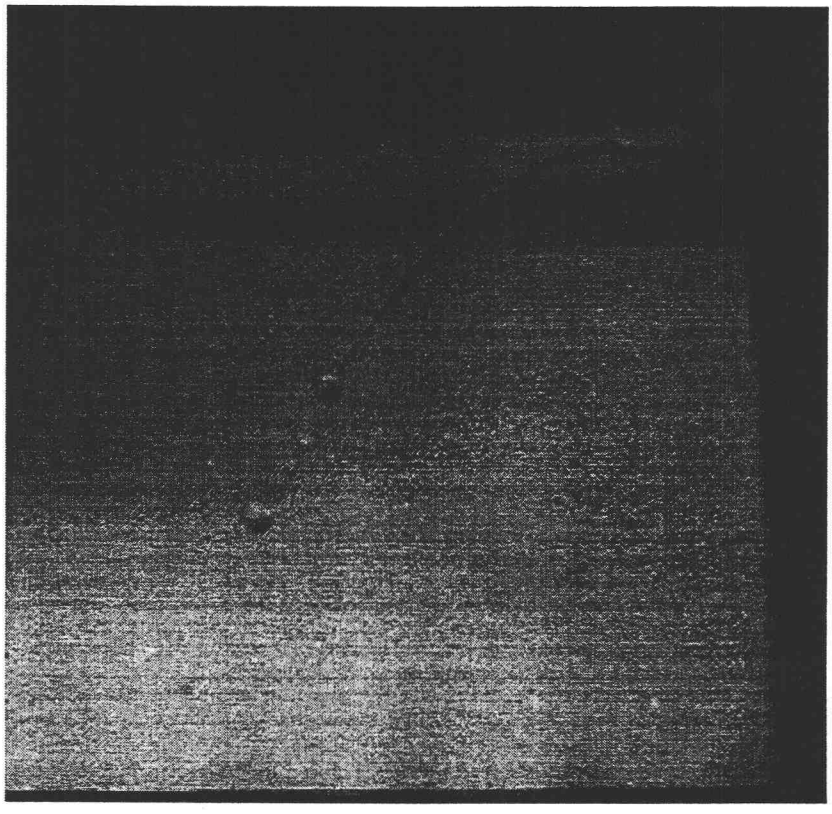

Figure B-6 Alginate Jet Breakup
Short Wavelengths, Large Amplitude

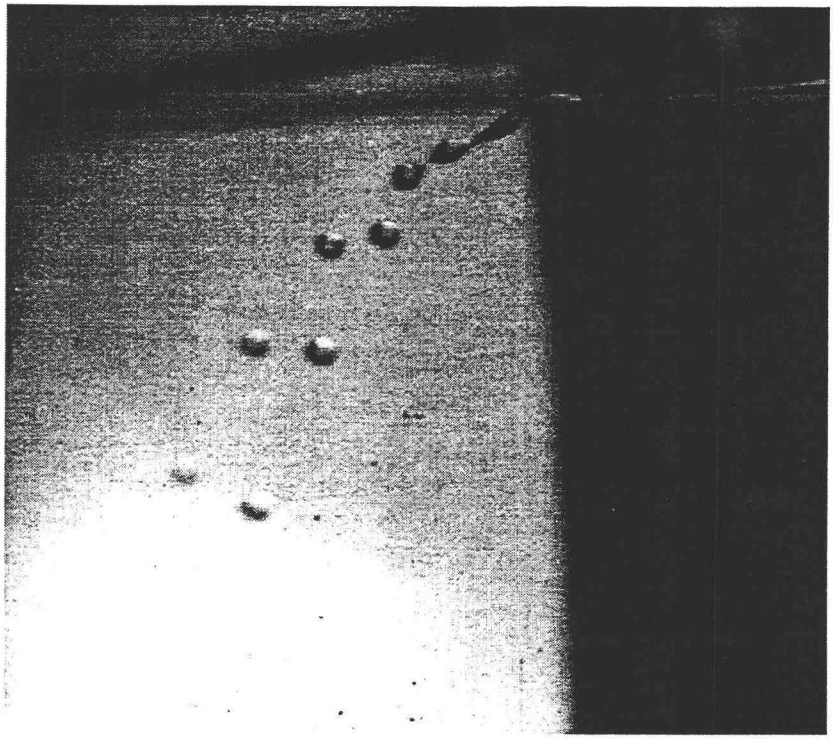

Figure B-7 Keltone LV 2% Droplet

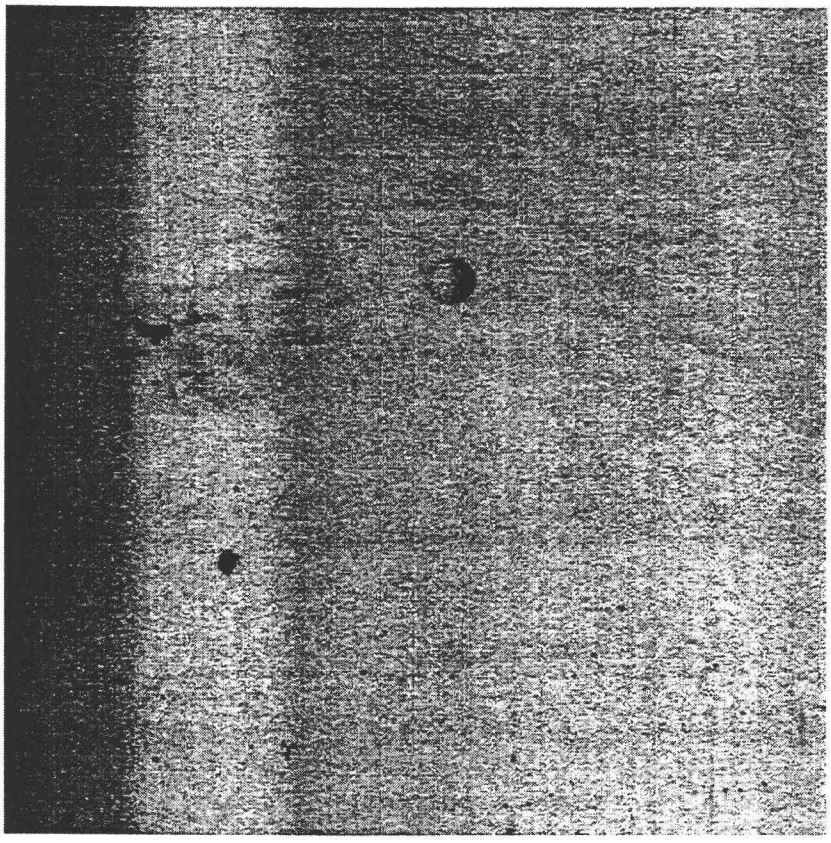

Figure B-8 Keltone LV 2% Crosslinked Bead

Figure B-9 Coalescence Of Two Droplets During Jet Breakup

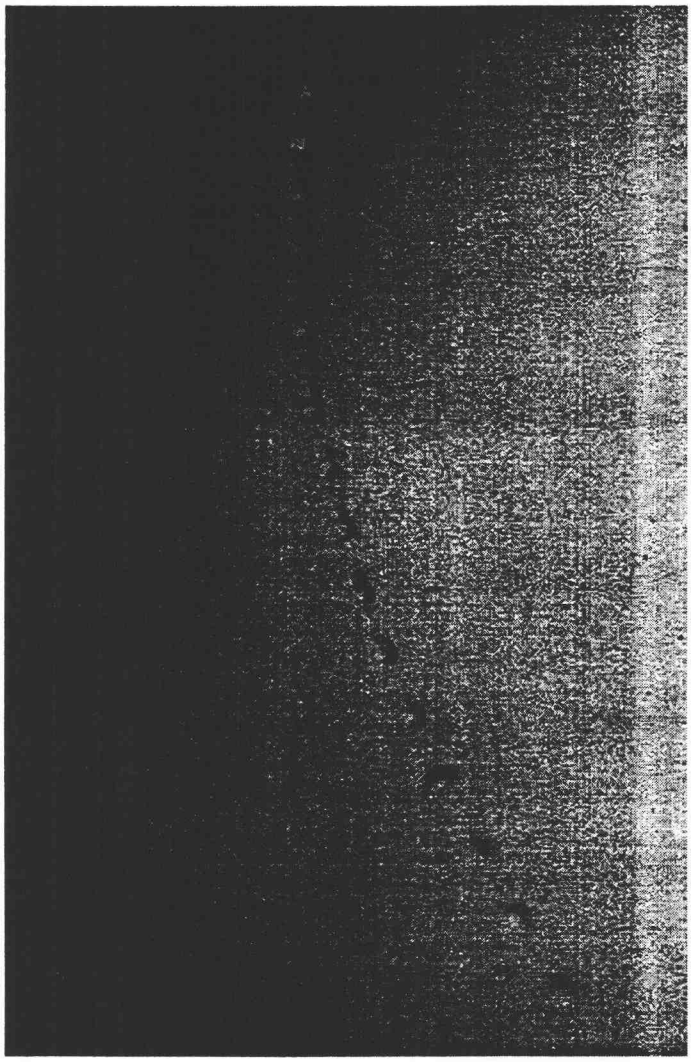

Figure B-10 Calcium Alginate Beads Produced By Unstimulated Jet Breakup

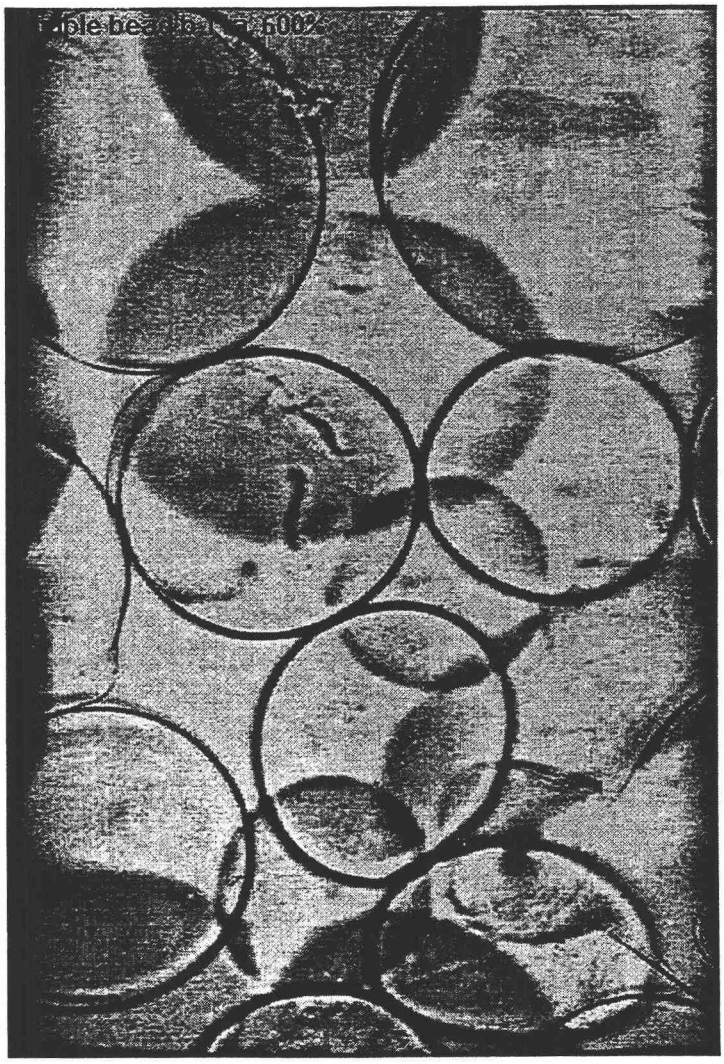

APPENDIX C

Figure C-1 List Of Investigators Who Used Stimulated Jet Breakup For Different Fluids

Investigator	Year	Droplet Diameter (microns)	Fluid
Schneider and Hendricks	1964	50-2000	water
Goedde and Yuen	1969	1820-4550	water water-glycerin
Rutland and Jameson	1971	---	water
Berglund and Lui	1973	12-46	DOP in ethanol Methylene blue in ethanol and water NaCl in water
Rajagopalan and Tien	1973	---	water-glycerin Human serum albumin
Wedding and Stukel	1974	3-25	DOP in ethanol
Wedding	1975	0.8-30	Uranine water
Haas	1975	500-1500	Thoria Sol
Taub	1976	---	Aq. Ink Soln.
Pimbley and Lee	1977	---	water
Araki and Masuda	1978	700-1300	Distilled water
Sakai and Hoshino	1980	600-1100	water-sugar solution
Kurabayaski and Karasawa	1982	1250-2120	water methanol-water
Schummer and Tebel	1982	---	water-glycerin 5% PVA-water
Lui and Pui	1982	25	DOP oleic acid
Barr, Carpenter and Newton	1984	15	oleic acid
Tramper	1985	1300-2500	Algin solution
Lin, Eversol and Campillo	1990	5-80	ethanol
Warnica, Reenen,Renksizbulut and Strong	1993	---	water
Blaisot, Ledoux, Ducret and Vendel	1994	100-500	water
Charuau, Tierce and Birocheau	1994	0.1-1	water
Moon, Kim, Lim, Go, Lee and Chang	1995	5-200	ethanol

APPENDIX D

Figure D-1 Graph For Bead Contraction With Time
Keltone 1% LV, 18 gage needle,
0.1M Calcium Chloride

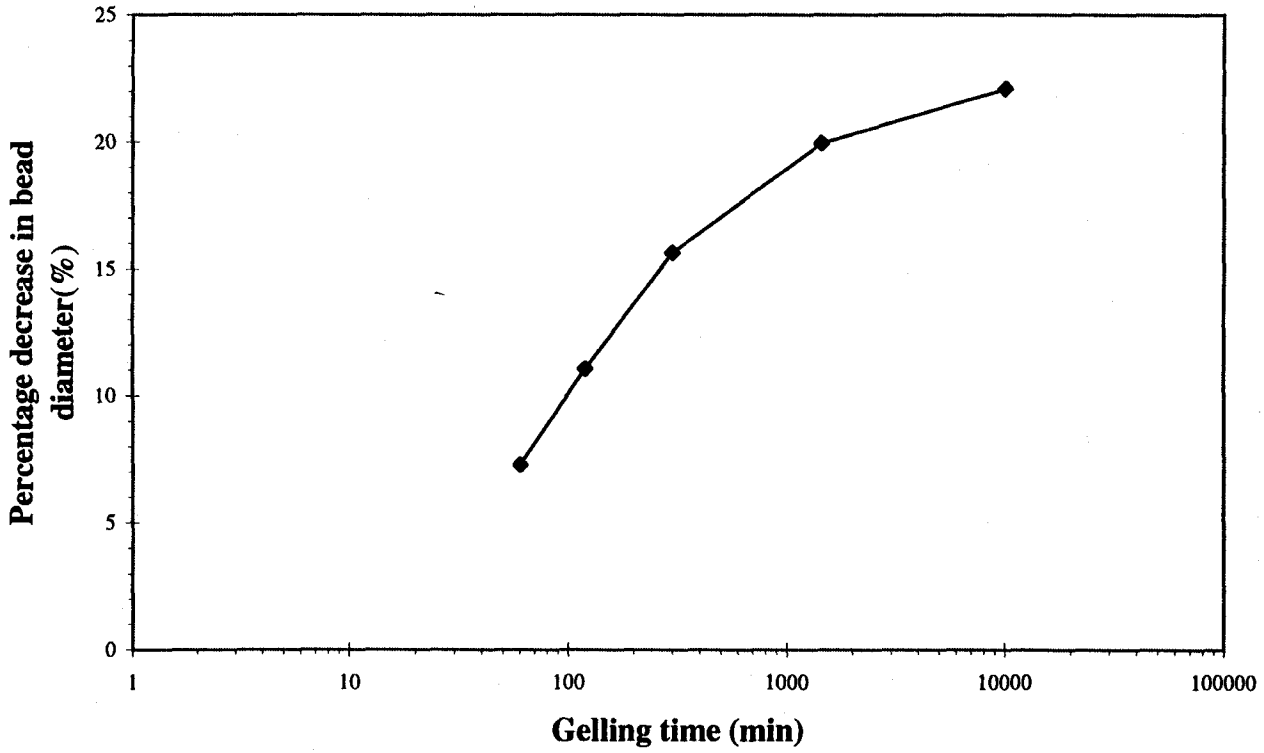

Figure D-2 Graph For Bead Contraction With Time
Keltone 1.5% LV, 18 gage needle,
0.1M Calcium Chloride

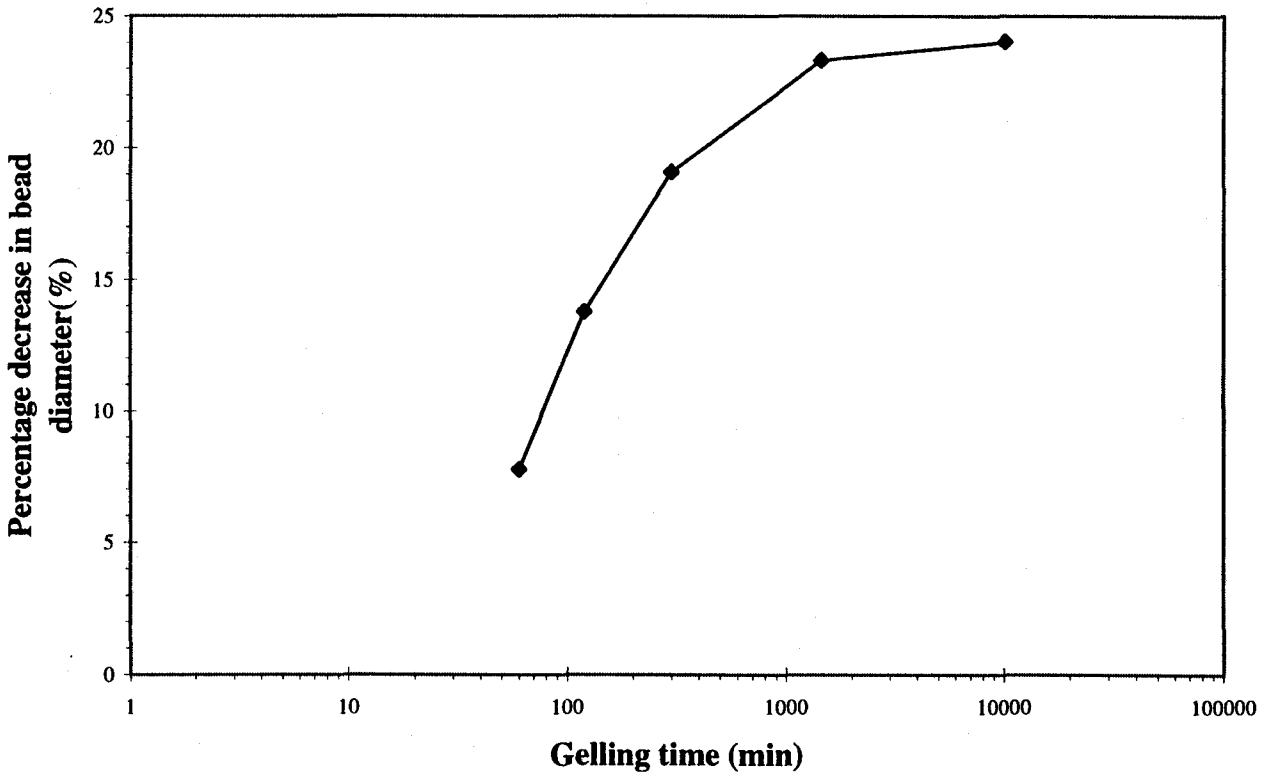

Figure D-3 Graph For Bead Contraction With Time
Keltone 2% LV, 18 gage needle,
0.1M Calcium Chloride

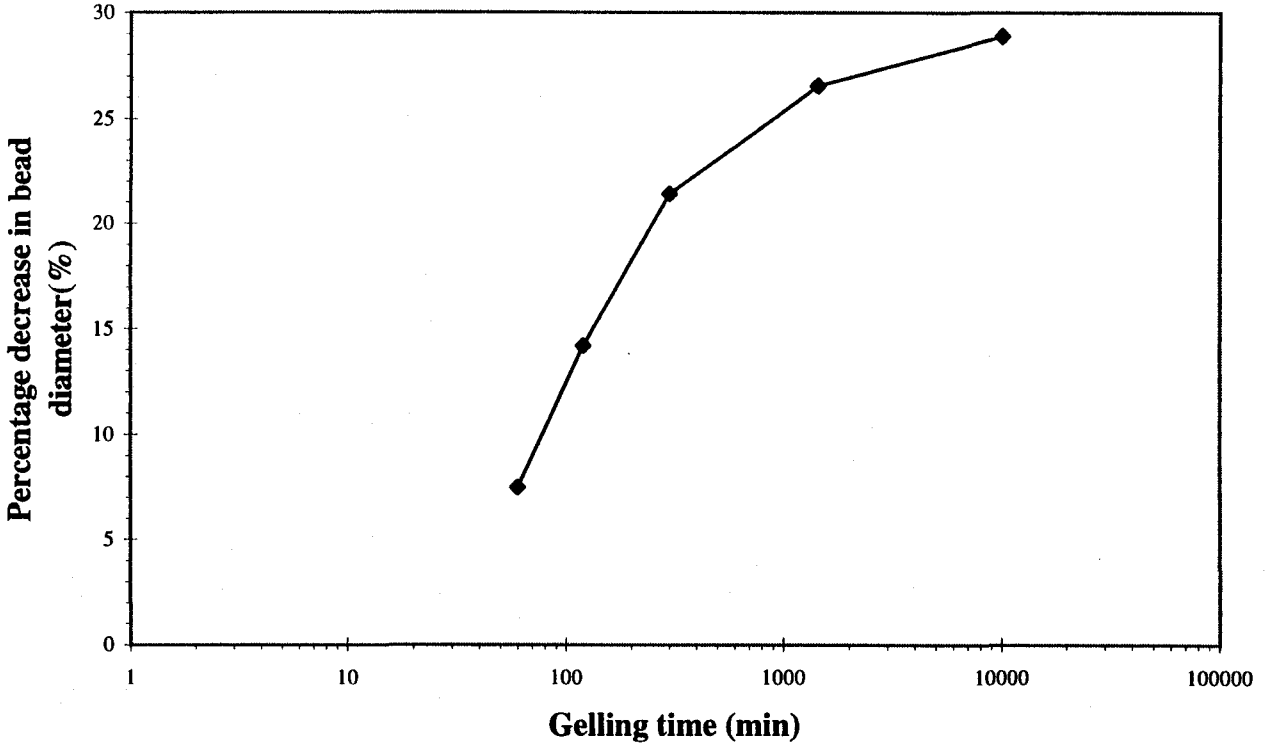

Figure D-4 Graph For Bead Contraction With Time
Keltone 2% LV, 22 gage needle,
0.1M Calcium Chloride

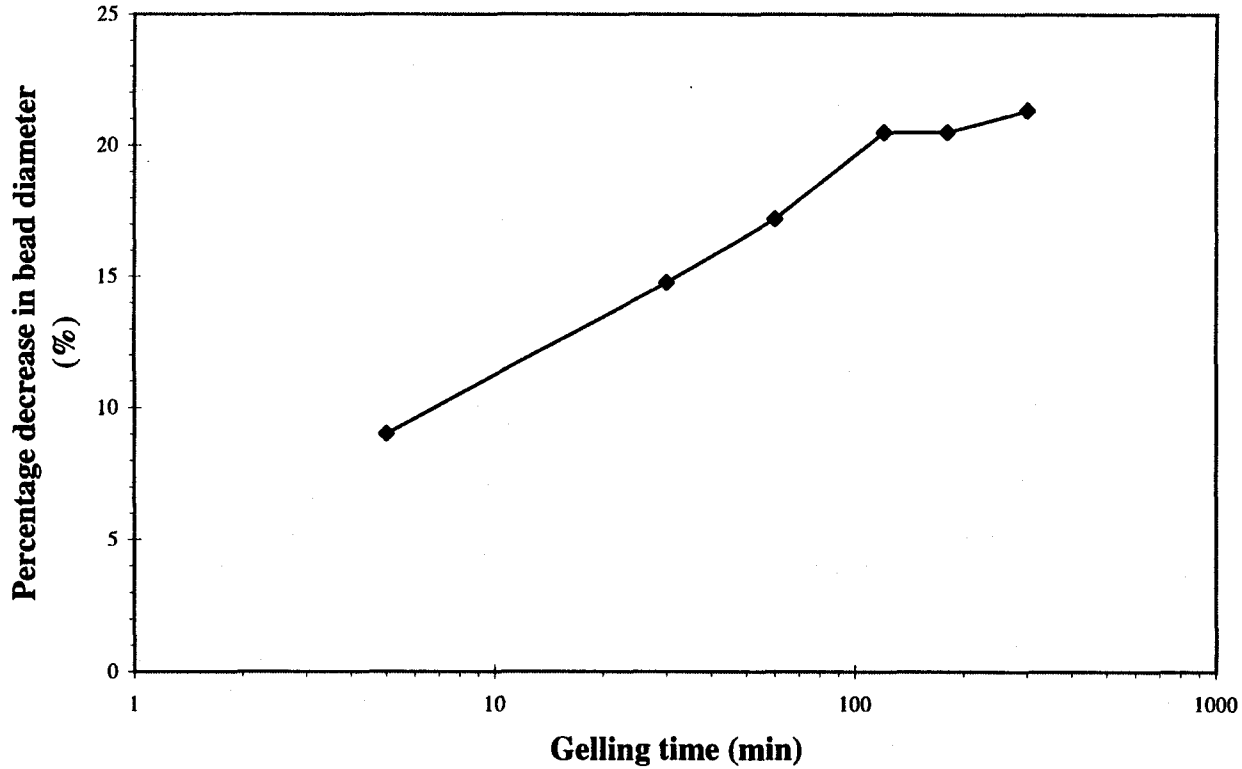

Figure D-5 Graph For Bead Contraction With Time
Keltone 1% LV, 27 gage needle,
0.1M Calcium Chloride

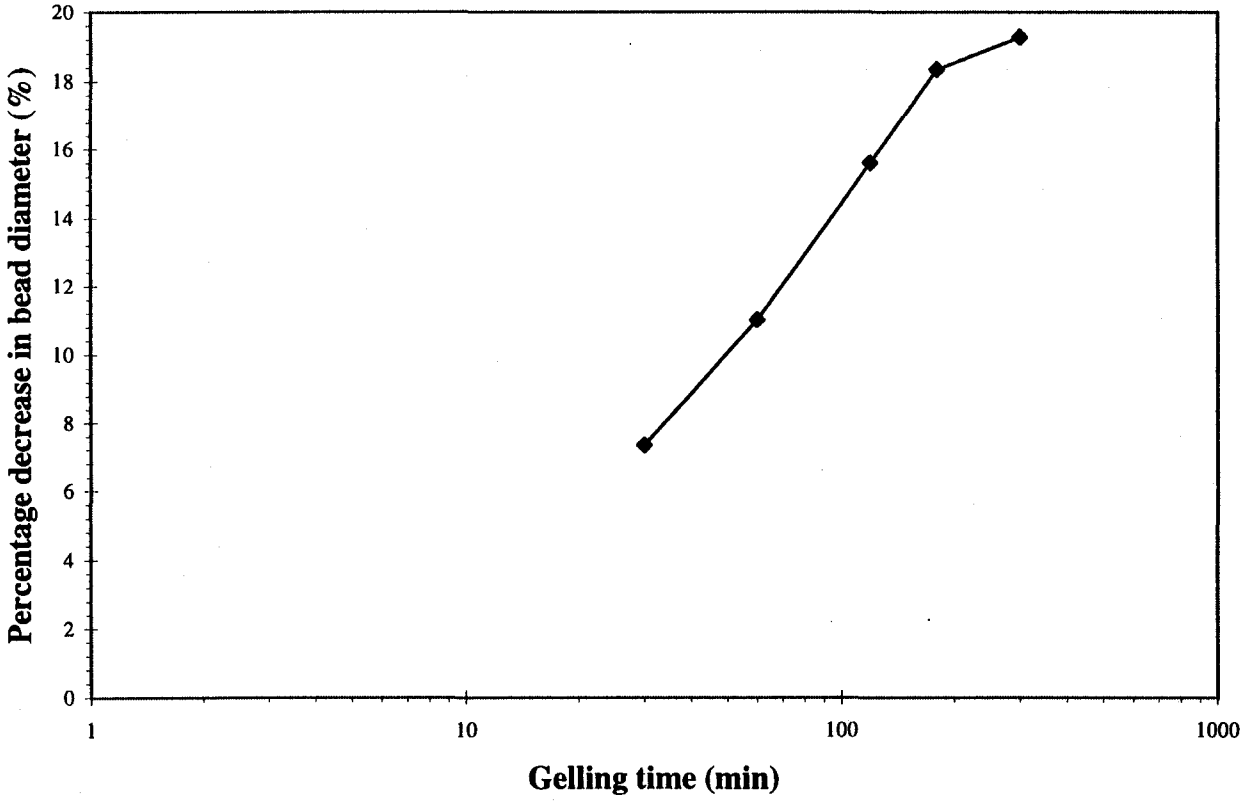

Figure D-6 Graph For Bead Contraction With Time
Keltone 2% LV, 27 gage needle,
0.1M Calcium Chloride